Correlated 2D Electron Aspects of the Quantum Hall Effect

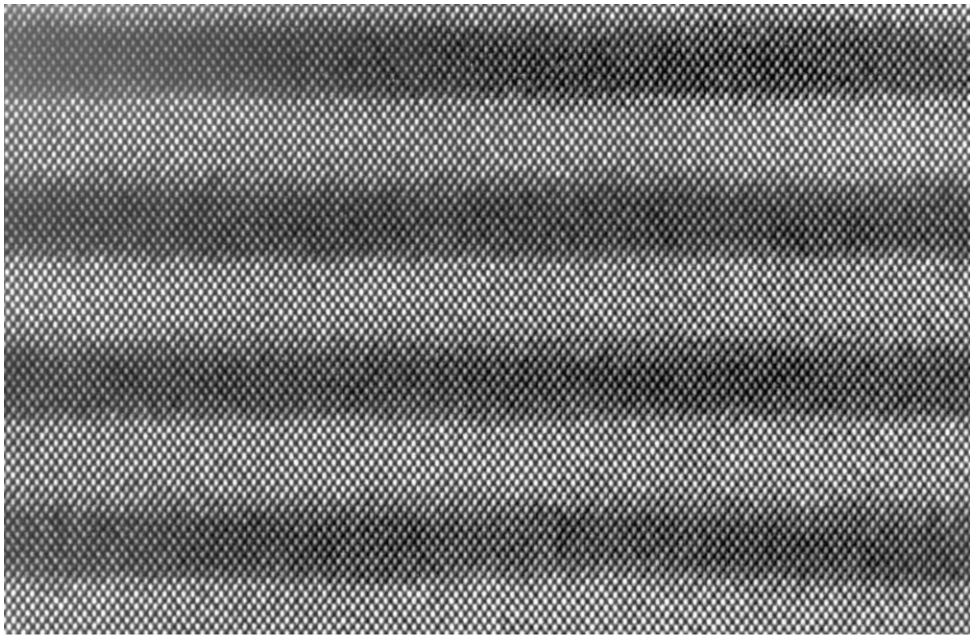

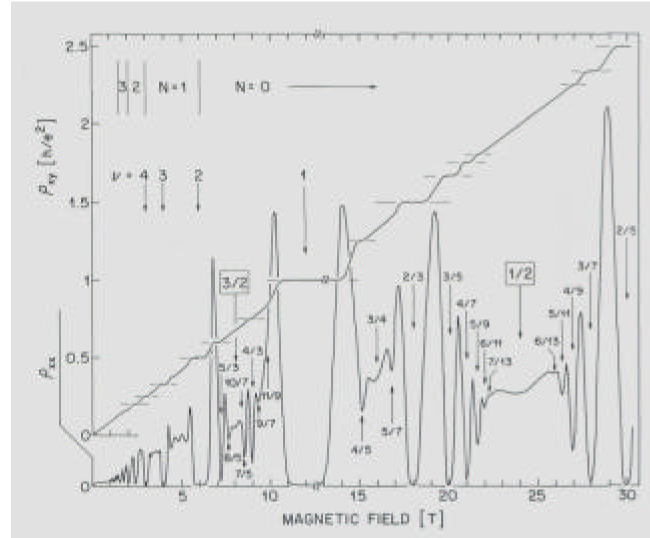

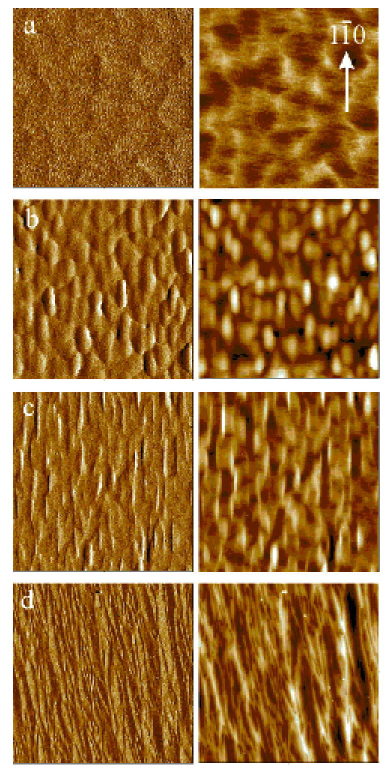

Outline:

I. Introduction: materials, transport, Hall effects

II. Composite particles – FQHE, statistical transformations

III. Quasiparticle charge and statistics

IV. Higher Landau levels

V. Other parts of spectrum: non-equilibrium effects, electron solid?

   A. Overview
   B. High magnetic fields – the electron solid
   C. Low magnetic fields – response to radiation

VI. Multicomponent systems: Bilayers

V. Other parts of the spectrum:
from the electron solid to
non-equilibrium effects

A. overview: now examine physics at the extreme ends of the magnetic field spectrum

2) A new finding near zero B-field, radiation induced oscillations

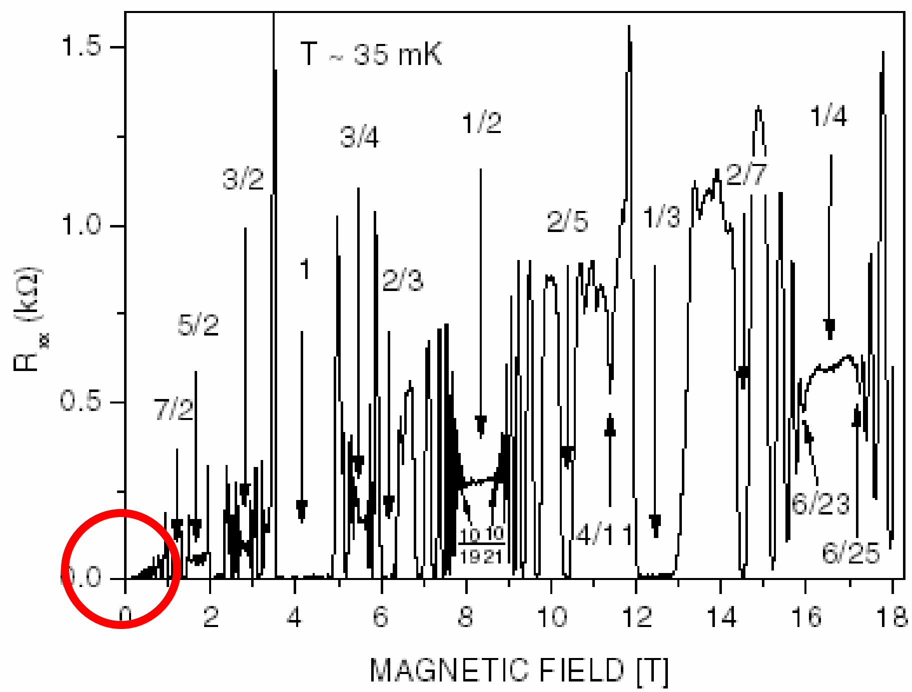

FIG. 1. Diagonal resistance R_{xx} of a sample of $n = 1.0 \times 10^{11}$ cm^{-2} and $\mu = 10 \times 10^6$ cm^2/V sec. Arrows mark several key fractional Landau level filling factors.

1) An old problem at high B-field, the proposed electron solid: what happens out here

Pan PRL '02

V. Other parts of the spectrum:
from the electron solid to
non-equilibrium effects

A. overview: some numbers

Contrast high and low field values
using standard density $1\times10^{11}cm^{-2}$

		0.1 Tesla	15 Tesla
Length scales:	magnetic length	813 Å	66 Å
	cyclotron radius	5220 Å	35 Å
	inter-particle spacing	350Å	
Energy scales:	Coulomb energy	16 K	193 K
	spin gap	0.03 K	4.3 K
	cyclotron energy	2 K	301 K

Different processes to consider:

high field = magnetic localization =>loss of collective effects

low field = no kinetic energy quenching => single particle physics

V. Other parts of the spectrum:
from the electron solid to
non-equilibrium effects

B. High magnetic fields – the electron solid?

Competition between collective effects (solid or liquid) and magnetic freeze-out

Ground state is expected to be Wigner solid for sufficiently large r_s at given small filling factor:

The FQHE states may be in competition with this, or

The ordering may be interrupted by defects, which if sufficiently strong, could localize the electrons.

Solid = both positional and orientational order

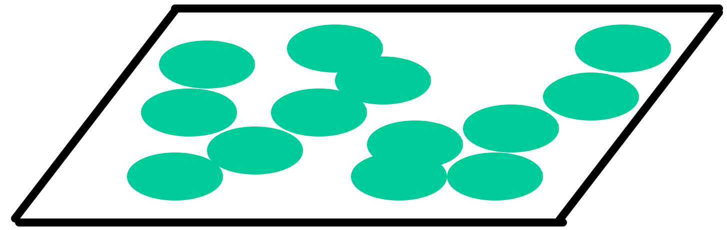

uncorrelated

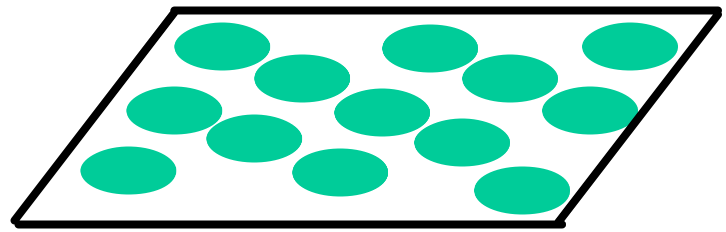

solid

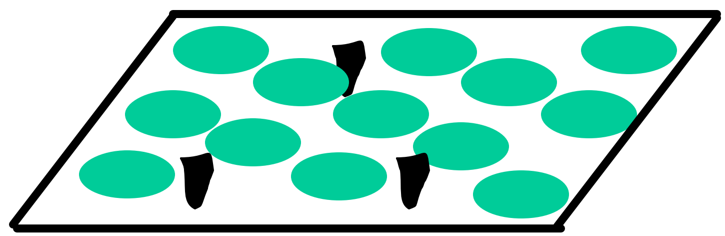

Pinned solid

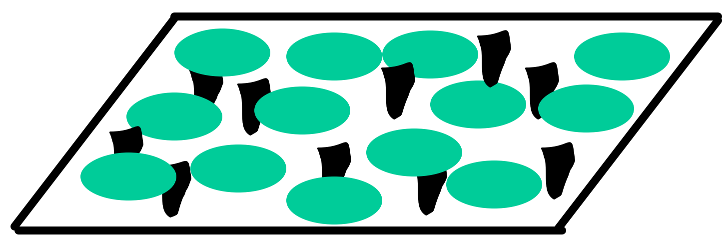

Magnetically localized, or severly pinned = glass

V. Other parts of the spectrum:
from the electron solid to
non-equilibrium effects

B. High magnetic fields – the electron solid?

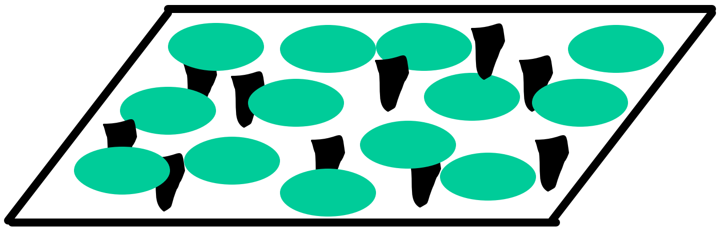

Magnetically localized, or
severly pinned = glass

The ordering may be interrupted by
defects, which if sufficiently strong, could
localize the electrons.

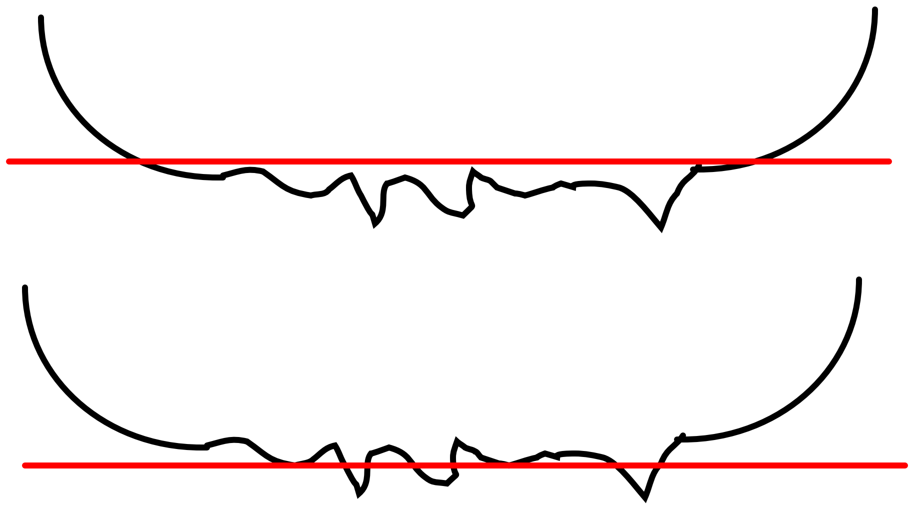

V. Other parts of the spectrum:
from the electron solid to
non-equilibrium effects

B. the electron solid?

Given r_s and filling factor ?,
what is expected for the phases and in transport?

Predictions for the electron solid:
(magnetically induced electron solid)

phase diagram line

✍increase in mass pushes onset to larger ?
✍increase r_s by decreasing density n

"Theoretical" phase diagram
(numerical studies)

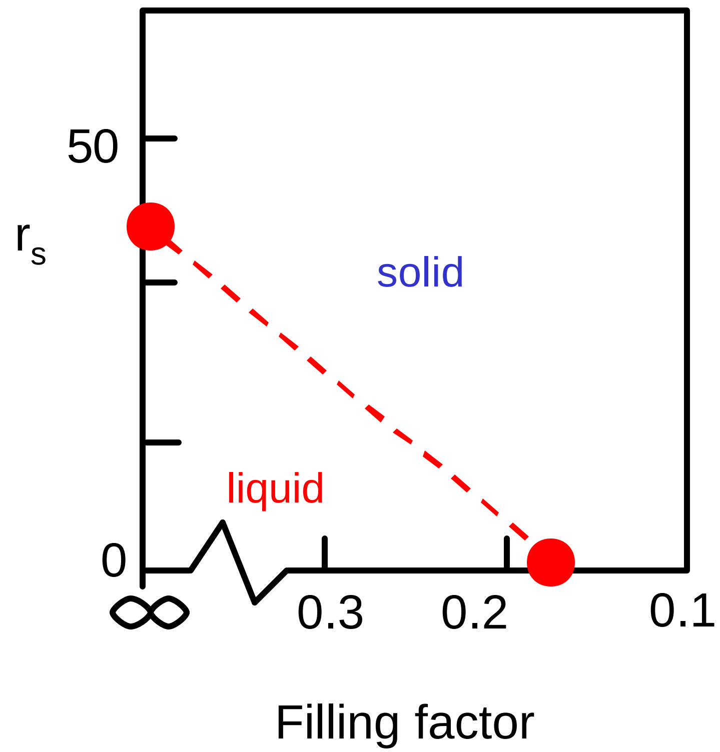

V. Other parts of the spectrum:
from the electron solid to
non-equilibrium effects

B. the electron solid?

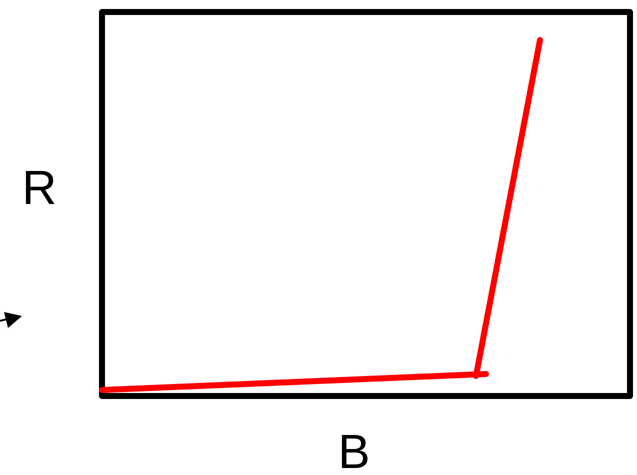

The pinned electron state should have two characteristics

In transport:

1) Insulating in the d.c. limit.
2) Oscillation modes of the electron solid about the pinning sites.

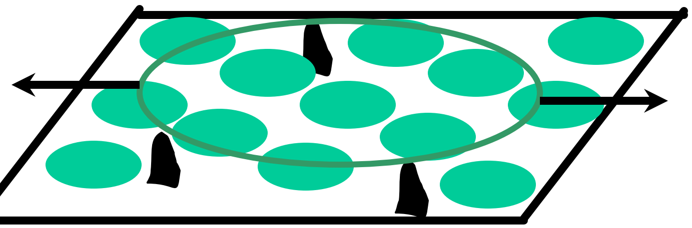

V. Other parts of the spectrum: from the electron solid to non-equilibrium effects

B. the electron solid?

For pinned solid or glassy solid, expect transport to show insulated properties

These are indeed apparent

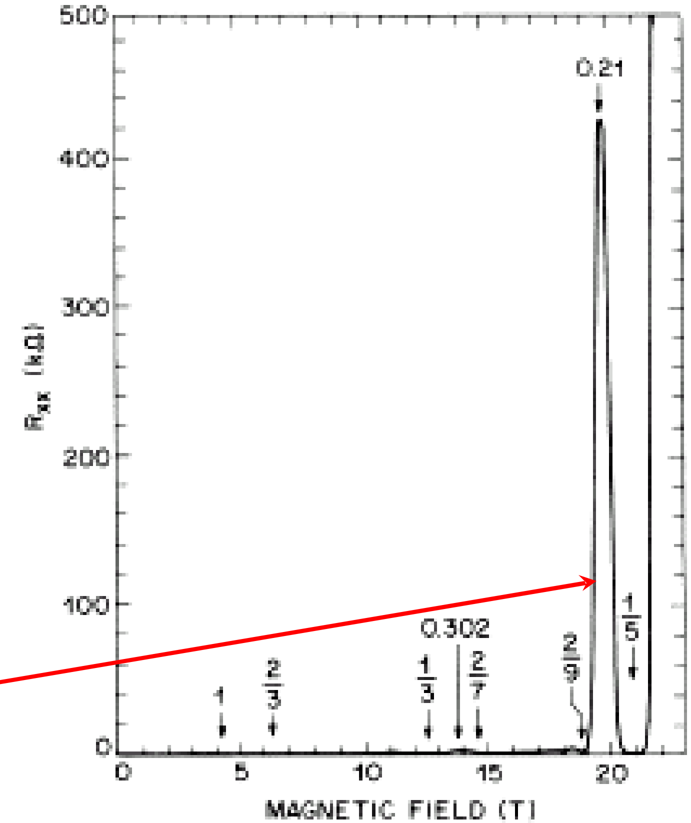

FIG. 1. Diagonal resistance R_{xx} vs magnetic field at $T \approx 90$ mK. Data are taken on a square sample so that $\rho_{xx} = \alpha R_{xx}$ with $\alpha \sim 1$. At $\nu = \frac{1}{5}$, $\rho_{xx} \to 0$ indicating that the $\nu = \frac{1}{5}$ quantum liquid forms the ground state. The resistivity ρ_{xx} in the sharp spike at $\nu \sim 0.21$ and for all $\nu \lesssim \frac{1}{5}$ is rising exponentially on lowering the temperature. All FQHE features at lower magnetic field are well developed but practically invisible on this scale. Inset: Result of a calculation for the total energy per flux quantum of the solid (E'_{WC}) and interpolated $1/m$ quantum liquids (E_L) as a function of filling factor (Ref. 4). A classical energy ($E_{class} = -0.782133\nu^{-1/2}$) is subtracted for clarity. The dashed lines represent the cusp in the total energy (Ref. 13) of the liquid at $\nu = \frac{1}{5}$. Its extrapolation intersects the solid at $\nu \sim 0.21$ and 0.19 suggesting *two* phase transitions from quantum liquid to solid around $\nu = \frac{1}{5}$.

Jiang PRL '89

V. Other parts of the spectrum:
from the electron solid to
non-equilibrium effects

B. the electron solid?

For pinned solid or glassy solid,
expect transport to show insulated
properties

These are indeed apparent

Temperature dependence of this
large resistance part of the
spectrum is

T~ exp(? /kT)

What are the current carrying
excitations in this system?

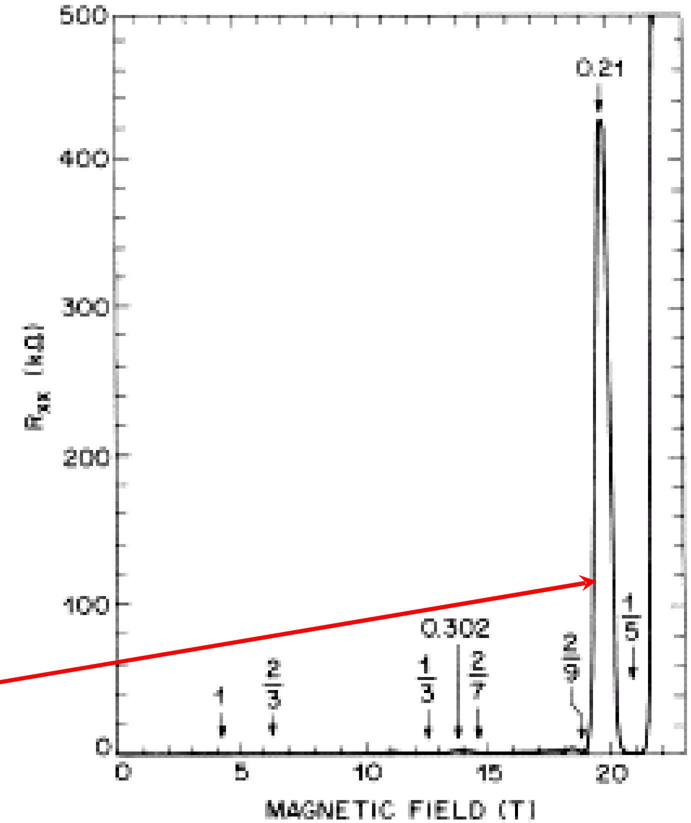

FIG. 1. Diagonal resistance R_{xx} vs magnetic field at $T \approx 90$ mK. Data are taken on a square sample so that $\rho_{xx} = \alpha R_{xx}$ with $\alpha \sim 1$. At $\nu = \frac{1}{5}$, $\rho_{xx} \to 0$ indicating that the $\nu = \frac{1}{5}$ quantum liquid forms the ground state. The resistivity ρ_{xx} in the sharp spike at $\nu \sim 0.21$ and for all $\nu \lesssim \frac{1}{5}$ is rising exponentially on lowering the temperature. All FQHE features at lower magnetic field are well developed but practically invisible on this scale. Inset: Result of a calculation for the total energy per flux quantum of the solid (E'_{WC}) and interpolated $1/m$ quantum liquids (E_L) as a function of filling factor (Ref. 4). A classical energy ($E_{class} = -0.782133\nu^{-1/2}$) is subtracted for clarity. The dashed lines represent the cusp in the total energy (Ref. 13) of the liquid at $\nu = \frac{1}{5}$. Its extrapolation intersects the solid at $\nu \sim 0.21$ and 0.19 suggesting *two* phase transitions from quantum liquid to solid around $\nu = \frac{1}{5}$.

Jiang PRL '89

V. Other parts of the spectrum: from the electron solid to non-equilibrium effects

B. the electron solid?

If this represents a correlated state, then its energy must be close to that of the FQHE states over some B-field range

Re-entrance of 1/5 state in insulating background observed for electrons

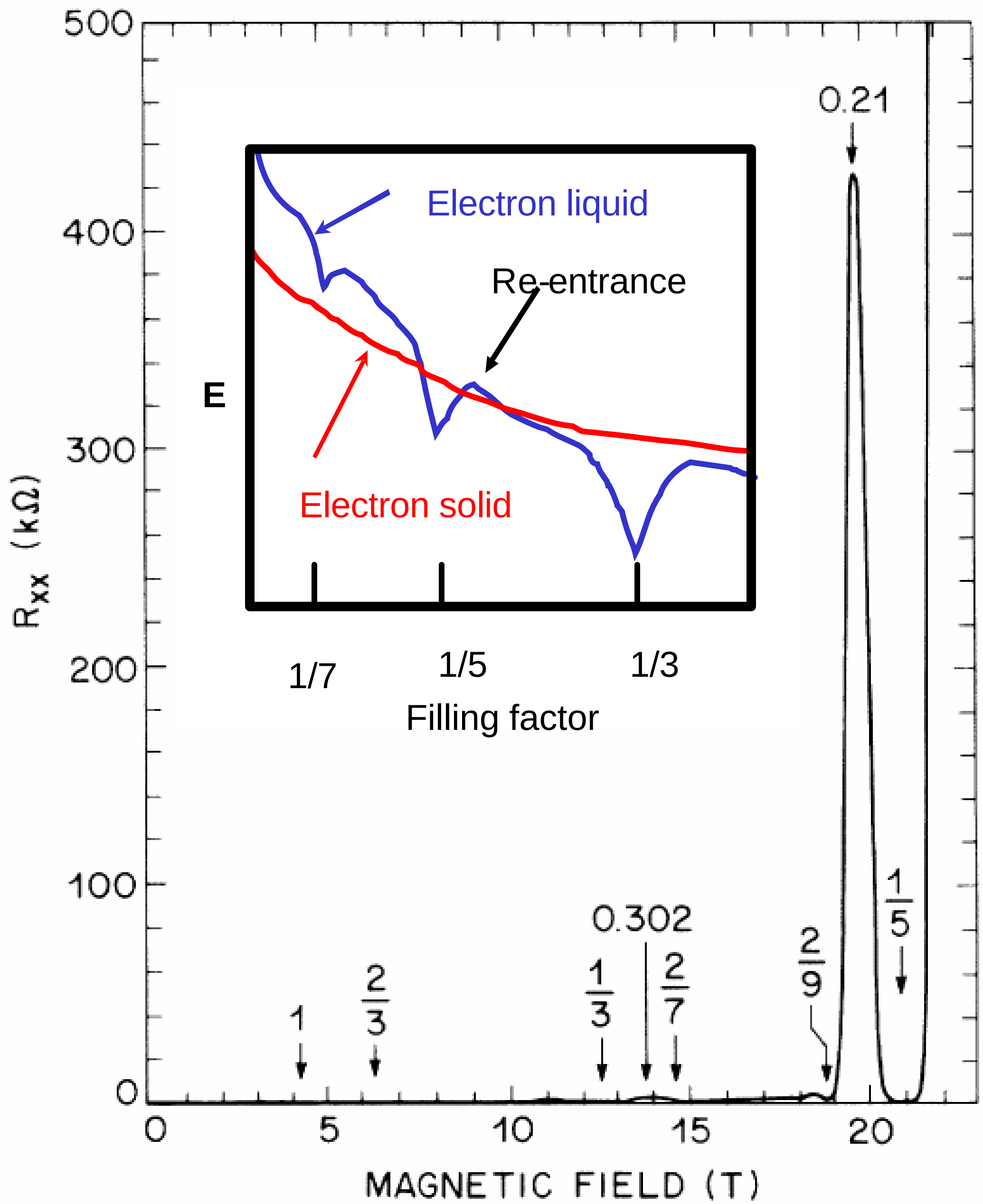

Jiang PRL ‘89

V. Other parts of the spectrum: from the electron solid to non-equilibrium effects

B. the electron solid?

At low densities (large r_s) re-entrance observed around 1/3 in holes, due to the larger effective mass

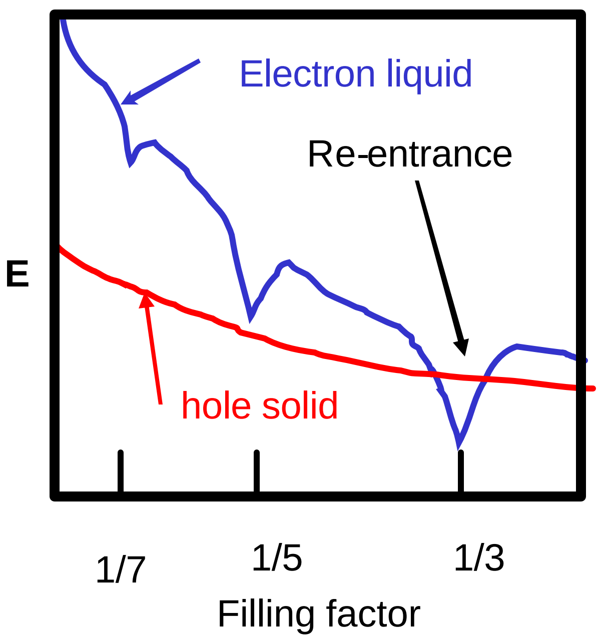

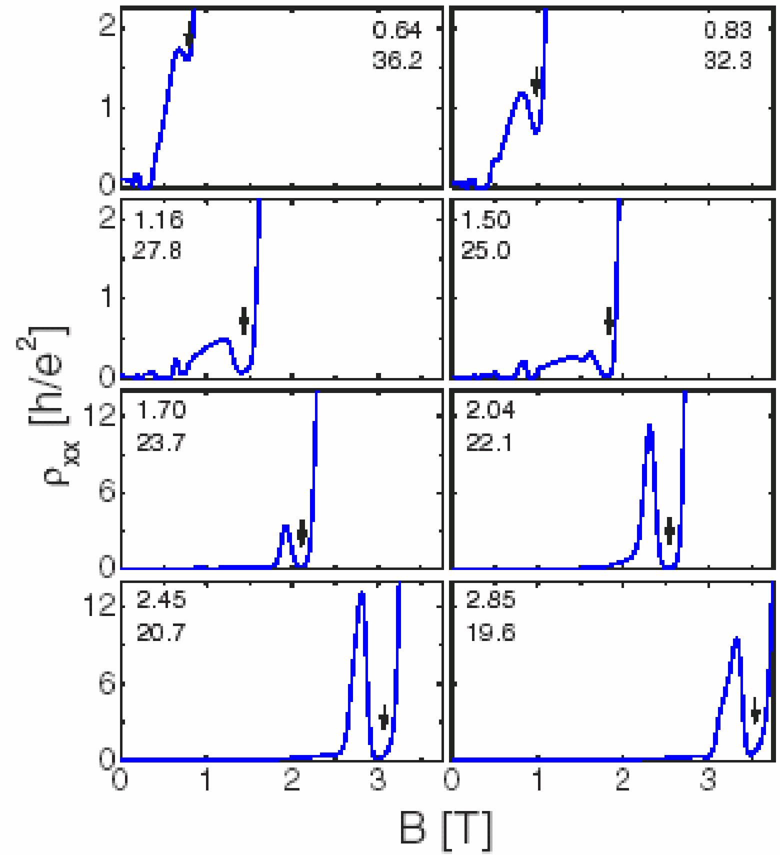

FIG. 1 (color online). The longitudinal resistivity ρ_{xx} in units of the quantum resistance h/e^2 versus B at 33 mK. Arrows mark $\nu = 1/3$. Each panel is labeled by the density in units of 10^{10} cm^{-2} (upper number) and the value of r_s (lower number). Note the change of the vertical scale for the four largest densities.

Csathy PRL ‘05

V. Other parts of the spectrum: from the electron solid to non-equilibrium effects

B. the electron solid?

At low densities (large r_s) re-entrance observed around 1/3 and 2/5: leads to an interesting phase diagram

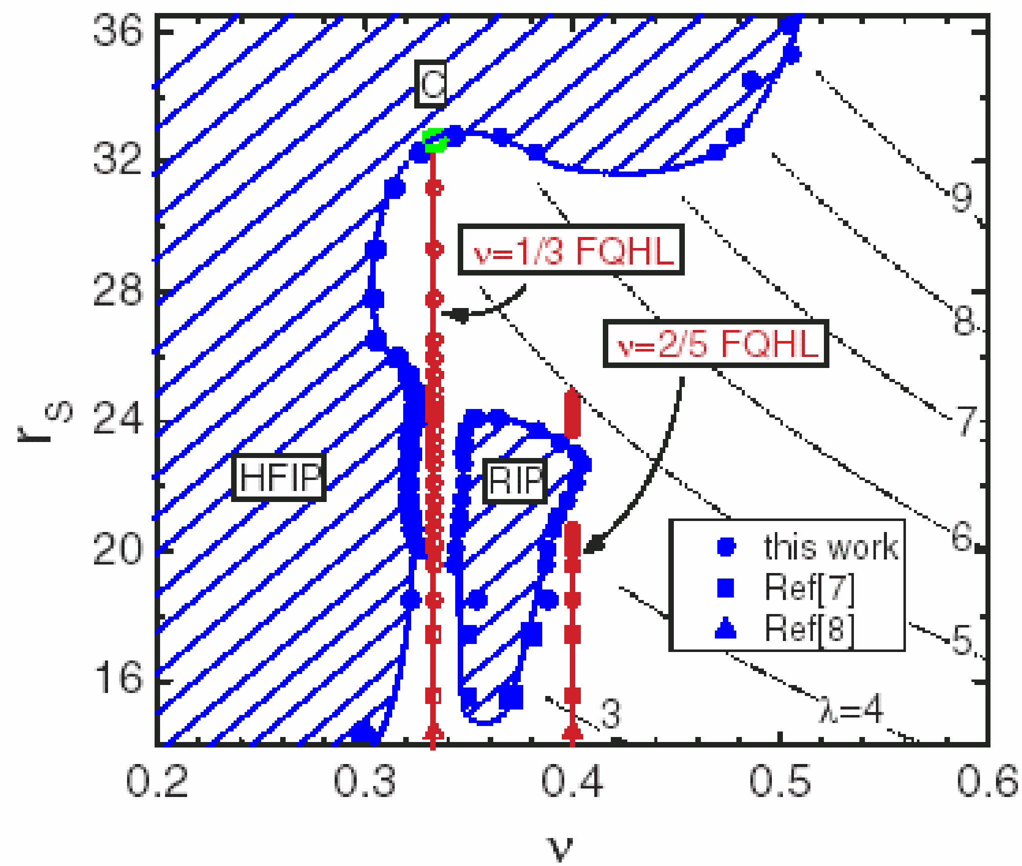

FIG. 4 (color online). The boundary of the insulating phases (solid symbols) and the $\nu = 1/3$ and $2/5$ FQHL (open symbols) in the $\nu - r_s$ phase space. Lines are guides to the eye. Dotted contours are loci of points obeying $E_c = \lambda\hbar\omega_c$ (see text).

Csathy PRL '05

V. Other parts of the spectrum: from the electron solid to non-equilibrium effects

B. the electron solid?

Transition from liquids to insulating complex:
Higher temperatures can reveal FQHE states

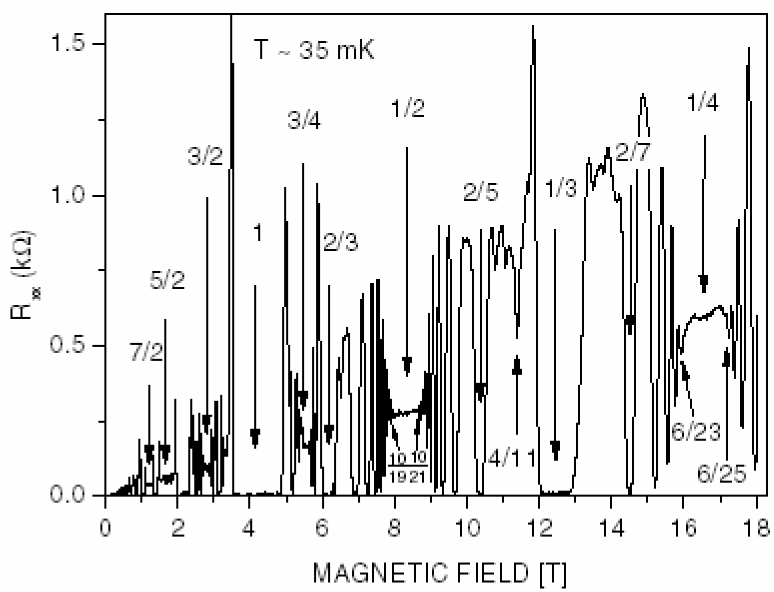

FIG. 1. Diagonal resistance R_{xx} of a sample of $n = 1.0 \times 10^{11}$ cm^{-2} and $\mu = 10 \times 10^6$ cm^2/V sec. Arrows mark several key fractional Landau level filling factors.

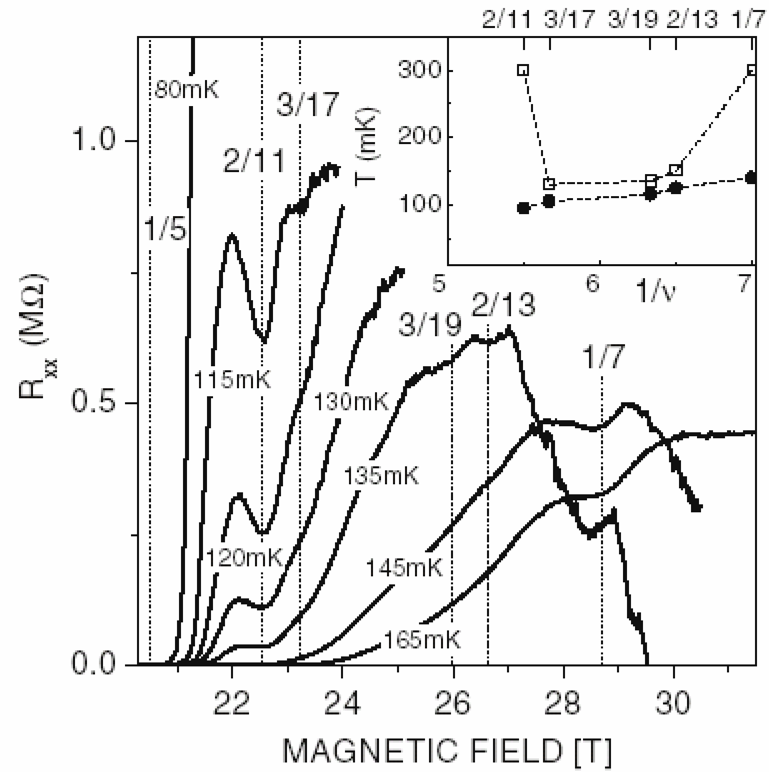

FIG. 2. R_{xx} above 20 T at various temperatures. The vertical, dashed lines show the positions of the Landau level filling factors $\nu = 1/5$, $2/11$, $3/17$, $3/19$, $2/13$, and $1/7$. The inset summarizes high-T limits (open squares) and low-T limits (solid dots) for the observation of features in R_{xx} at various ν. The dashed line is only a guide to the eye. The low-T limits may be viewed as the melting line from Wigner crystal to FQHE liquids and the high-T limits are measures of the energy gap of FQHE states (see text for details).

Pan PRL '02

V. Other parts of the spectrum: from the electron solid to non-equilibrium effects

B. the electron solid?

For pinned solid or glassy solid, expect transport to show insulated state

What other properties distinguish a solid from a liquid? What other tests can be performed?

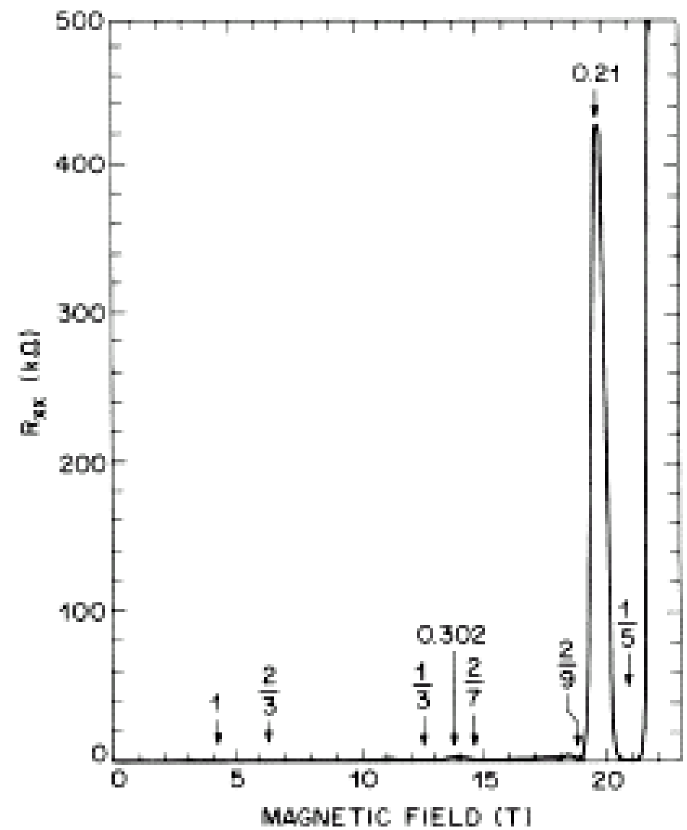

Jiang PRL '89

V. Other parts of the spectrum:
from the electron solid to
non-equilibrium effects

B. the electron solid?

The pinned state should have two characteristics
In transport:

1) Insulating in the d.c. limit.
2) Oscillation modes of the electron solid about the pinning sites.

Are there simple models for pinned electron solid?

Mode may be complicated due to
the mixing by the magnetic field

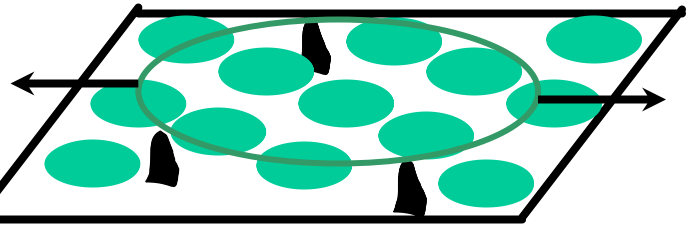

V. Other parts of the spectrum: from the electron solid to non-equilibrium effects

B. the electron solid?

The pinned state should have two characteristics

In transport:

1) Insulating in the d.c. limit.
2) Oscillation modes of the electron solid about the pinning sites.

Wavevector dependence should be observed if the electron solid domains are sufficiently large

Excitation modes in the electron solid

solid supports phonons, B-field mixes longitudinal and transverse modes

ideal Wigner Crystal : (Cote '91, Normand '92)

$$\omega_+(q) = \omega_c + \frac{\omega_\ell^2(q)}{2\omega_c}$$

$$\omega_-(q) = \frac{\omega_t(q)\,\omega_\ell(q)}{\omega_c} \sim q^{3/2}$$

where

plasma mode $\omega_\ell(q) = \left(ne^2/2m^*\varepsilon\varepsilon_0\right)^{1/2} q^{1/2}$

transverse mode $\omega_t(q) = c_t q$

pinned Wigner Crystal : (Normand '92)

using harmonic oscillator approximation of the pinning potential and pinning frequency ω_0

$$\omega_-(q) = \left[\left(\omega_\ell^2(q)+\omega_0^2\right)\left(\omega_t^2(q)+\omega_0^2\right)\right]^{1/2}/\omega_c$$

results for weak pinning :

clean limit $\frac{\omega_\ell\omega_t}{\omega_c} \sim q^{3/2}$ $\lambda < \xi$

intermediate $\frac{\omega_\ell\omega_0}{\omega_c} \sim q^{1/2}$

dirty limit $\frac{\omega_0^2}{\omega_c} \neq f(q)$

with coherent crystal domain size ξ

strong pinning : (Li '95)

$\omega_0^2 \simeq e^2 n_i / 2\pi\varepsilon\varepsilon_0 m^*$, n_i = 3d residual impurity density

$\xi \sim (n_i/a)^{-1/2}$

V. Other parts of the spectrum: from the electron solid to non-equilibrium effects

B. the electron solid?

The pinned state should have two characteristics

In transport:

1) Insulating in the d.c. limit.
2) Oscillation modes of the electron solid about the pinning sites.

For disordered systems, the pinning mode will be wavevector independent:

Resonance mode should be present

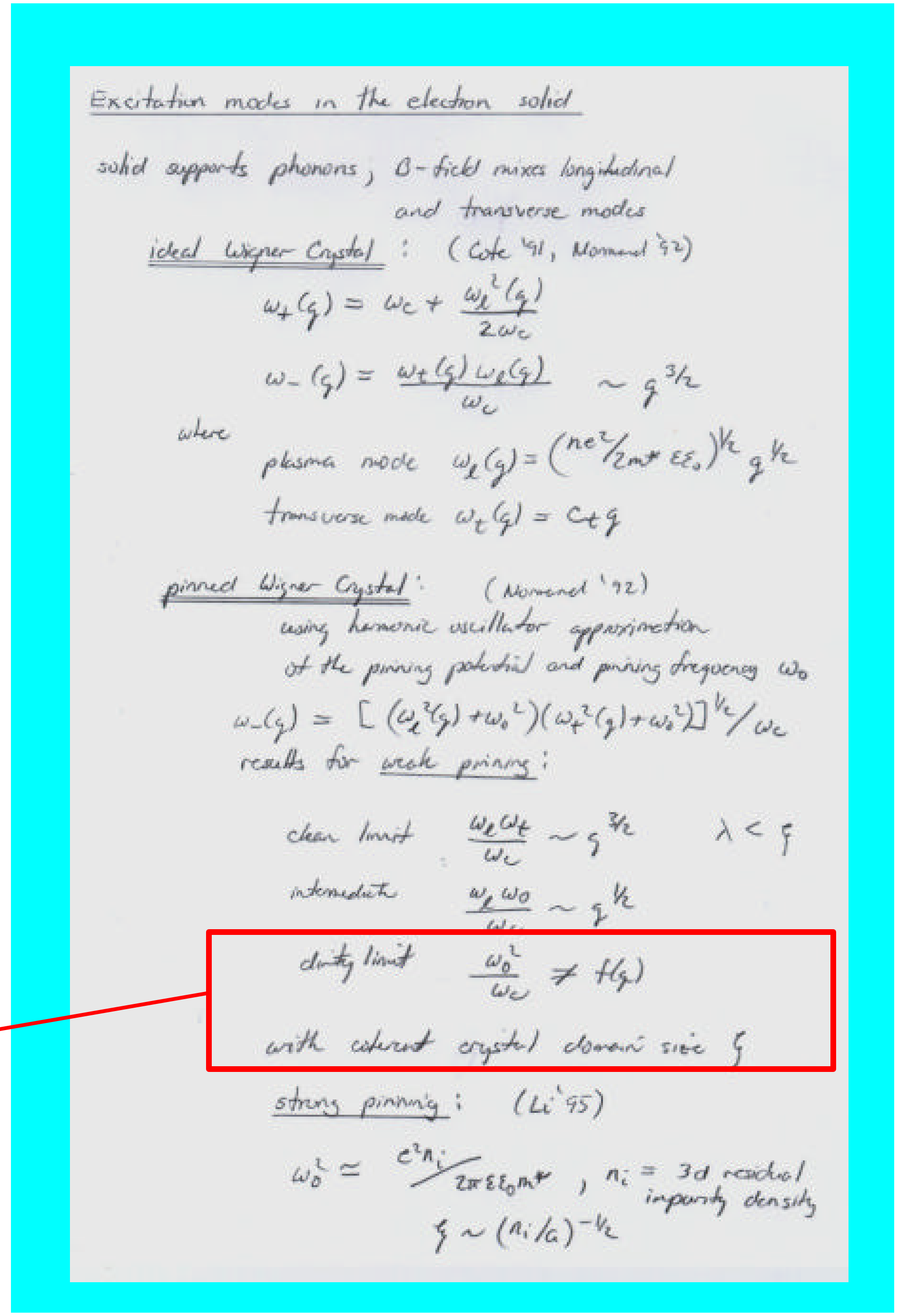
Excitation modes in the electron solid

solid supports phonons, B-field mixes longitudinal and transverse modes

ideal Wigner Crystal: (Côté '91, Normand '92)

$$\omega_+(q) = \omega_c + \frac{\omega_\ell^2(q)}{2\omega_c}$$

$$\omega_-(q) = \frac{\omega_t(q)\,\omega_\ell(q)}{\omega_c} \sim q^{3/2}$$

where

plasma mode $\omega_\ell(q) = (ne^2/2m^*\epsilon\epsilon_0)^{1/2} q^{1/2}$

transverse mode $\omega_t(q) = c_t q$

pinned Wigner Crystal: (Normand '92)

using harmonic oscillator approximation of the pinning potential and pinning frequency ω_0

$$\omega_-(q) = [(\omega_\ell^2(q)+\omega_0^2)(\omega_t^2(q)+\omega_0^2)]^{1/2}/\omega_c$$

results for weak pinning:

clean limit $\frac{\omega_\ell\omega_t}{\omega_c} \sim q^{3/2}$ $\lambda < \xi$

intermediate $\frac{\omega_\ell\omega_0}{\omega_c} \sim q^{1/2}$

dirty limit $\frac{\omega_0^2}{\omega_c} \neq f(q)$

with coherent crystal domain size ξ

strong pinning: (Li '95)

$\omega_0^2 \simeq \frac{e^2 n_i}{2\pi\epsilon\epsilon_0 m^*}$, n_i = 3d residual impurity density

$\xi \sim (n_i/a)^{-1/2}$

V. Other parts of the spectrum:
from the electron solid to
non-equilibrium effects

B. the electron solid?

An electron solid can demonstrate shear mode propagation or the wavevector independent pinned mode:

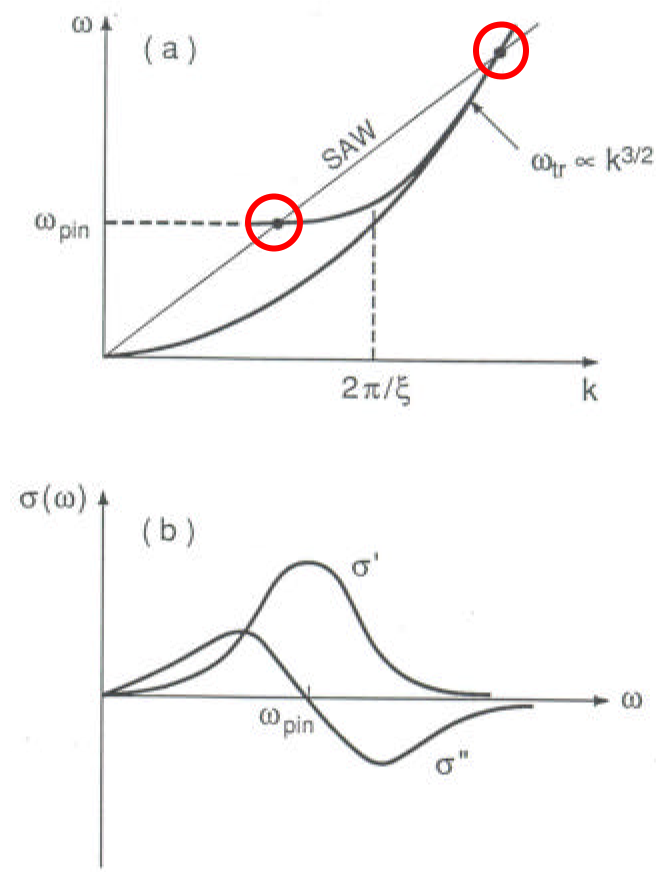

This may be detected using surface acoustic waves:
Contribution to ? ’(?), ? ”(?) when SAW dispersion and electron solid modes cross
Also true for other frequency, wavevector dependent techniques

V. Other parts of the spectrum:
from the electron solid to
non-equilibrium effects

B. the electron solid?

Instead of distinct mode crossings,
a broad resonance structure was found near 1GHz

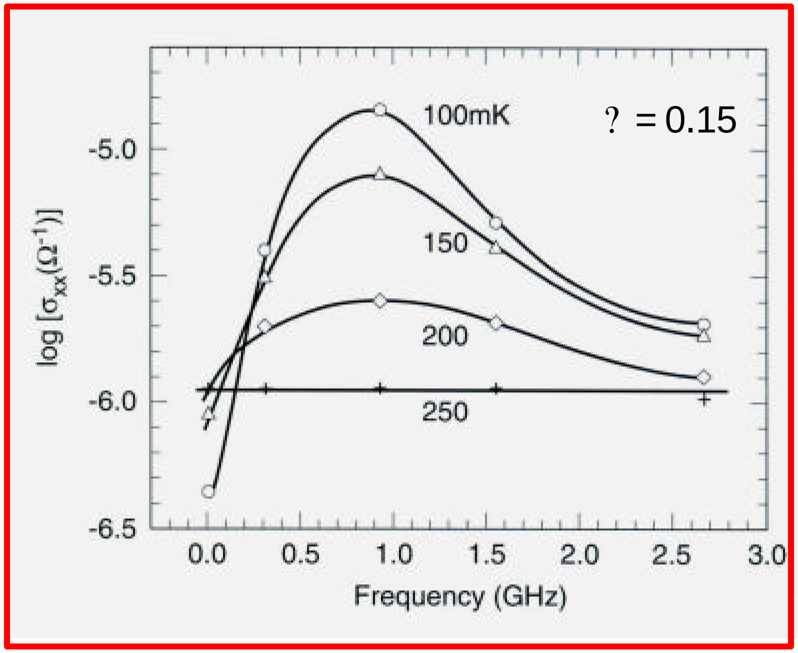

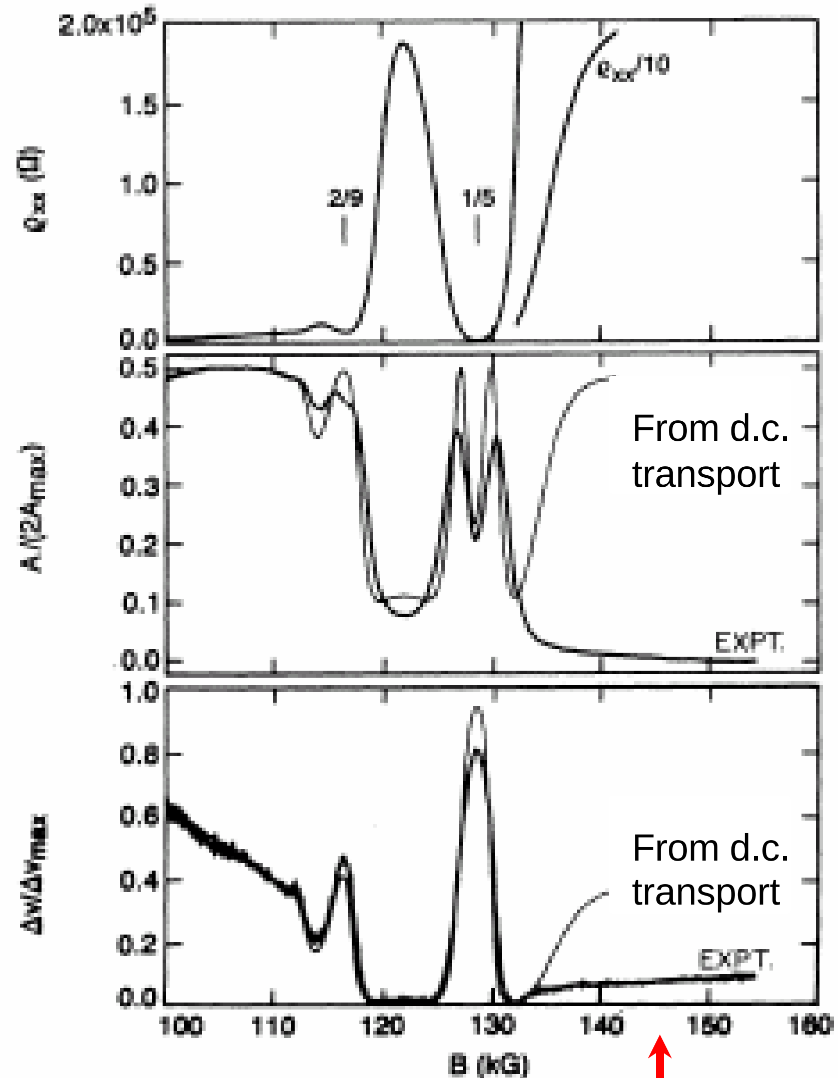

FIG. 1. Magnetic-field dependence of dc resistance ρ_{xx}, normalized SAW attenuation, and velocity shifts in sample 1 at 80 mK and 235 MHz. The theory lines are calculated from Eq. (1) using ρ_{xx}(dc).

V. Other parts of the spectrum: from the electron solid to non-equilibrium effects

B. the electron solid?

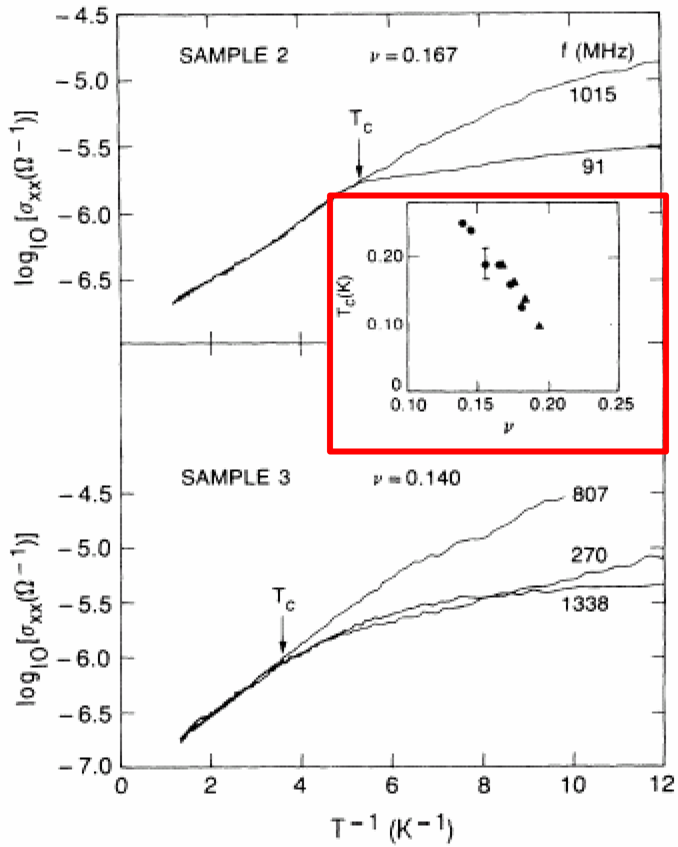

FIG. 4. High-frequency conductivity $\sigma_{xx}(k,\omega)$ of a 2DEG in the Wigner crystallization regime as a function of inverse temperature. The inset shows T_c as a function of filling factor ν.

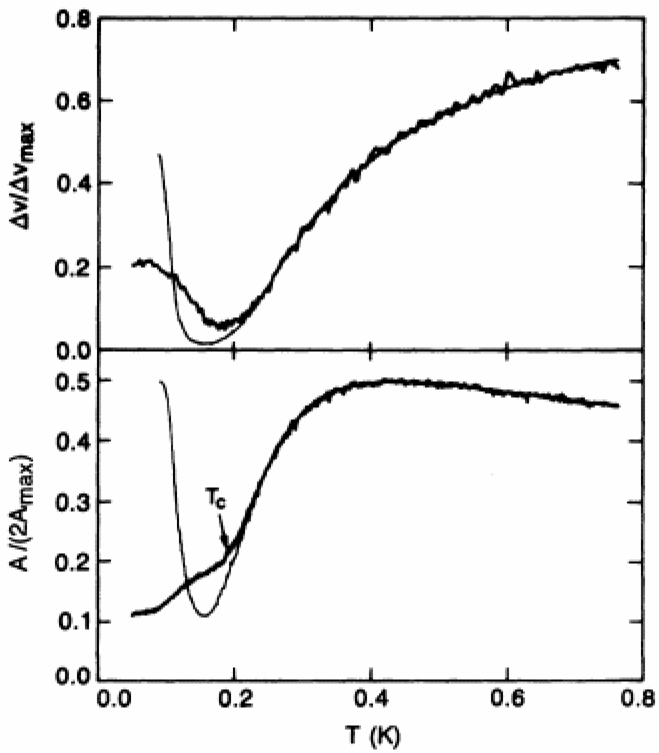

FIG. 2. Temperature dependence of normalized velocity shift and attenuation in sample 2 at 160 kG (ν=0.167) and 91 MHz. The theory lines are based on Eq. (1) and on the simultaneously measured ρ_{xx}(dc) values.

As temperature is lowered, the onset to this mode can be traced over filling factor range:

Temperature versus ? phase diagram

V. Other parts of the spectrum:
from the electron solid to
non-equilibrium effects

B. the electron solid?

coplanar waveguide can also be used to look for $?_{xx}(?)$:

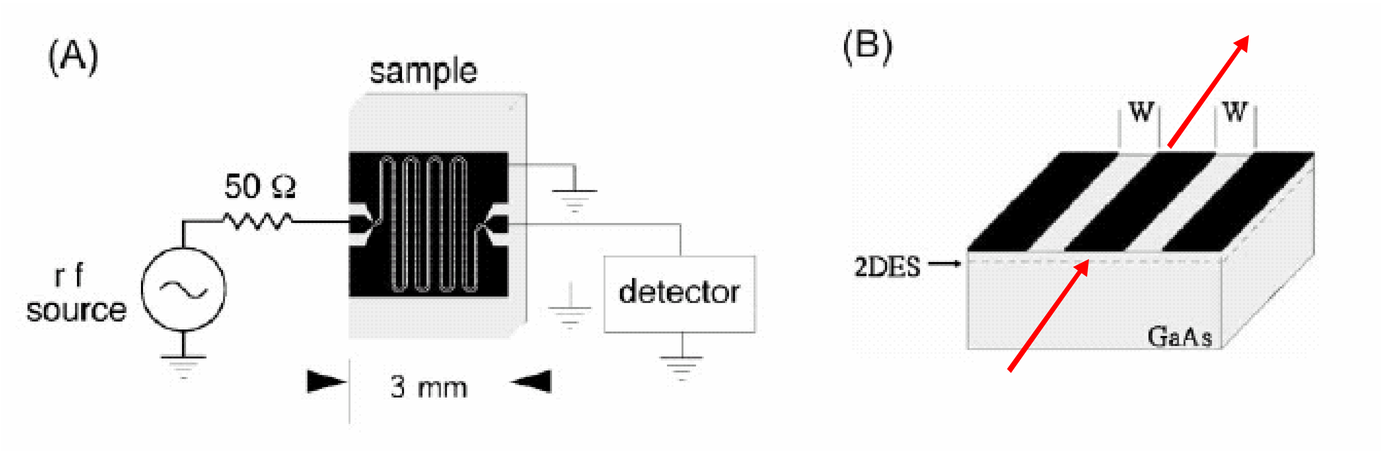

Power absorption $P=\exp\{(2l/Z_0/w)\mathrm{Re}\,[?_{xx}(?)]\}$,
w=width, *l*=length of waveguide

$\mathrm{Re}(?_{xx}(?))$~ln(absorbed power, P)

q ~ ?/w, w=30-80?m

V. Other parts of the spectrum: from the electron solid to non-equilibrium effects

B. the electron solid?

With cleaner samples and in hole samples this mode structure is observed

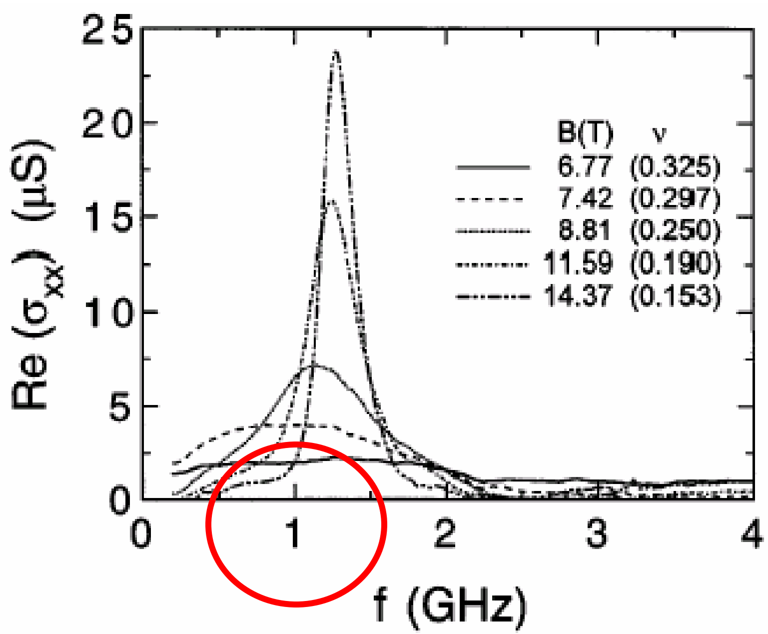

FIG. 2. Real part of diagonal conductivity vs frequency for several magnetic fields, $T = 50$ mK.

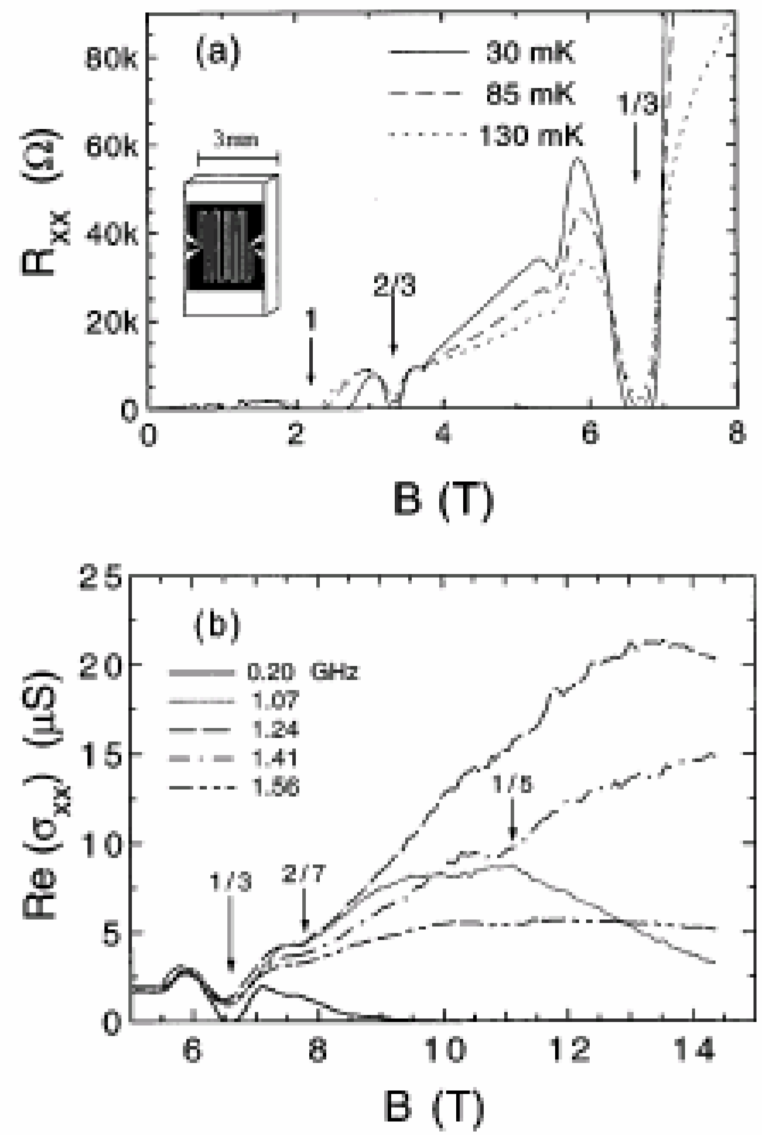

coplanar waveguide:
Re(?$_{xx}$(?))~In(absorbed power)

Chen PRL '97

V. Other parts of the spectrum:
from the electron solid to
non-equilibrium effects

B. the electron solid?

Higher mobilities show sharper, multiple modes at lower frequencies:
(may reflect fewer pinning sites)

One mode at B-field lower than 1/5,
disappears at high fields

Also, possible wavevector dependence

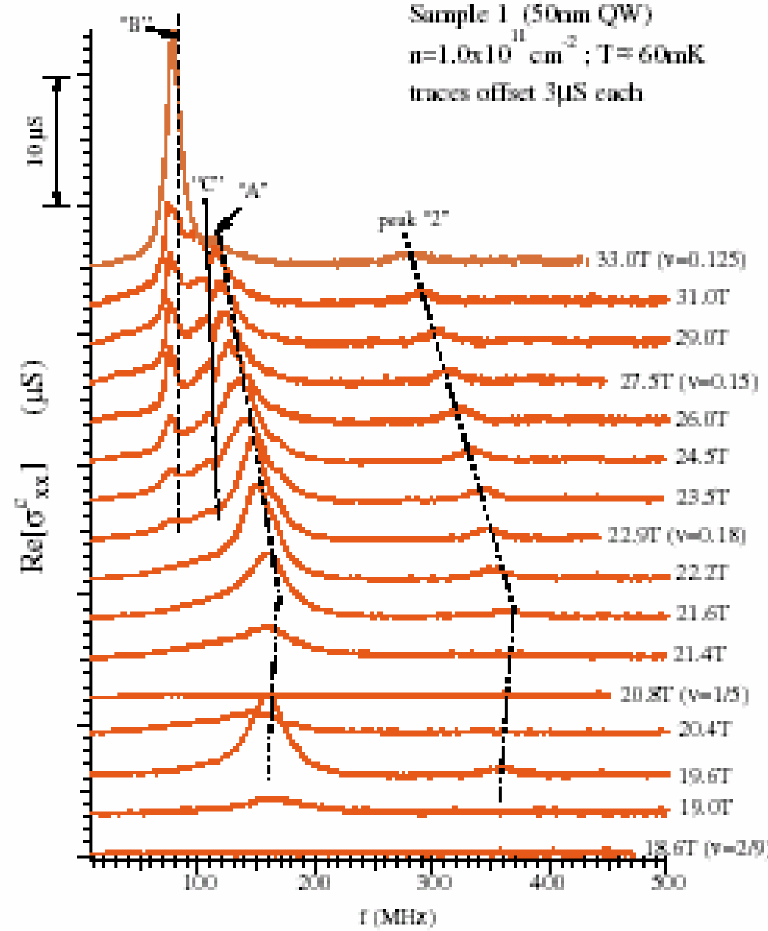

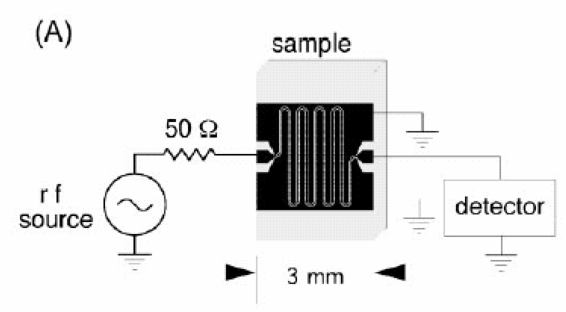

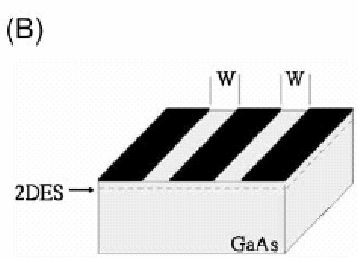

FIG. 2 (color online). Sample 1: Re[$\sigma^c_{xx}(f)$] spectra at various B, in increasing order from $B = 18.6$ (bottom) to 33 T (top). Adjacent traces are offset by 3 μS from each other for clarity. Magnetic fields (and selected ν's) are labeled at the right. Measurements were performed at $T \sim 60$ mK. From left to right, the long dashed line, dotted line, dot-dashed line, and short dashed line are guides to the eye, corresponding to peaks "B", "C", "A", and "2", respectively, as explained in the text

Coplanar waveguide technique

Chen PRL '04

V. Other parts of the spectrum: from the electron solid to non-equilibrium effects

B. the electron solid?

The pinned state should have two

characteristics +

In transport:

1) Insulating in the d.c. limit.
2) Oscillation modes of the electron solid about the pinning sites.
3) Depinning, or non-linear I-V

Non-linear Current-Voltage Characteristics:

threshold electric field E_T to de-pin lattice determined by balancing pinning force and external force/domain

$$(\xi/a)^2 e E_T = \alpha \eta a \qquad a)$$

with $(\xi/a)^2$ electrons/domain, and η the Wigner crystal shear modulus

$$\eta \doteq 0.2 e^2 n^{3/2} / 4\pi\varepsilon\varepsilon_0$$

with α a numerical prefactor of 0.1 [Normand '92, Bonsall '77, Esfarjani '91].

With above and $E_T \sim 1$ mV/cm

$\Rightarrow \xi/a \gg 10$

In CDW (Gruner '88), relate pinning frequency ω_0 to threshold field E_T

$$e E_T \simeq m^* \omega_0^2 a / 2\pi \qquad b)$$

But a) + b) above produce $\xi/a \sim 1$, and ω_0 from measurements $\Rightarrow$ E_T too large!!!

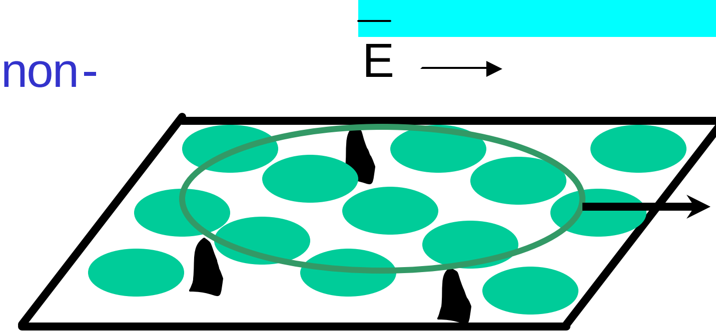

Depinning thresholds and microwave resonances not consistent

V. Other parts of the spectrum: from the electron solid to non-equilibrium effects

B. the electron solid?

The pinned state should have two characteristics

In transport:

1) Insulating in the d.c. limit.
2) Oscillation modes of the electron solid about the pinning sites.
3) Depinning, or non-linear I-V

Non-linear I-V observed

Shayegan '93

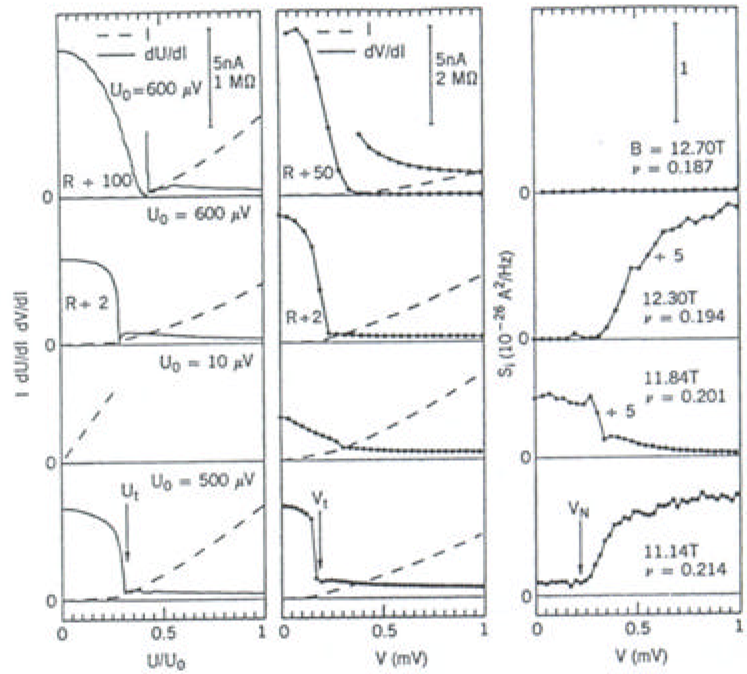

Figure 9.5. (*Top*) B dependence of R_{xx} near $\nu = 1/5$ and the configuration of the sample contacts (inset). (*Bottom*) Current–voltage and noise characteristics: (*left*) four-terminal I and dU/dI versus U (note that U is normalized to the indicated U_0); (*center*) two-terminal I and dV/dI versus V; (*right*) current noise power density S_i averaged between 500 and 775 Hz as a function of V. The data are taken at $T = 22$ mK and at the four B-field values listed in the right panel. (Data from [Li 1991].)

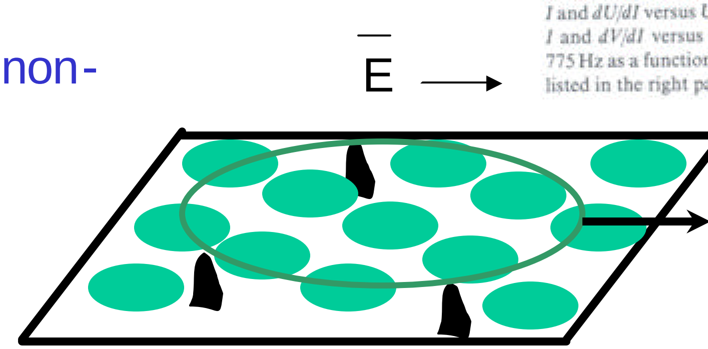

Depinning thresholds and microwave resonances not consistent in models

V. Other parts of the spectrum: from the electron solid to non-equilibrium effects

B. the electron solid?

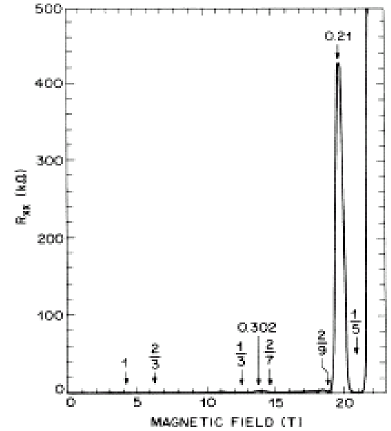

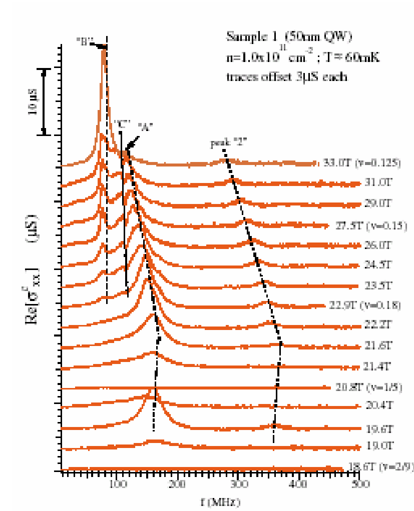

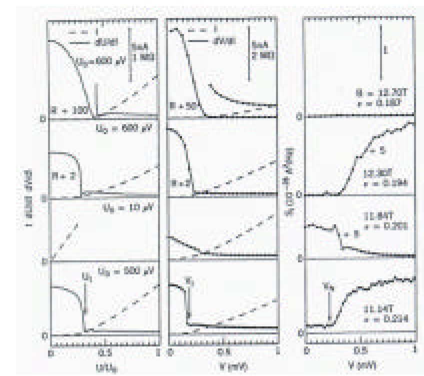

Summary:

1) Insulating state observed at small filling factors
2) Competition between insulating state and fractional quantum Hall states
3) Radio frequency mode observed – broad and high frequency for low mobility, narrow for cleaner samples
4) Non-linear I-V

NO DIRECT OBSERVATION OF ORDERING: we still don't know if we are observing a true ordered electron system or a glass

V. Other parts of the spectrum:
from the electron solid to
non-equilibrium effects

C. Low magnetic fields: response to radiation

Pertinent numbers for small magnetic fields: 0.1T, $1x10^{11}cm^{-2}$

1) Fermi energy 41 K
2) Spin gap 0.03 K
3) Cylotron energy 2.0 K
4) Coulomb energy 16 K
5) Cyclotron radius 5200 Å

With little magnetic field to quench kinetic energy, single particle effects more prominent

V. Other parts of the spectrum:
from the electron solid to
non-equilibrium effects

C. Low magnetic fields: response to radiation

Apply high frequency radiation (50-120GHz)
through waveguide onto 2D electron system and
look at low B-field end

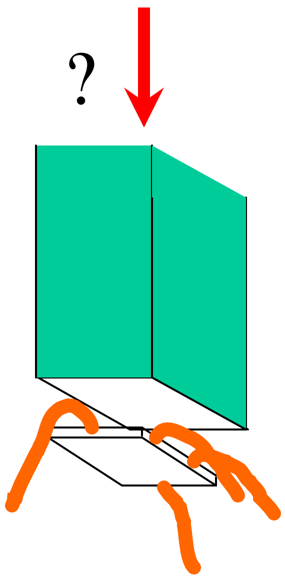

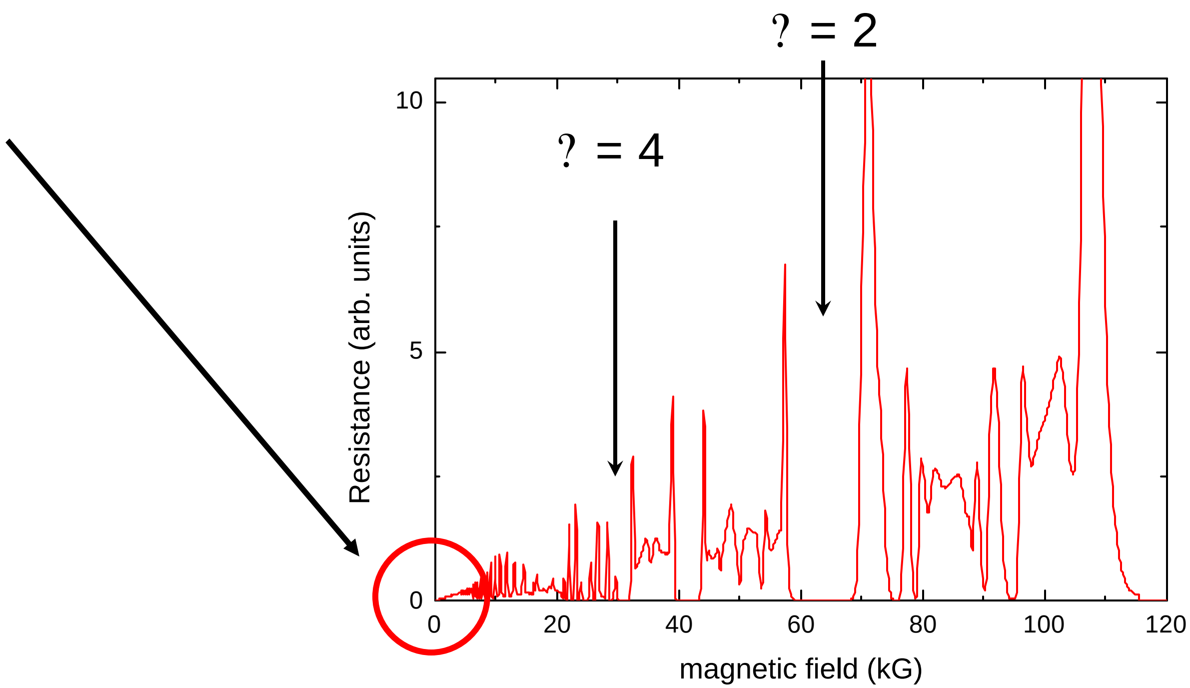

V. Other parts of the spectrum:
from the electron solid to
non-equilibrium effects

C. Low magnetic fields: response to radiation

Zudov PRB ‘01

Upon radiation on a high mobility sample with GHz radiation, **oscillations are observed near zero magnetic field**

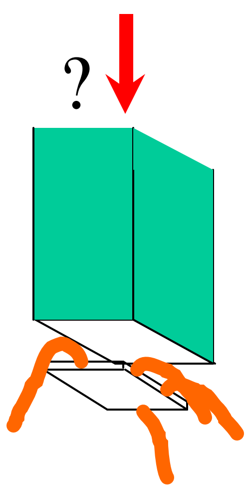

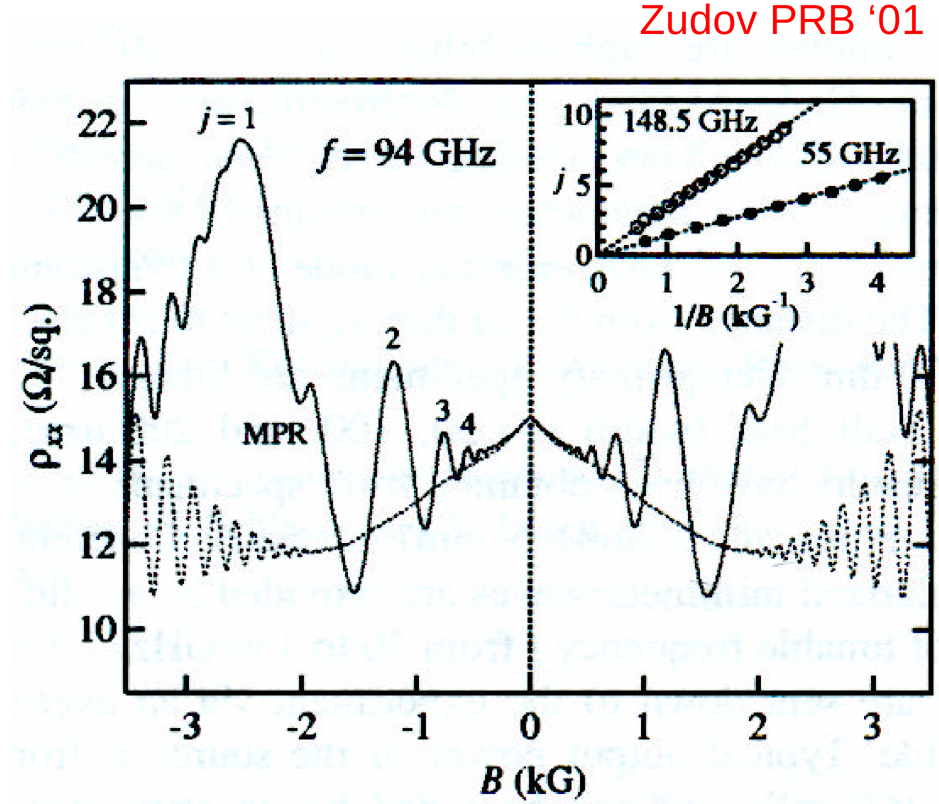

Minima at ? ?? $_{C}$ = j+1/2,
j=1,2,3,…

V. Other parts of the spectrum:
from the electron solid to
non-equilibrium effects

C. Low magnetic fields: response to radiation

Zudov PRB ‘01

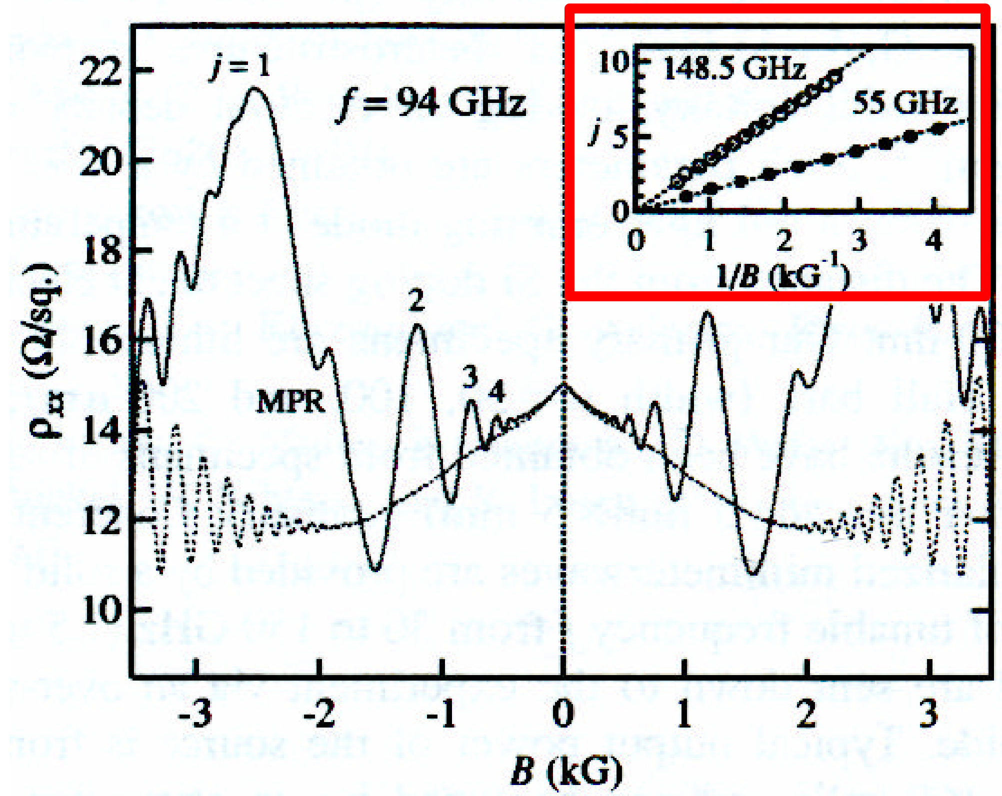

✍oscillations are observed near zero magnetic field

✍minima at ? ?? $_C$ = j+1/2, j=1,2,3,…
(? $_C$ = e/Bm*, m* bare GaAs mass)

✍no dependence upon filling factor (density)

What’s causing this?

Zudov PRL '03

V. Other parts of the spectrum:
from the electron solid to
non-equilibrium effects

C. Low magnetic fields: response to radiation

For higher mobility samples, the minima look like **quantum Hall effect zeroes**

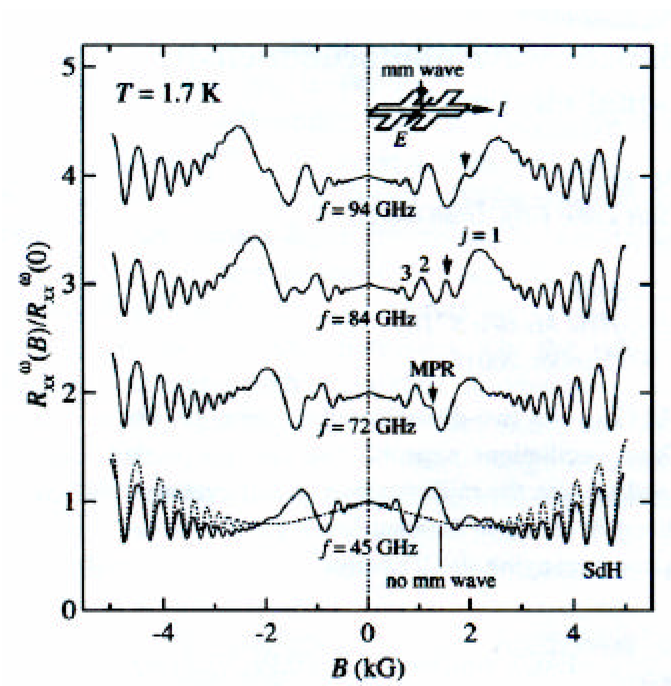

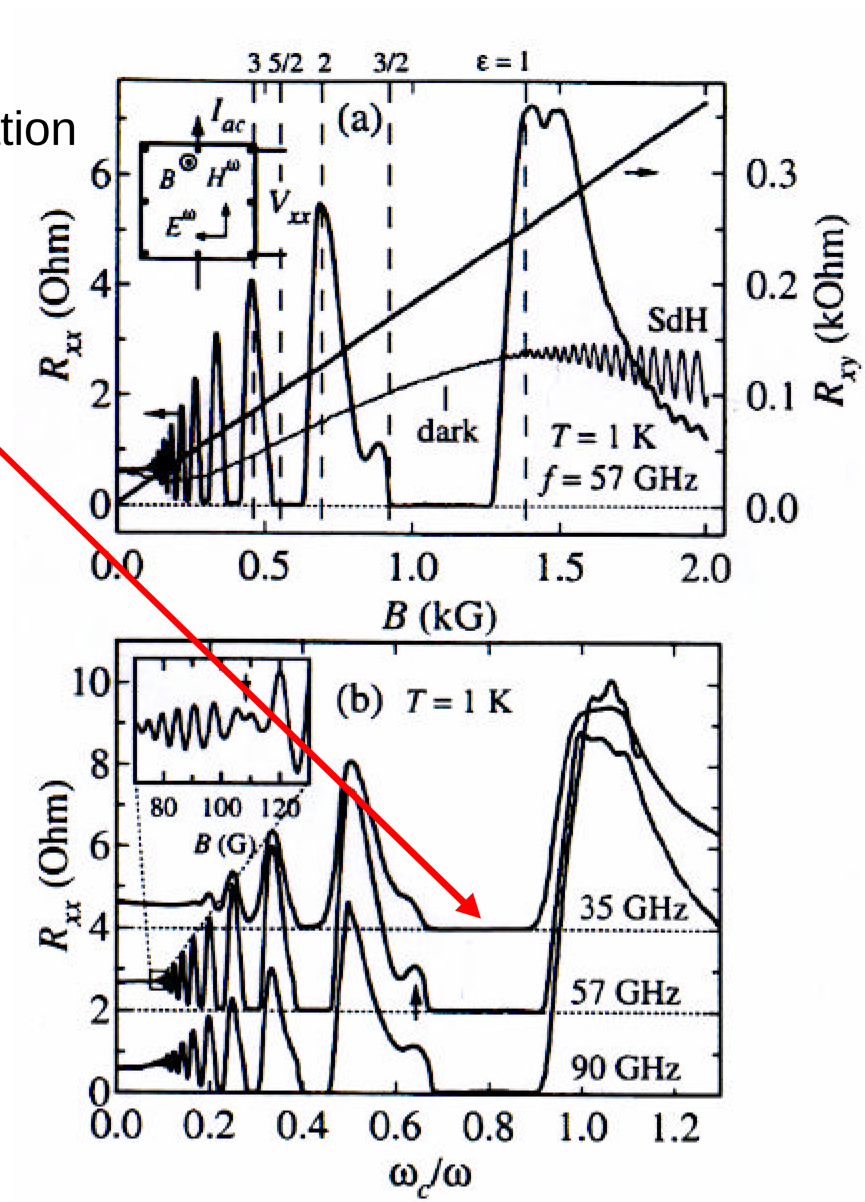

V. Other parts of the spectrum:
from the electron solid to
non-equilibrium effects

C. Low magnetic fields: response to radiation

✍Minima show activated temperature dependence:

consistent with an energy gap

✍Large activation energies:
activation energy E
photon energy $E_?$
E >> $E_?$

Gap energy E~18K, $E_?$~3K
for ? =57GHz, j=1

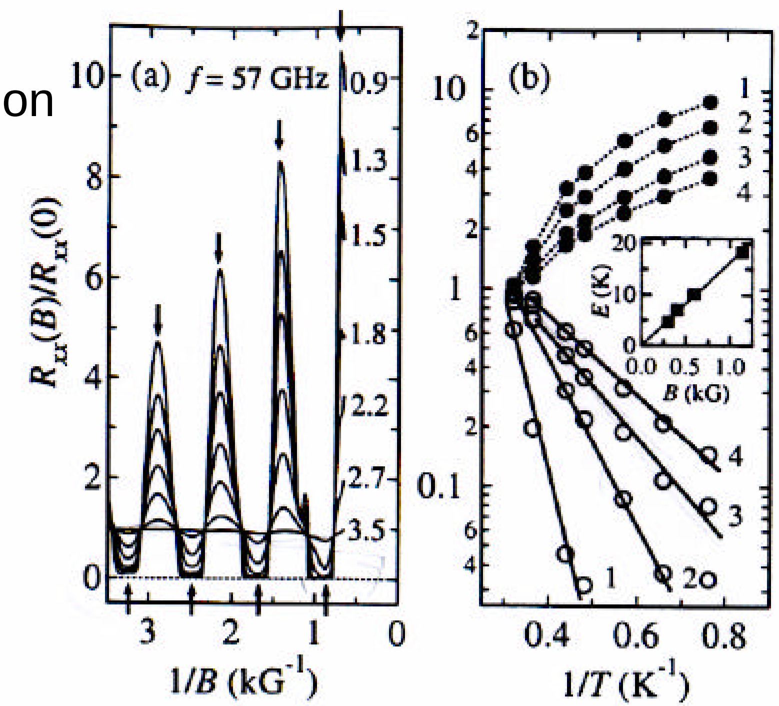

FIG. 2: (a) $R_{xx}(B)/R_{xx}(0)$ under MW (f = 57 GHz) illumination, plotted vs. $1/B$ at different T from 0.9 K to 3.5 K. Upward arrows mark positions of the minima suggesting a roughly periodic series in $1/B$. (b) $R_{xx}(B)/R_{xx}(0)$ at the minima series (open circles) and at the j = 1, 2, 3, and 4 maxima series (solid circles), as a function of $1/T$. Solid lines are fits to $R_{xx}(T) \propto \exp(-E/T)$. The inset shows the values of the fitting parameter E as a function of B revealing roughly linear dependence with a slope of $\simeq$ 18 K/kG.

Zudov PRL '03, see also Mani Science '03

V. Other parts of the spectrum:
from the electron solid to
non-equilibrium effects

C. Low magnetic fields: response to radiation

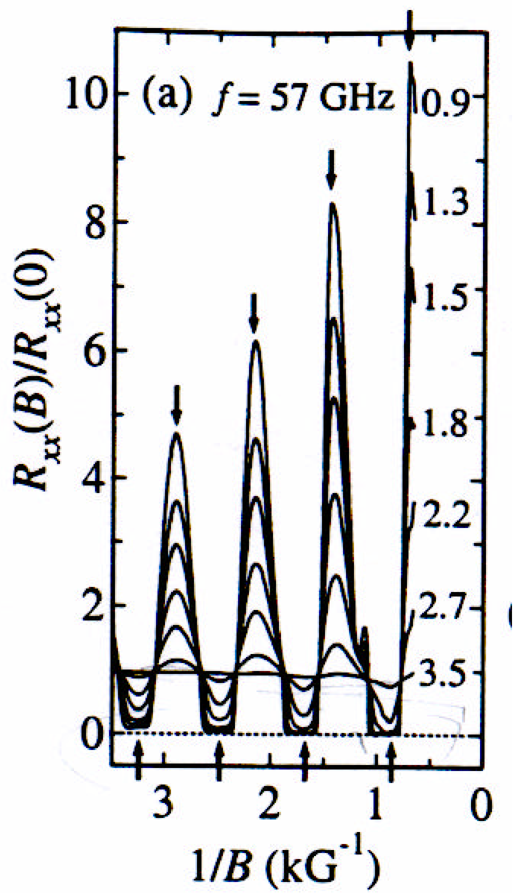

Zudov PRL ’03, see also Mani Science ‘03

✍what causes the oscillations?
✍what causes the zeroes?

V. Other parts of the spectrum:
from the electron solid to
non-equilibrium effects

C. Low magnetic fields:
response to radiation

Further work showed that oscillations can be observed at lower frequencies, revealing same physics

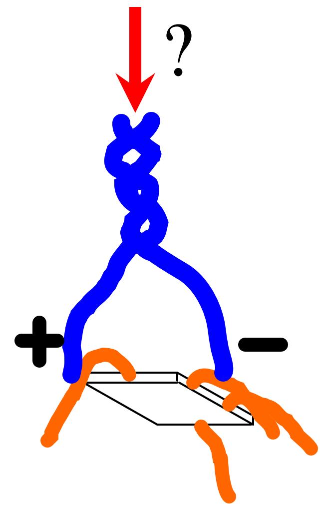

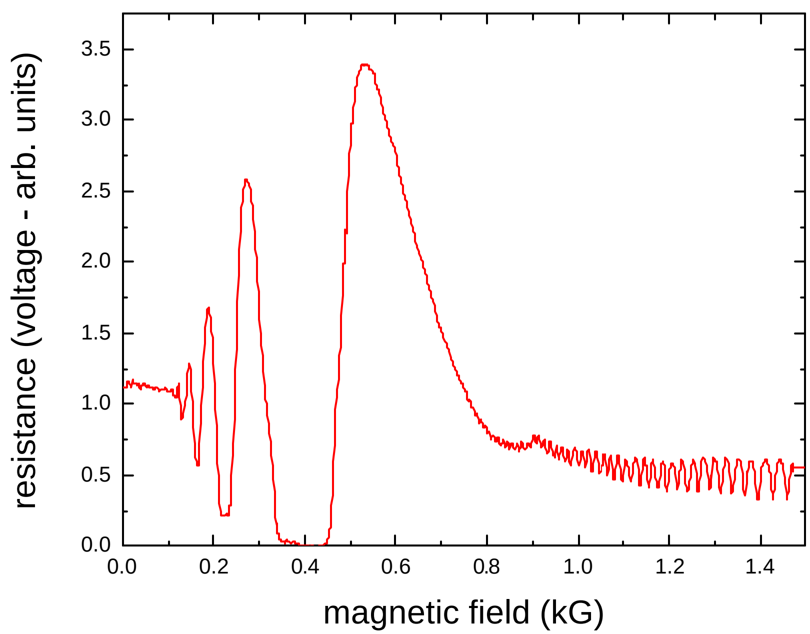

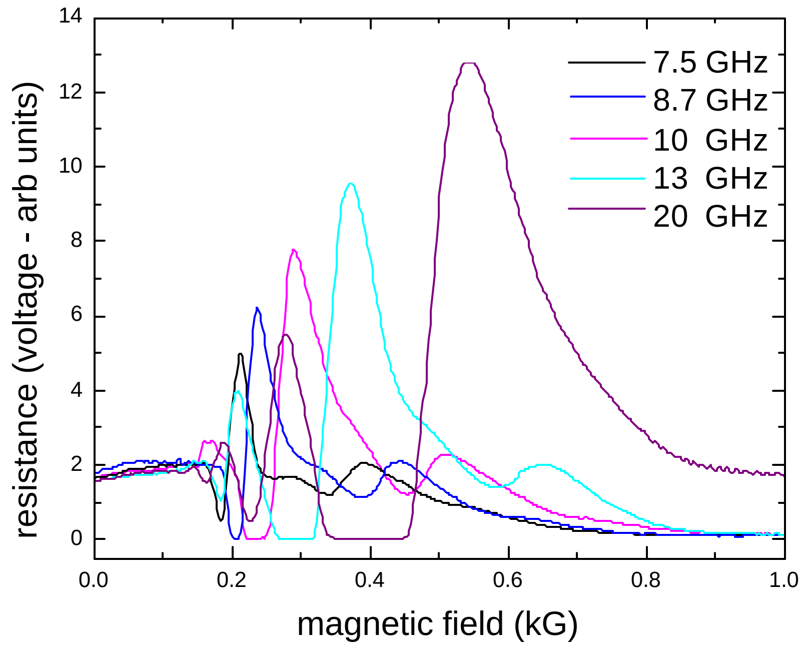

RLW PRL '04

V. Other parts of the spectrum:
from the electron solid to
non-equilibrium effects

C. Low magnetic fields:
response to radiation

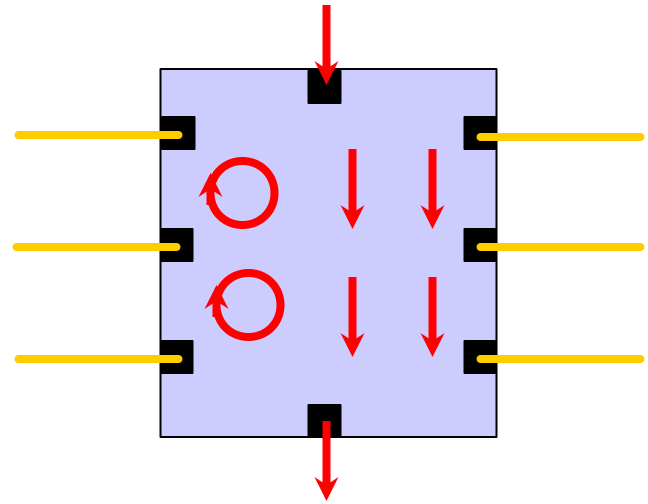

Using lower frequencies, consider possible anomalous current paths due to radiation

V. Other parts of the spectrum:
from the electron solid to
non-equilibrium effects

C. Low magnetic fields:
response to radiation

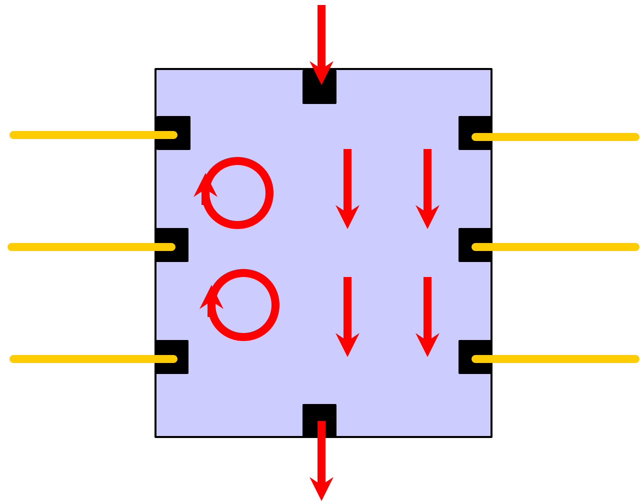

Using lower frequencies, consider possible anomalous current paths due to radiation

By looking at different contact configurations around samples, found

Zeroes not always zeroes

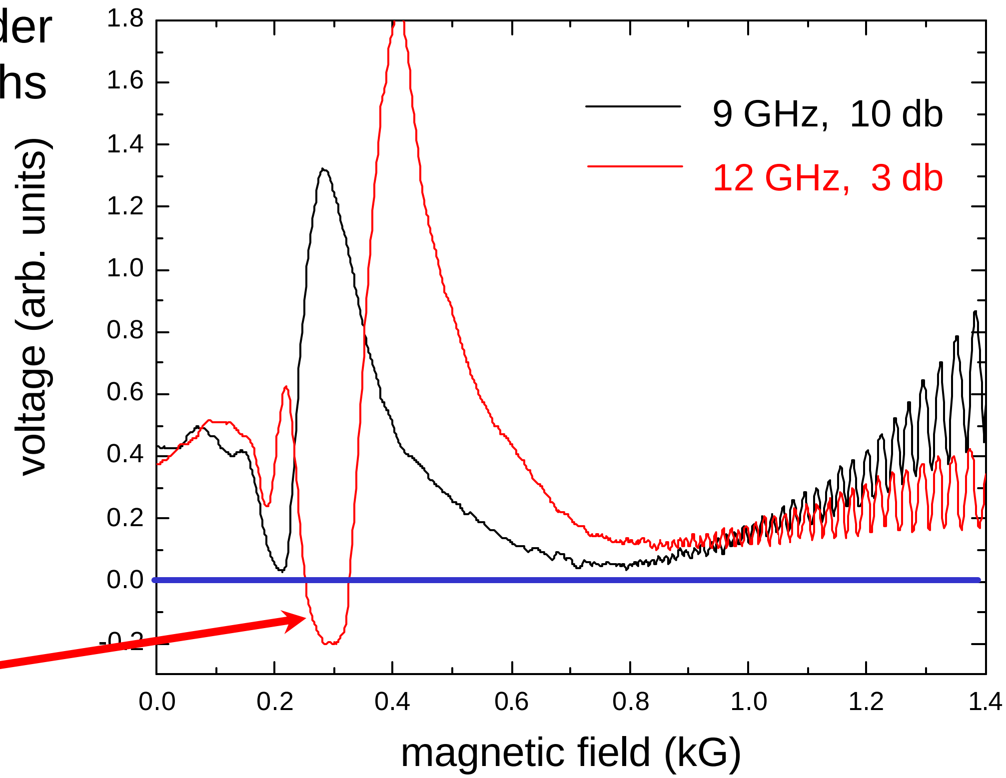

RLW PRL '04

V. Other parts of the spectrum:
from the electron solid to
non-equilibrium effects

C. Low magnetic fields:
response to radiation

Using lower frequencies, consider possible anomalous current paths due to radiation

By looking at different contact configurations around samples, found

Zeroes not always zeroes

Common structure
in non-zeroes

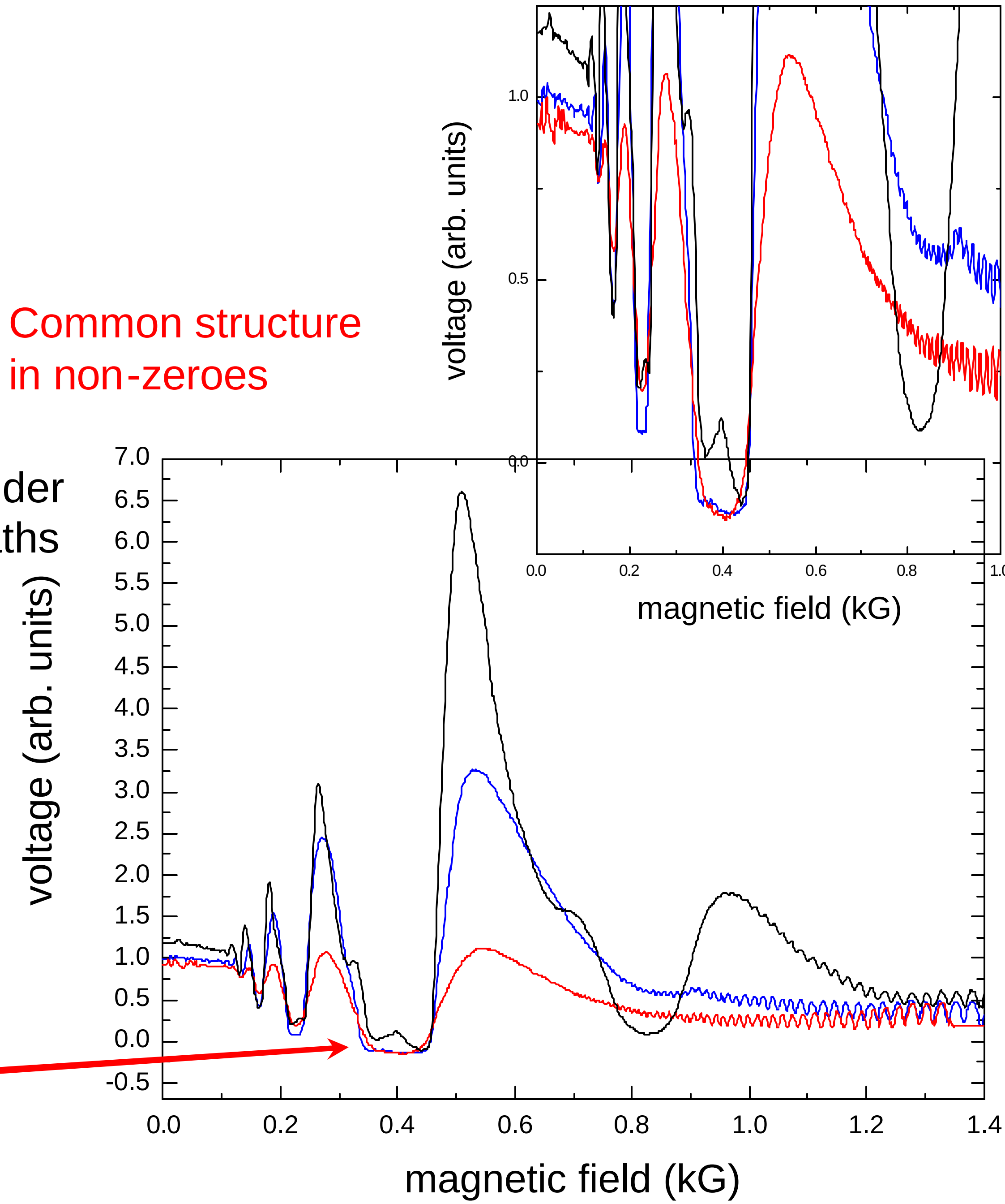

RLW PRL ‘04

V. Other parts of the spectrum: from the electron solid to non-equilibrium effects

C. Low magnetic fields: response to radiation

Consider possible anomalous current paths due to radiation

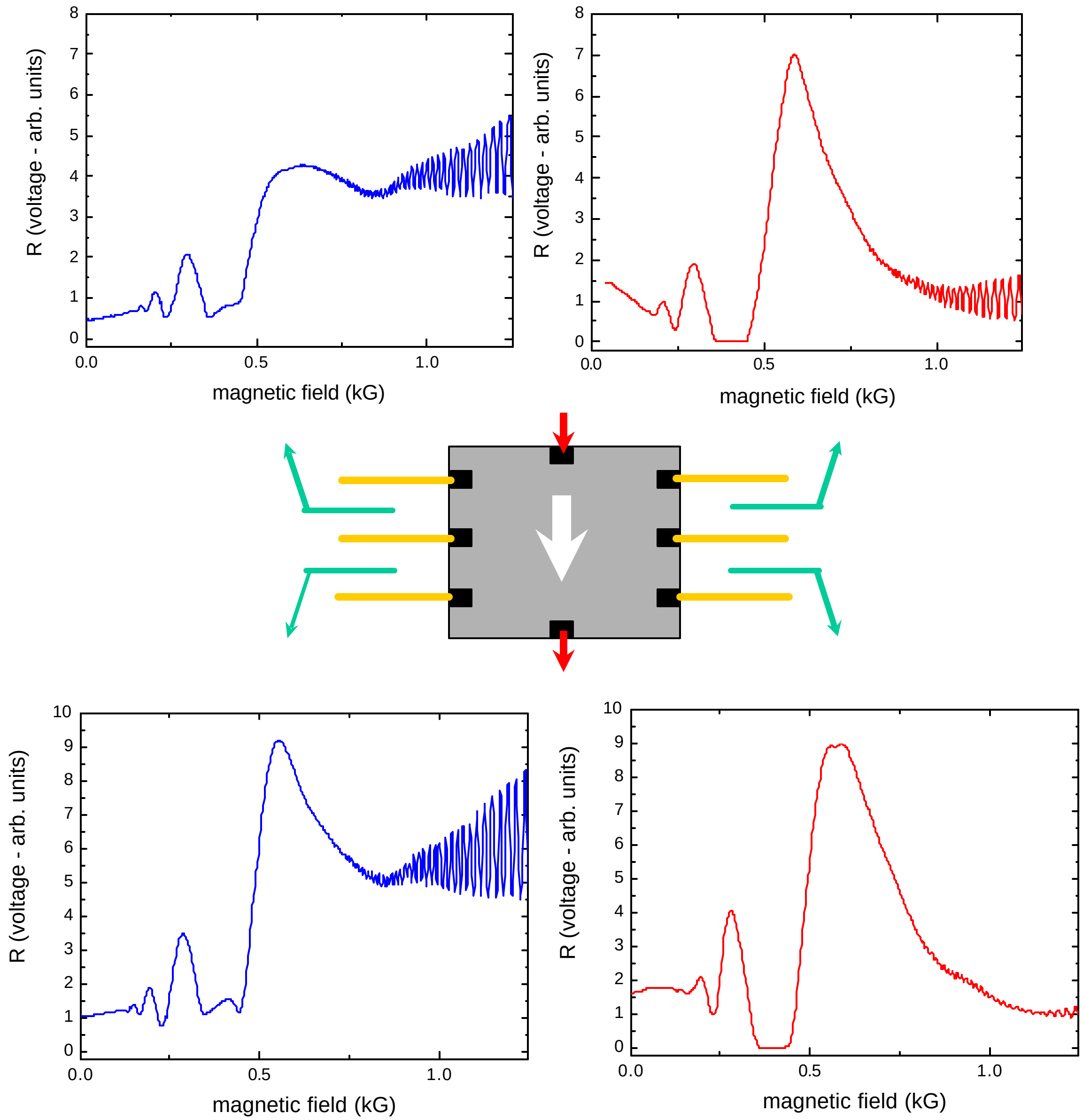

In addition to non-zeroes, found

systematic differences in zeroes around sample perimeter

V. Other parts of the spectrum:
from the electron solid to
non-equilibrium effects

C. Low magnetic fields: response to radiation

In addition to non-zeroes, found

systematic differences in zeroes around sample perimeter

And anomalous response to reversing B-field

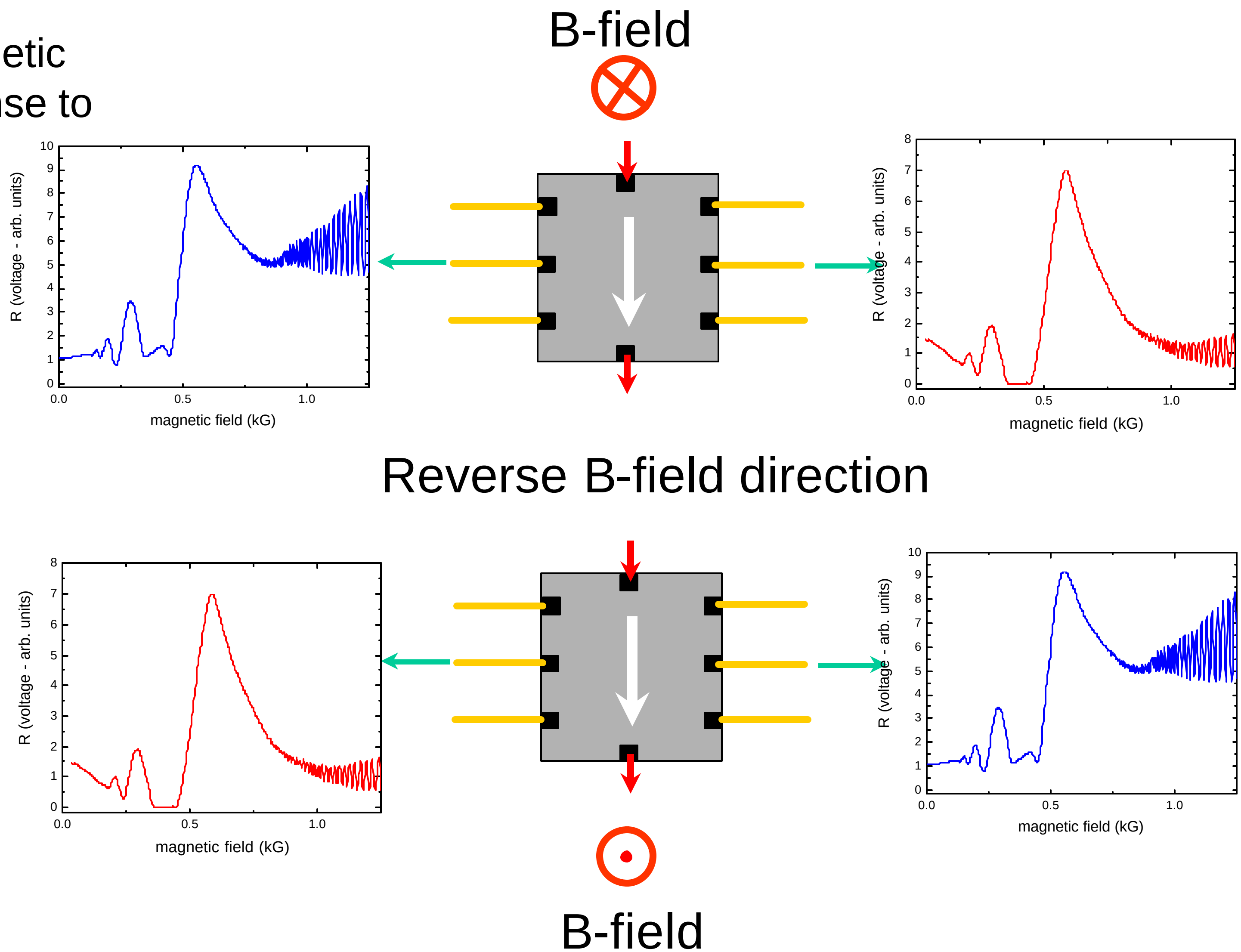

V. Other parts of the spectrum: from the electron solid to non-equilibrium effects

C. Low magnetic fields: response to radiation

Clearly odd current paths at work

In addition to non-zeroes, found

systematic differences in zeroes around sample perimeter

And anomalous response to reversing B-field

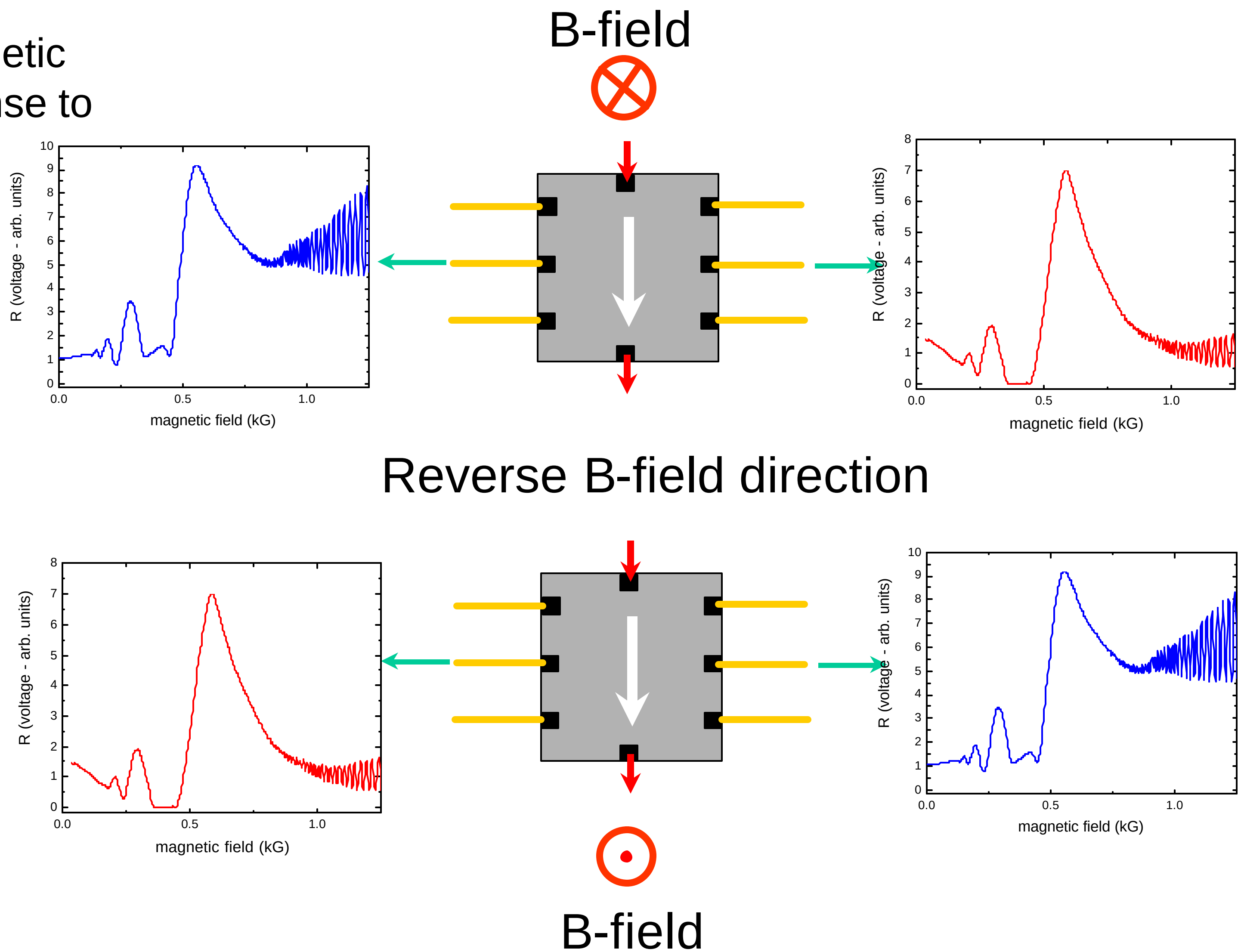

V. Other parts of the spectrum:
from the electron solid to
non-equilibrium effects

C. response to radiation:
Theory of oscillations

Among many,
two theories developed to explain
radiation induced magneto-oscillations:

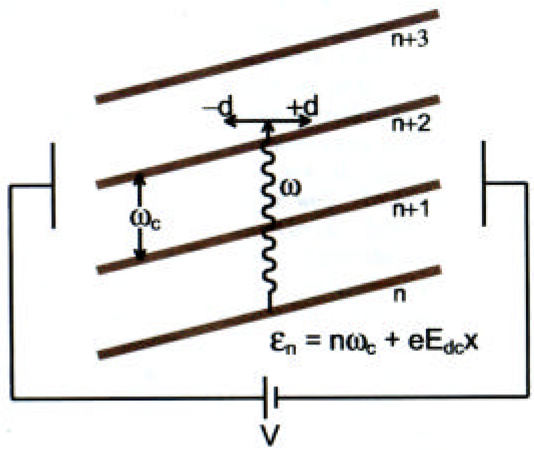

FIG. 1: Simple picture of radiation-induced disorder-assisted current. Landau levels are tilted by the applied dc bias. Electrons absorb photons and are excited by energy ω. Photo-excited electrons are scattered by disorder and kicked to the right or to the left by a distance $\pm d$. If the density of states to the left exceeds that to the right, current is enhanced. If vice versa, current is diminished.

1) Radiation induced,
disorder assisted current

Durst, et. al. PRL '03

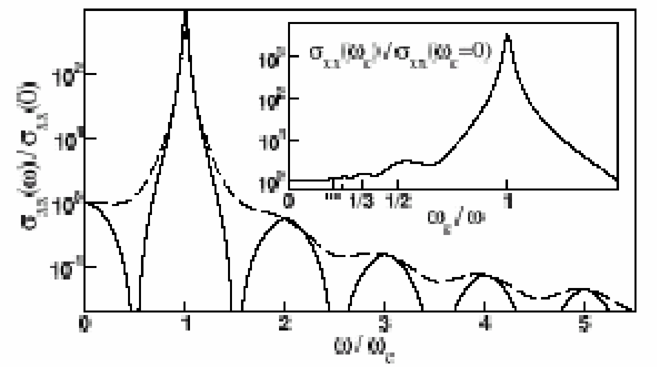

FIG. 2. Magneto-oscillations of the dynamical conductivity for a system with smooth disorder, $\tau_{tr,0}/\tau_{s,0} = 10$. Solid line: separated LLs, $\omega_c\tau_{s,0}/\pi = 3.25$; dashed line: overlapping LLs, $\omega_c\tau_{s,0}/\pi = 1$. Inset: σ_{xx} for fixed $\omega\tau_{s,0}/2\pi = 1$ as a function of ω_c.

Cyclotron-Resonance Harmonics in the ac Response of a 2D Electron Gas with Smooth Disorder

I. A. Dmitriev,[1,*] A. D. Mirlin,[1,2,†] and D. G. Polyakov[1,*]

[1]*Institut für Nanotechnologie, Forschungszentrum Karlsruhe, 76021 Karlsruhe, Germany*
[2]*Institut für Theorie der Kondensierten Materie, Universität Karlsruhe, 76128 Karlsruhe, Germany*

(Received 23 April 2003; published 24 November 2003)

The frequency-dependent conductivity $\sigma_{xx}(\omega)$ of 2D electrons subjected to a transverse magnetic field and smooth disorder is calculated. The interplay of Landau quantization and disorder scattering gives rise to an oscillatory structure that survives in the high-temperature limit. The relation to recent experiments on photoconductivity by Zudov *et al.* and Mani *et al.* is discussed.

2) Radiation induces change in electron
distribution function

Dmitriev, et al. PRL '03

V. Other parts of the spectrum:
from the electron solid to
non-equilibrium effects

C. response to radiation: Theory of oscillations

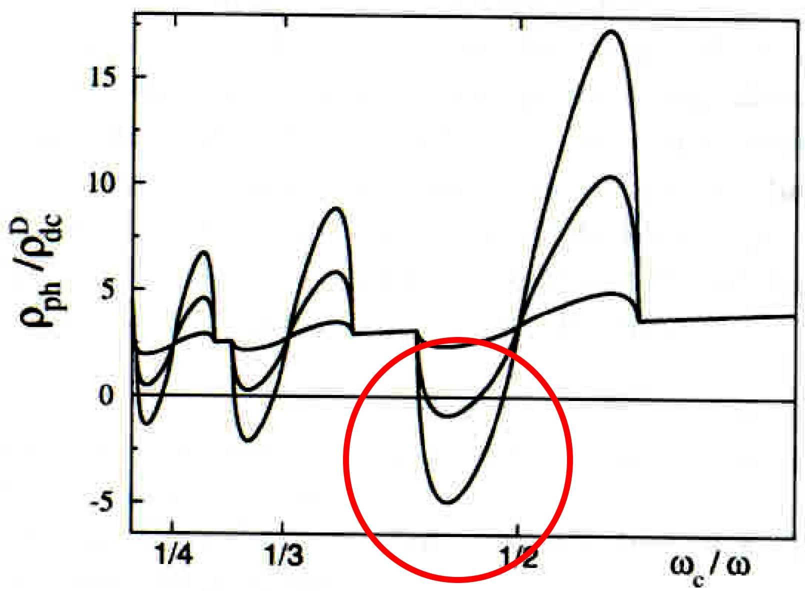

FIG. 3. Photoresistivity (normalized to the dark Drude value) for separated Landau levels vs ω_c/ω at fixed $\omega\tau_q = 16\pi$. The curves correspond to different levels of microwave power $\mathcal{P}_\omega^{(0)} = \{0.004, 0.02, 0.04\}$.

Both theories deduce

a) Oscillatory resistivity with period ~1/B

b) negative local microscopic resistivity due to radiation

✍ Magneto-oscillations covered

Dmitriev, et al. cond-mat/0310668

V. Other parts of the spectrum: from the electron solid to non-equilibrium effects

C. response to radiation: Theory of zeroes

Dynamical Symmetry Breaking as the Origin of the Zero-dc-Resistance State in an ac-Driven System

A.V. Andreev,[1,2] I. L. Aleiner,[3] and A. J. Millis[3]
[1]*Physics Department, University of Colorado, Boulder, Colorado 80309, USA*
[2]*Bell Labs, Lucent Technologies, Room 1D-267, Murray Hill, New Jersey 07974, USA*
[3]*Physics Department, Columbia University, New York, New York 10027, USA*
(Received 3 February 2003; published 1 August 2003)

Under a strong ac drive the zero-frequency linear response dissipative resistivity $\rho_d(j=0)$ of a homogeneous state is allowed to become negative. We show that such a state is absolutely unstable. The only time-independent state of a system with a $\rho_d(j=0)<0$ is characterized by a current which almost everywhere has a magnitude j_0 fixed by the condition that the nonlinear dissipative resistivity $\rho_d(j_0^2)=0$. As a result, the dissipative component of the dc-electric field vanishes. The total current may be varied by rearranging the current pattern appropriately with the dissipative component of the dc-electric field remaining zero. This result, together with the calculation of Durst *et al.*, indicating the existence of regimes of applied ac microwave field and dc magnetic field where $\rho_d(j=0)<0$, explains the zero-resistance state observed by Mani *et al.* and Zudov *et al.*.

any microscopic mechanism of nonequilibrium drive resulting in $\rho_d(j^2=0)<0$ leads to the observed [1,2] *zero dissipative differential resistance*:

$$\frac{dV_x}{dI_{dc}} = 0. \tag{5}$$

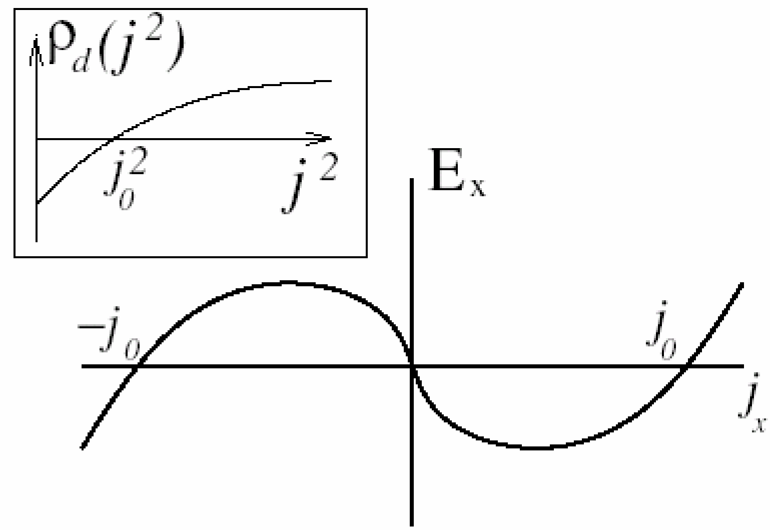

FIG. 1. Assumed dependence of the dissipative (parallel to current) component of the local electric field E_x on the current density j_x. Inset: dependence of the dissipative resistivity on the square of the current.

Negative local resistivity explains the zeroes:

system unstable with ?<0, current circulations form

Andreev, et al. PRL ‘03

V. Other parts of the spectrum:
from the electron solid to
non-equilibrium effects

C. response to radiation: Theory of oscillations

Negative local resistivity explains the zeroes:

system unstable with ?<0:
current circulations form.
These spontaneous current domains can result in the observed zero resistance.

Suggested to try to examine voltage drop from inner to outer contacts

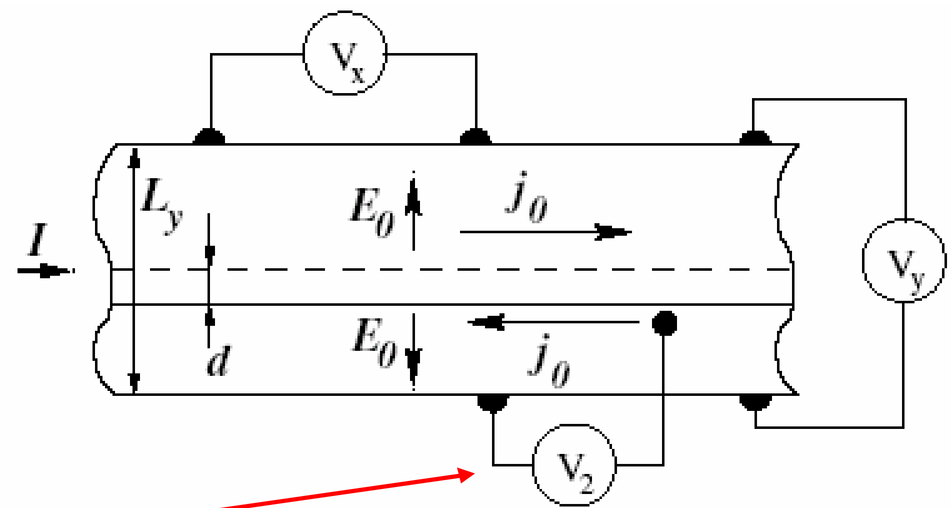

FIG. 2. The simplest possible pattern of the current distribution—domain wall. The net current, I, is accommodated by a shift of the position of the domain wall by the distance d; see text. The electric field in the domain is $E_0 = \rho_H j_0$. The current pattern in the Corbino disc geometry is obtained by connecting the broken edges into a ring.

Andreev, et al. PRL ‘03

V. Other parts of the spectrum:
from the electron solid to
non-equilibrium effects

C. response to radiation:

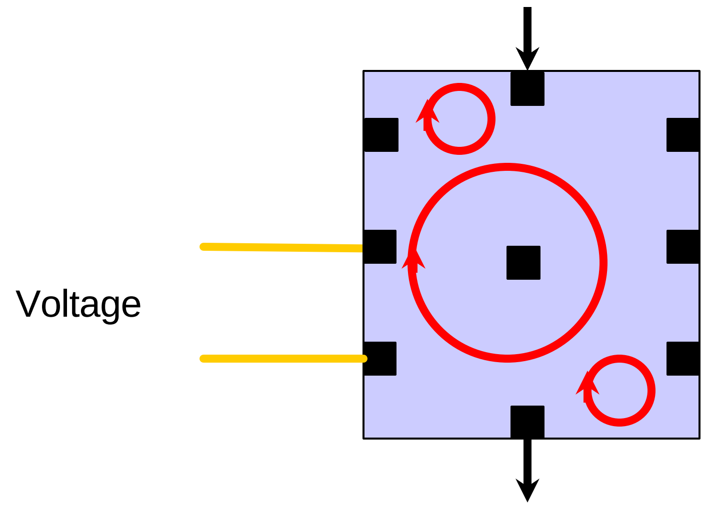

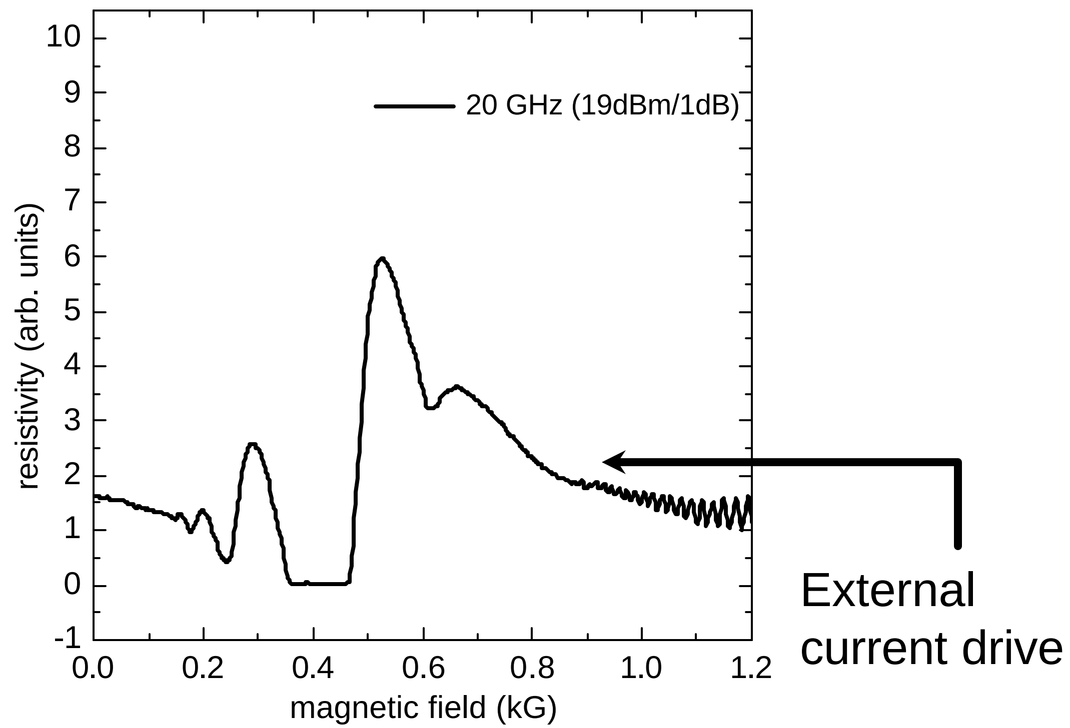

V. Other parts of the spectrum: from the electron solid to non-equilibrium effects

C. Low magnetic fields: response to radiation

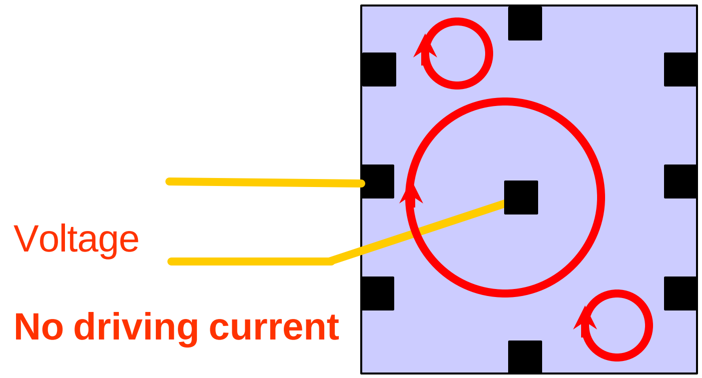

Currents induced by radiation:

No current driven through sample from external source, yet voltage pickup from internal to external contact

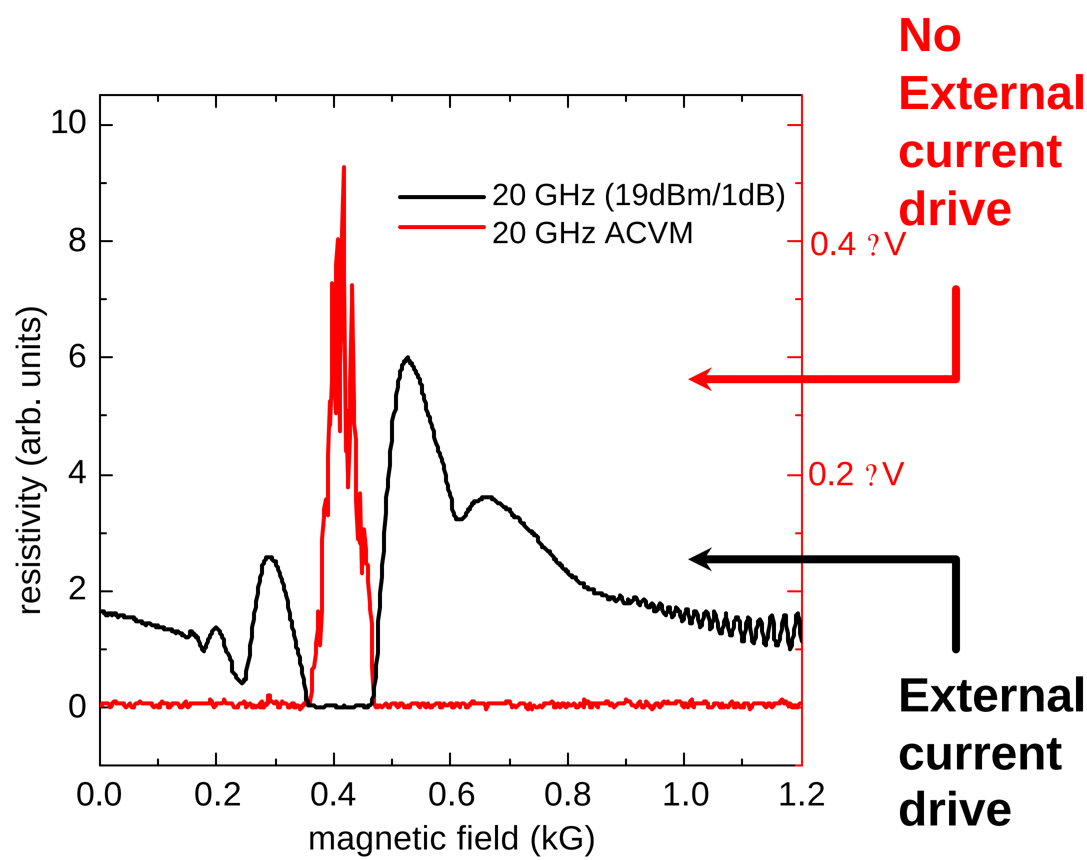

V. Other parts of the spectrum: from the electron solid to non-equilibrium effects

C. response to radiation: experiment and theory of zeroes

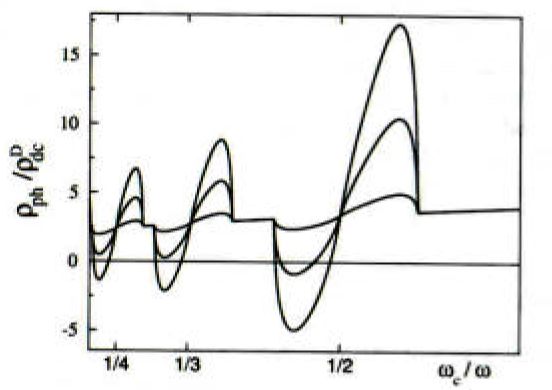

Microscopic
? ≺ 0

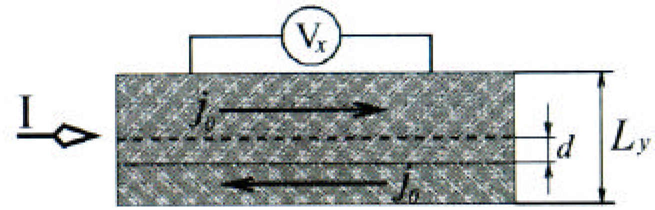

FIG. 2: The simplest possible pattern of the current distribution – domain wall. The net current, I, is accommodated by a shift of the position of the domain wall by the distance d, see text.

Negative local resistivity explains the zeroes:

system unstable with ?<0, current circulations form

Vortices within the sample, induced by the radiation, and if large enough potentially detectable

These may be observed in experiments

Macroscopic currents

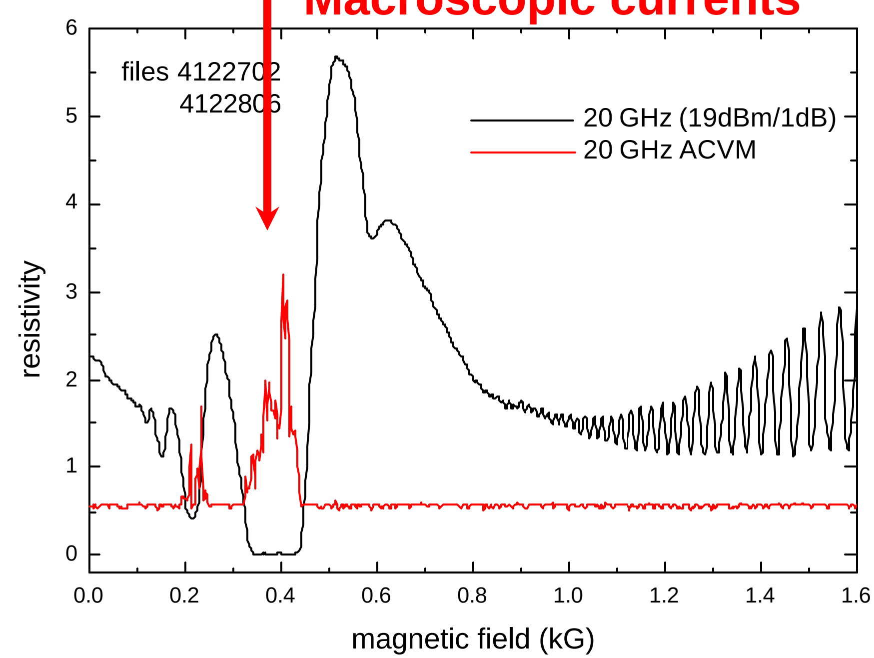

V. Other parts of the spectrum:
from the electron solid to
non-equilibrium effects

C. Low magnetic fields:
response to radiation

Summary:

1) Resistance oscillations of period ~? ??$_c$ occur with GHz radiaiton
2) Higher mobility samples show zeroes in oscillation minima
3) oscillations explained as due to non-equilibrium electron distribution function
4) Negative local resistivity can result, these induce current vortices
5) Current vortices observed experimentally as induced sample voltages

Outline:

I. Introduction: materials, transport, Hall effects

II. Composite particles – FQHE, statistical transformations

III. Quasiparticle charge and statistics

IV. Higher Landau levels

V. Other parts of spectrum: non-equilibrium effects, electron solid?

VI. Multicomponent systems: Bilayers

   A. Overview - materials
   B. Experiments – drag, tunneling, QHE
   C. Recent experiments and excitonic Bose-Einstein condensation

For review see also J.P. Eisenstein, Les Houches ‘04

VI. Multicomponent systems: bilayers

A. materials

To produce a bilayer system make two AlGaAs wells: the important parameters now are the well separation d and the electron separation l_o.

Interesting physics when d close to l_o, so that d is < 20nm.

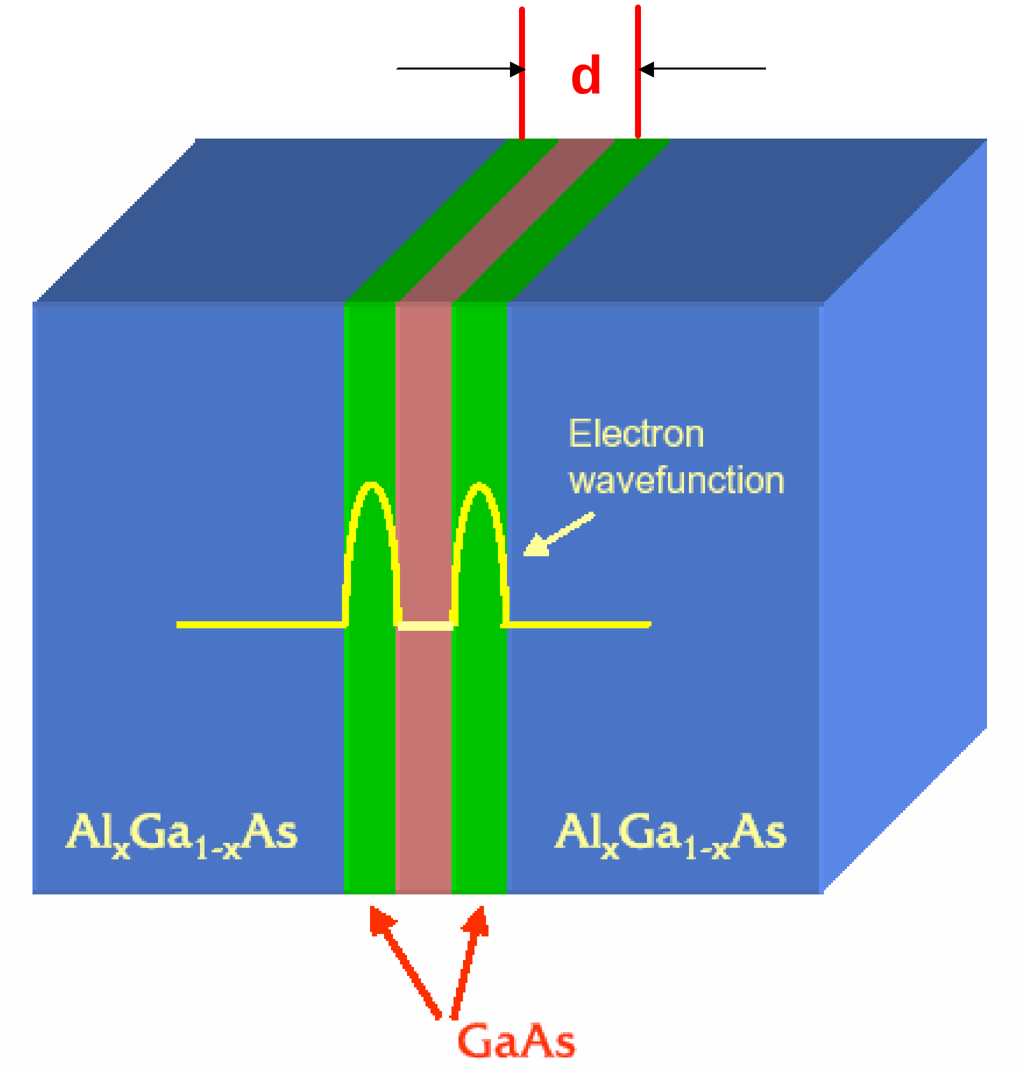

VI. Multicomponent systems: bilayers

A. materials

To produce a bilayer system make two AlGaAs wells: the important parameters now are the well separation d and the electron separation l_o.

AlAs barrier is *dirty*. This limits mobility of the individual layers.

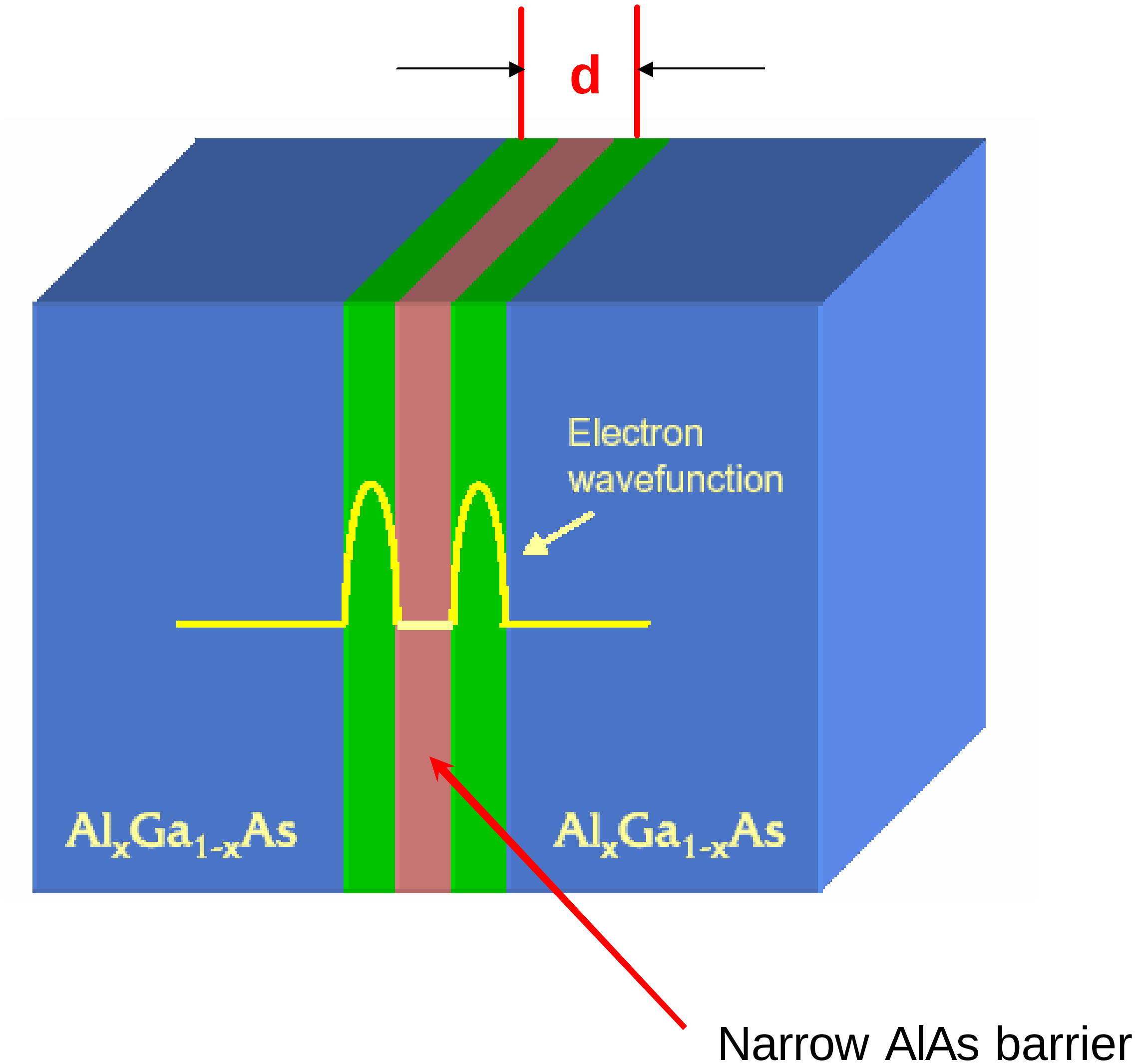

Typical GaAs layer thickness 20nm, AlAs thickness 3nm

VI. Multicomponent systems: bilayers

A. materials

In producing such a structure, the problem of the reverse interface is confronted: a smoother surface occurs when growing from GaAs to AlGaAs than from AlGaAs to GaAs.

This fact and the necessary doping scheme mean that the mobilities for these bilayer structures are not as high as for the single interface structures.

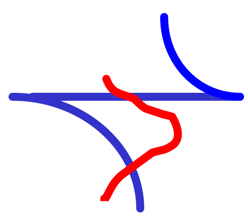

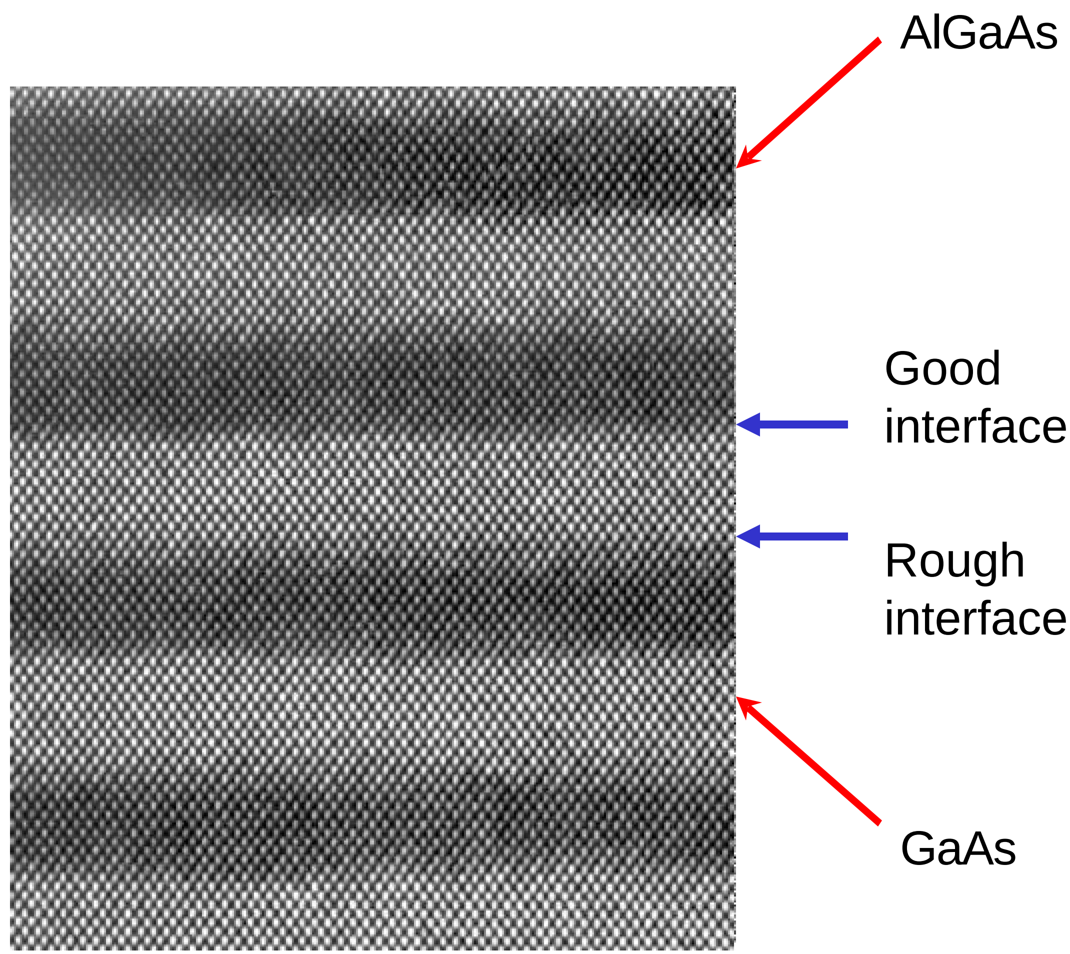

VI. Multicomponent systems: bilayers

A. materials

Experimentally need to contact the layers independently to really study the interactions between the two layers.

Use a set of gates on the top and on the bottom of the sample to accomplish this.

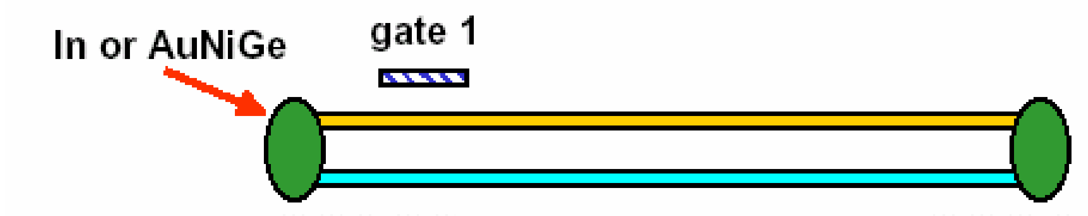

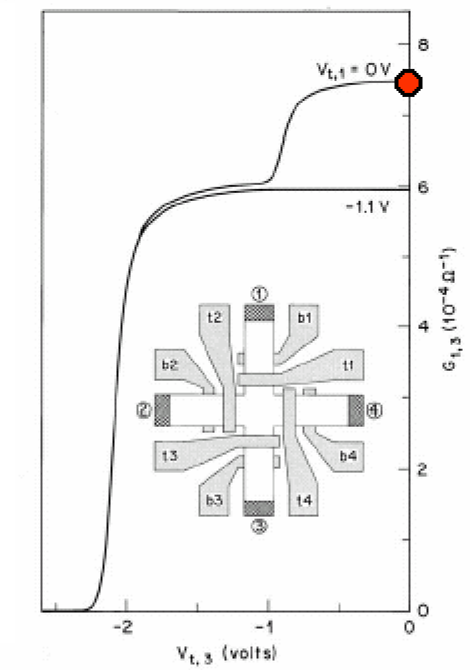

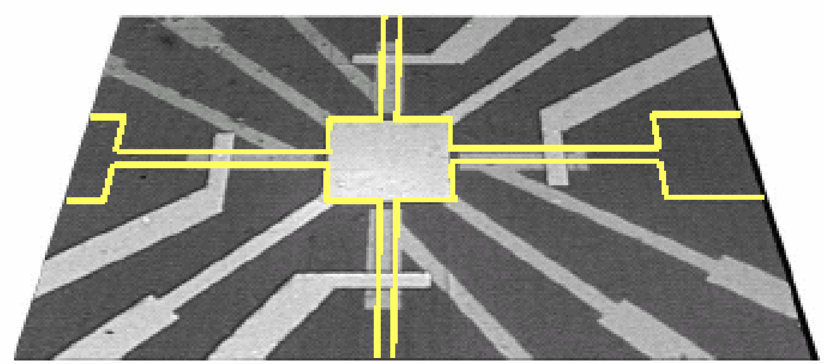

Gramilla '91

VI. Multicomponent systems: bilayers

A. materials

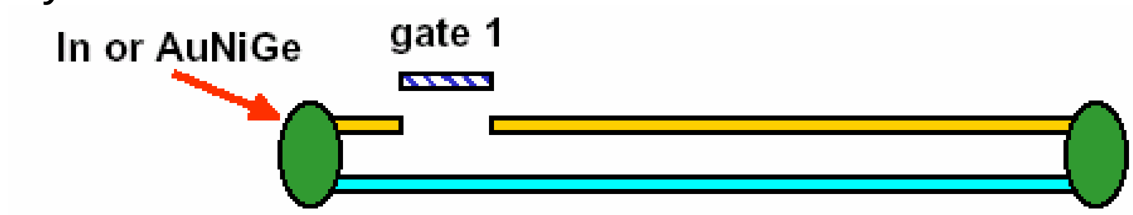

Experimentally need to contact the layers independently to really study the interactions between the two layers.

Use a set of gates on the top and on the bottom of the sample to accomplish this.

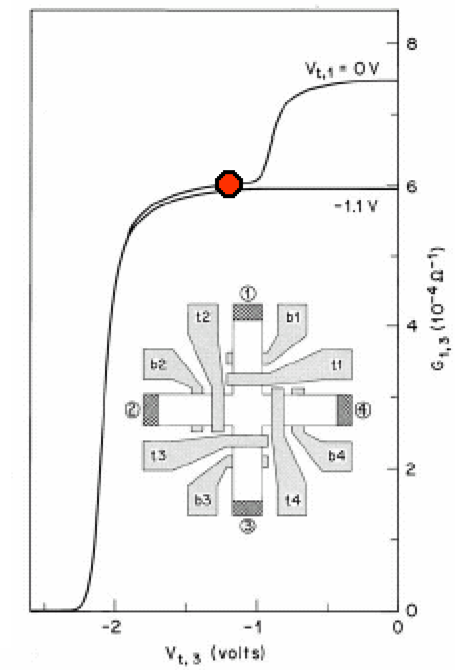

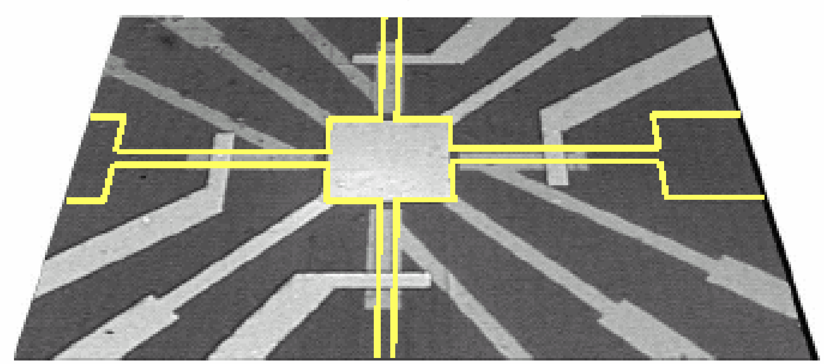

Gramilla '91

VI. Multicomponent systems: bilayers

A. materials

Experimentally need to contact the layers independently to really study the interactions between the two layers.

Use a set of gates on the top and on the bottom of the sample to accomplish this.

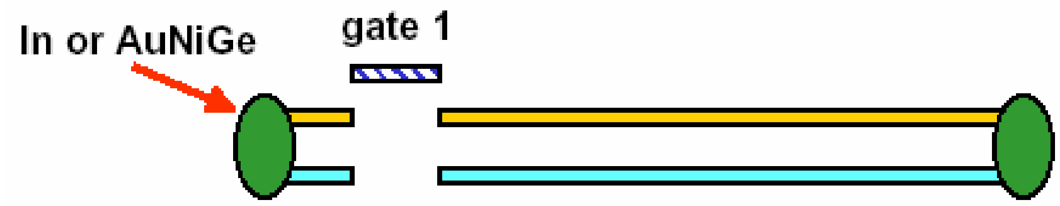

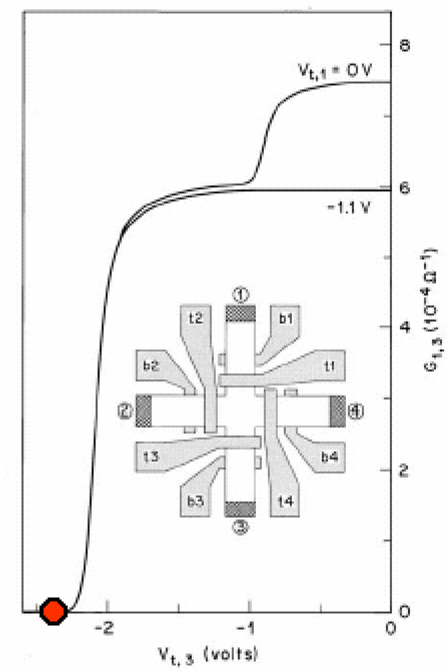

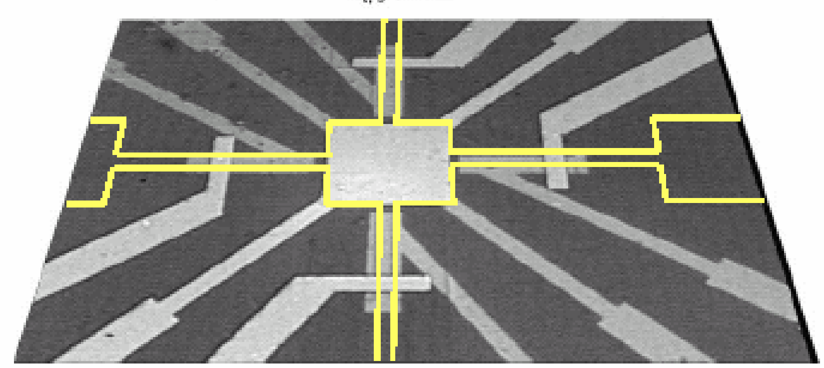

Gramilla '91

VI. Multicomponent systems: bilayers

A. materials

Experimentally need to contact the layers independently to really study the interactions between the two layers.

Use a set of gates on the top and on the bottom of the sample to accomplish this.

Backgating possible by allignment through sample

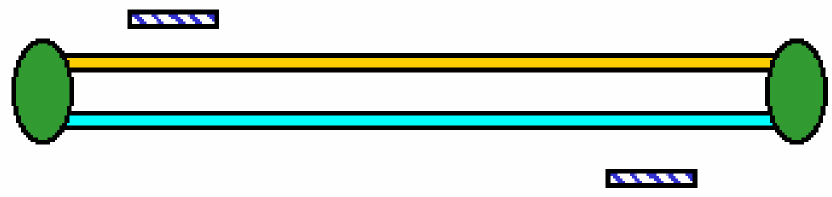

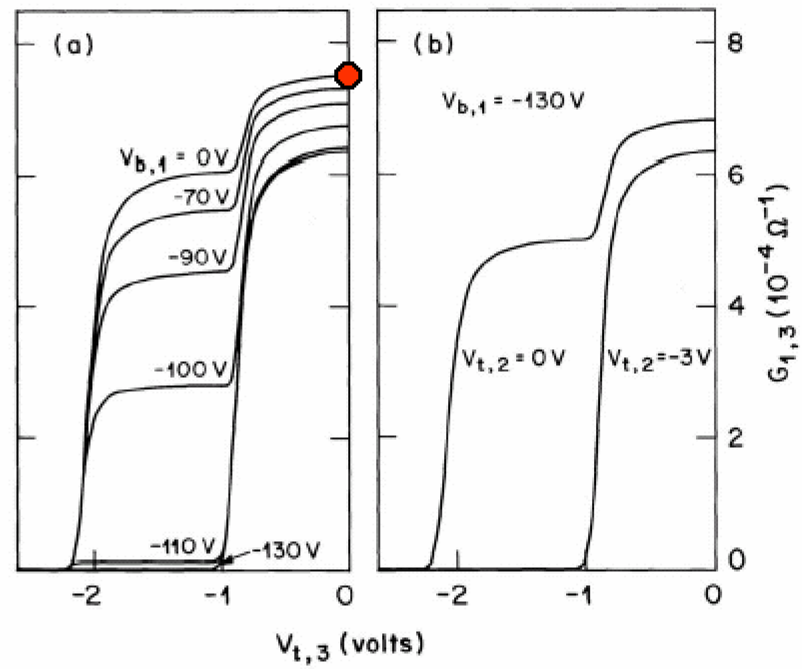

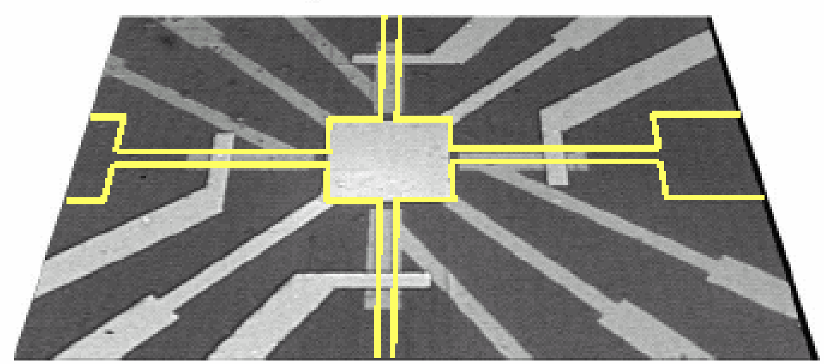

Gramilla ‘91

VI. Multicomponent systems: bilayers

A. materials

Experimentally need to contact the layers independently to really study the interactions between the two layers.

Use a set of gates on the top and on the bottom of the sample to accomplish this.

Backgating possible by allignment through sample

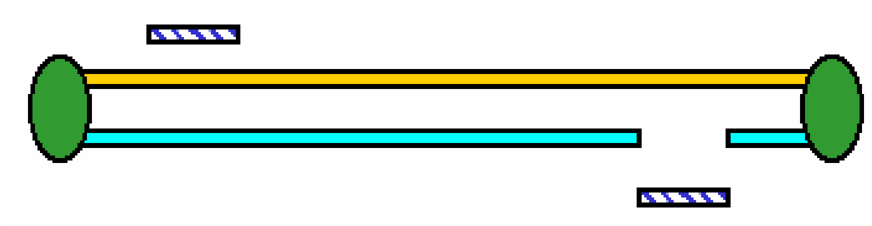

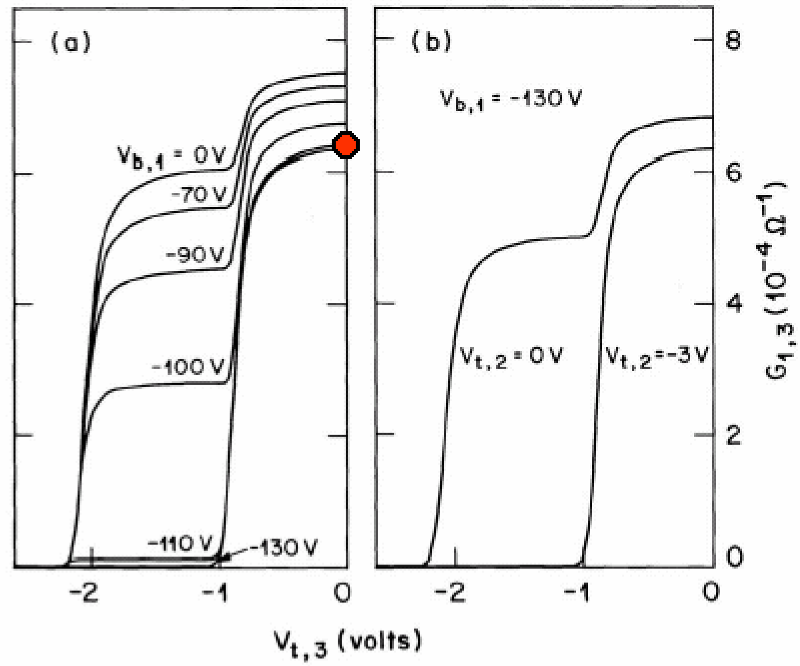

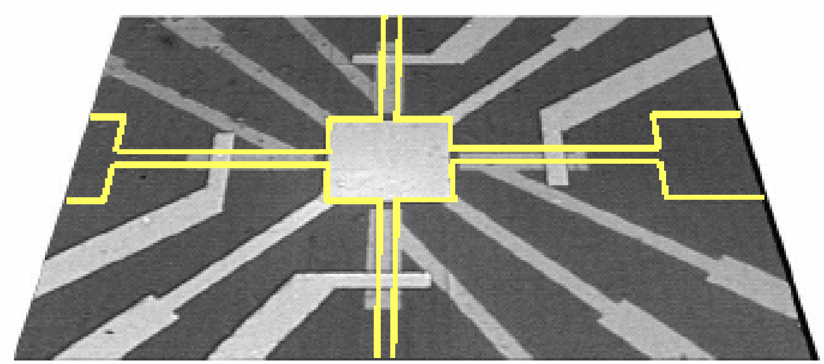

Gramilla '91

VI. Multicomponent systems: bilayers

A. materials

Experimentally need to contact the layers independently to really study the interactions between the two layers.

Use a set of gates on the top and on the bottom of the sample to accomplish this.

Backgating possible by allignment through sample

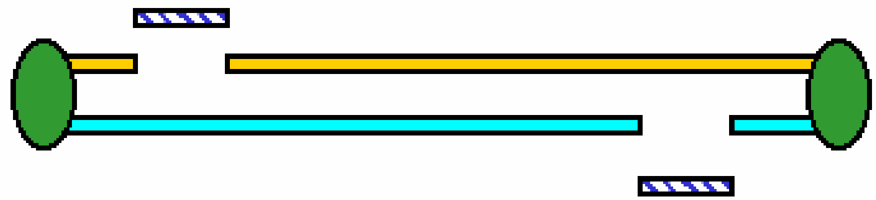

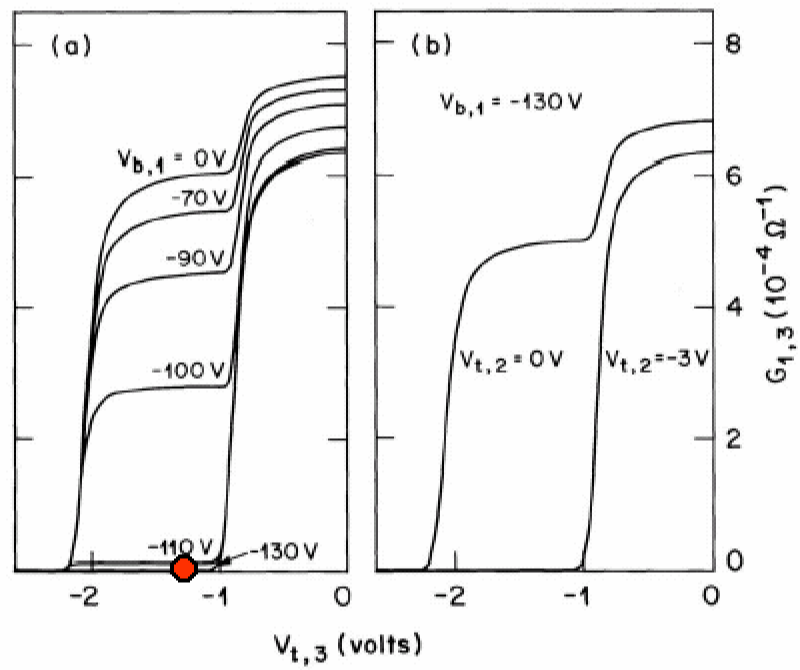

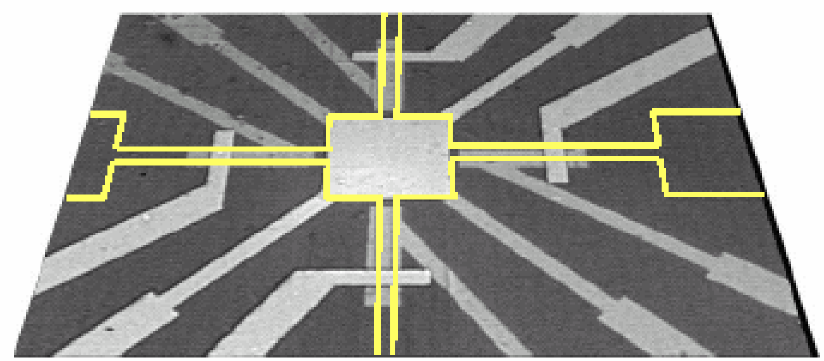

Gramilla '91

VI. Multicomponent systems: bilayers

A. materials

Independent contacting facilitates a series of experiments:

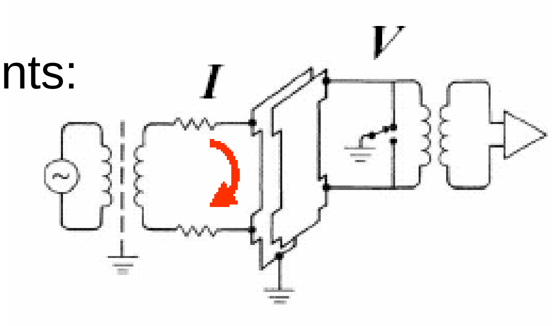

1) Drag measurements: probing adjacent layer interactions

2) Tunneling measurements: response to injecting charge

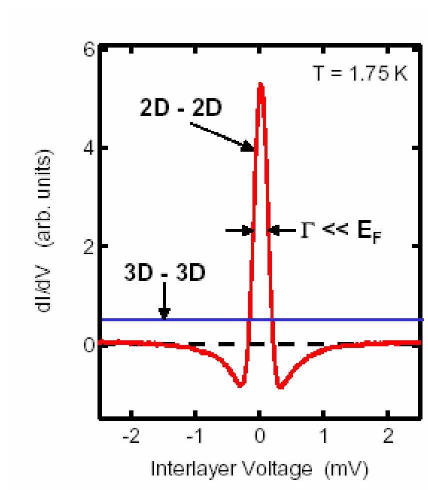

3) bilayer transport measurements showing QHE: collective state of two adjacent layers

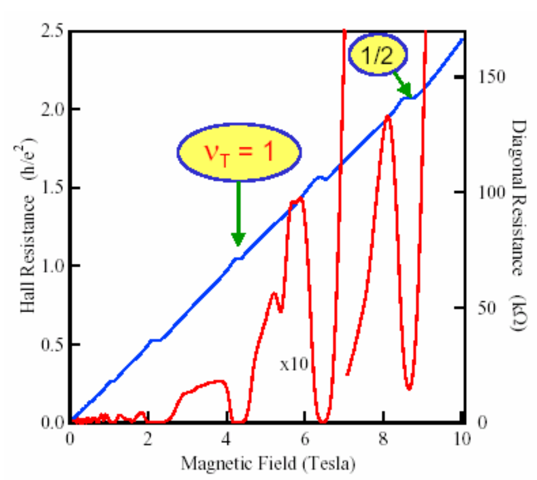

VI. Multicomponent systems: bilayers

B. experiments: 1) drag

"large" separation (>100Å)

$$\boxed{R_D \equiv \frac{V}{I}}$$

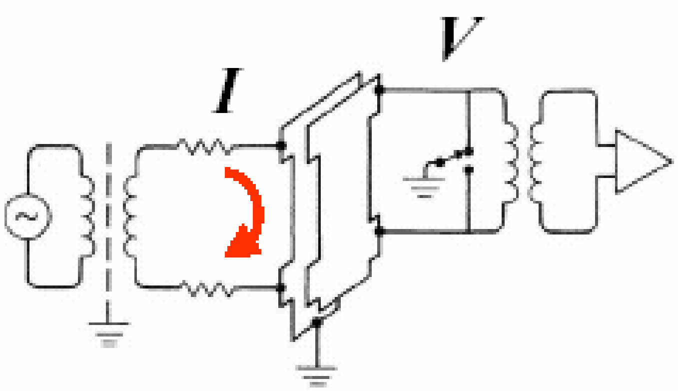

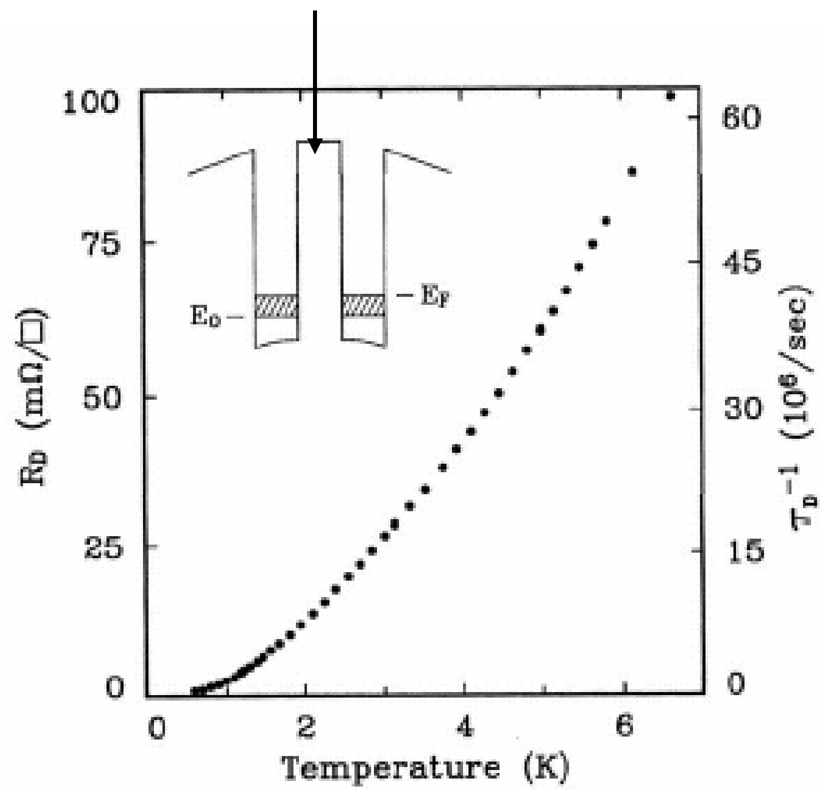

Examines Coulomb scattering
between layers

Gramila, et al. 1991

VI. Multicomponent systems: bilayers

B. experiments: 1) drag

Guess that R_D (~?$^{-}{}_{D}{}^{-1}$) ? T^2
From phase space argument

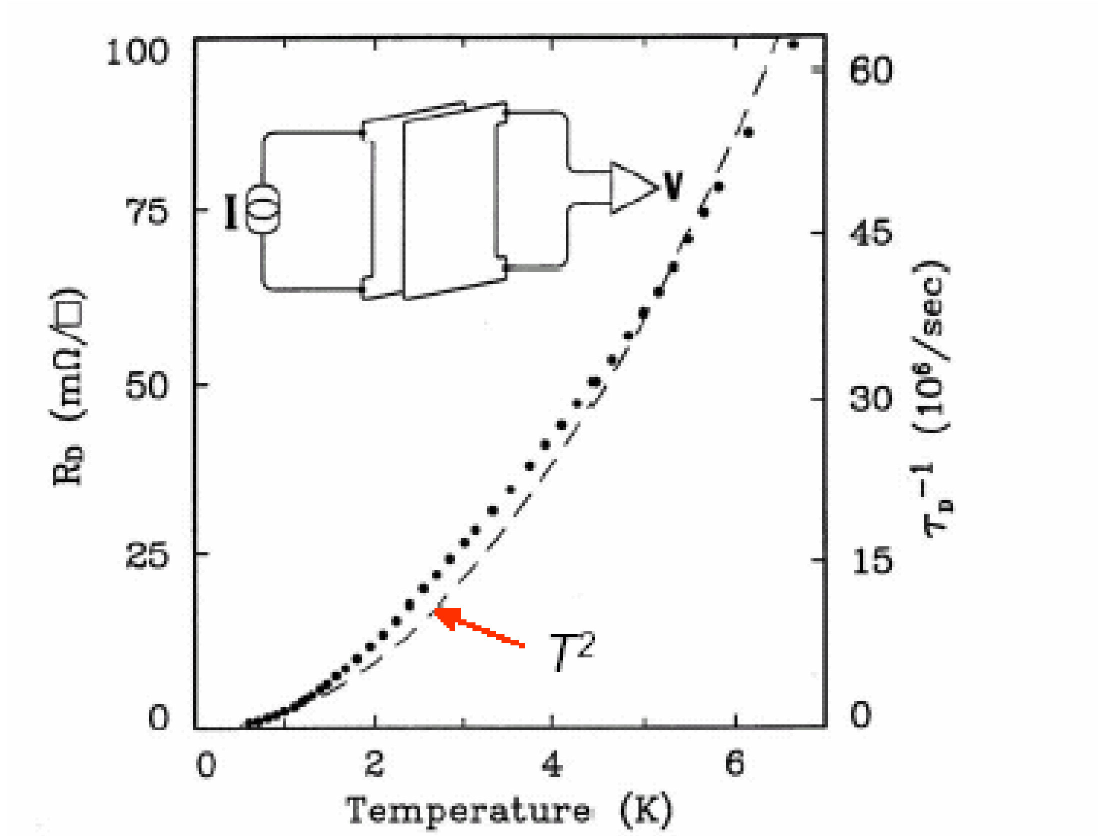

Gramila, et al. 1991

VI. Multicomponent systems: bilayers

B. experiments: 1) drag

Note!

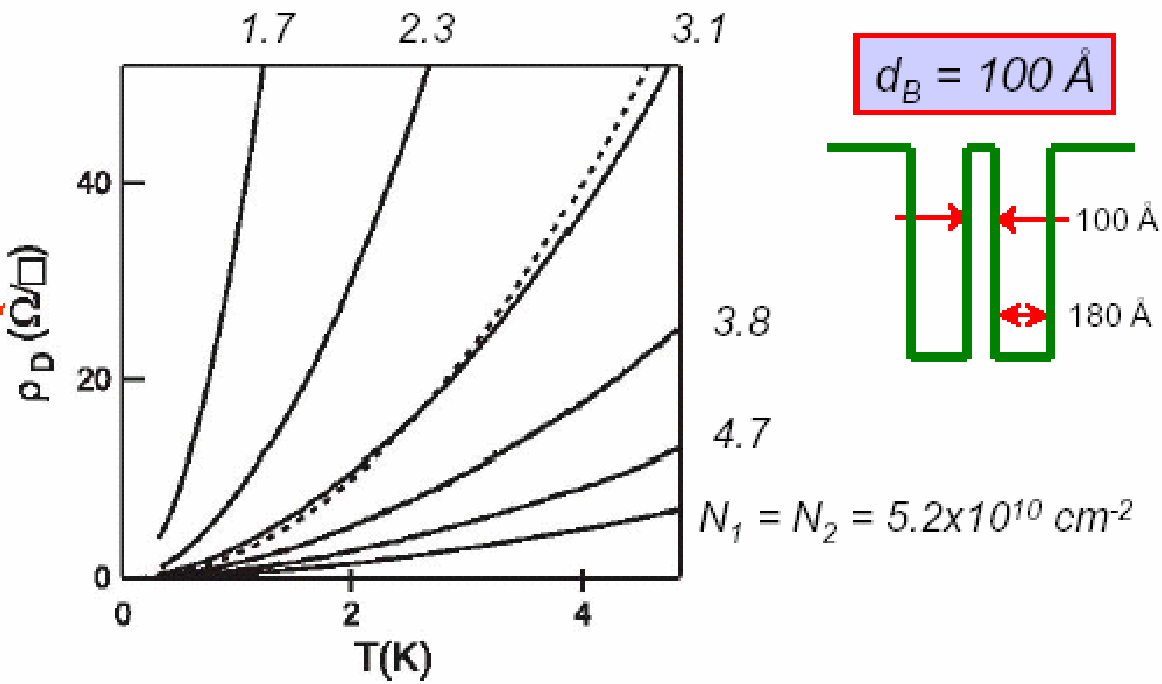

Theory: $\rho_D \propto \dfrac{T^2}{N^3 d^4}$

MacDonald '91
Jauho & Smith '93

M. Kellogg, et al. 2002

VI. Multicomponent systems: bilayers

B. experiments: 1) drag and composite fermions

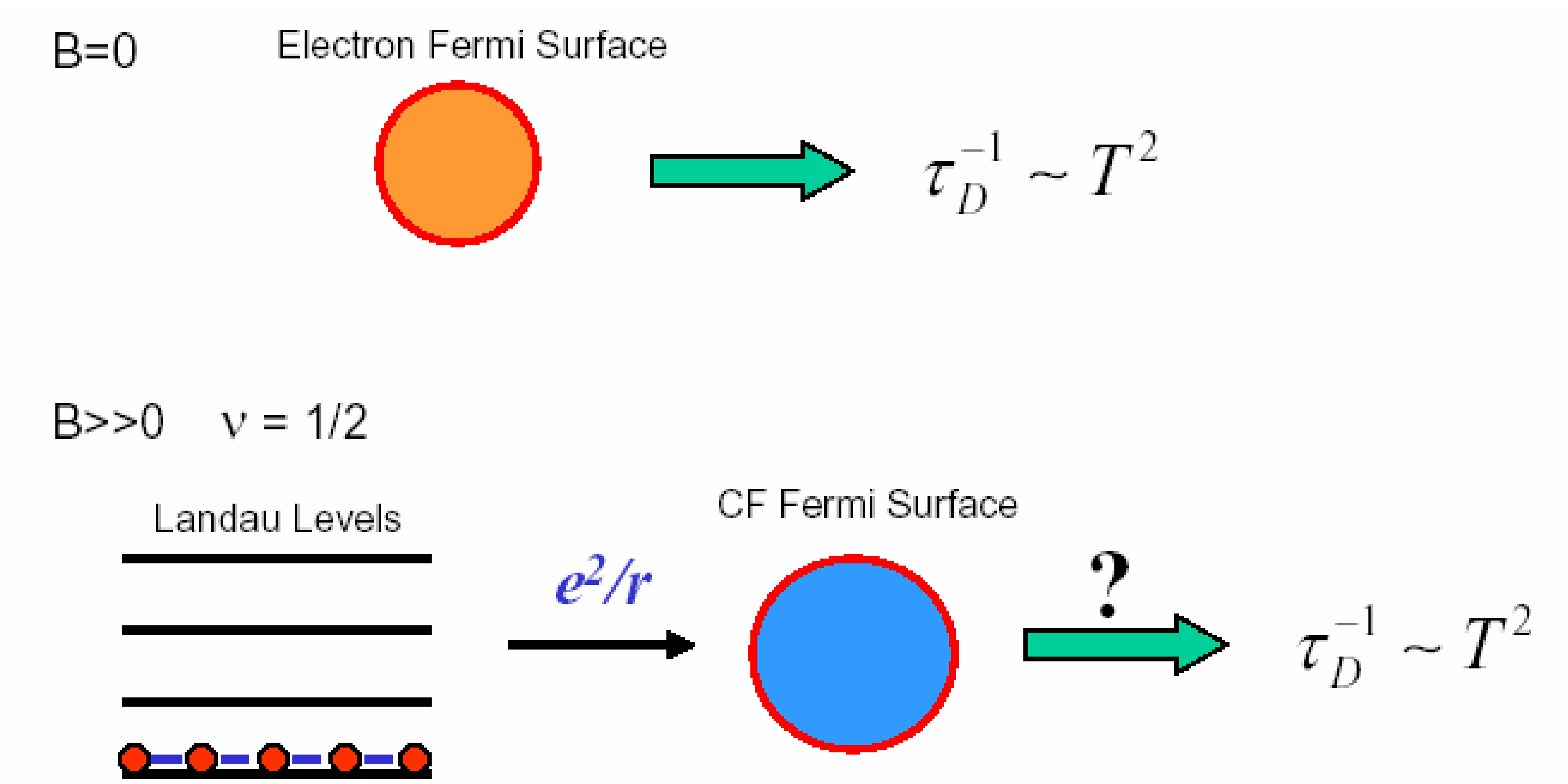

VI. Multicomponent systems: bilayers

B. experiments: 1) drag and composite fermions

Drag resistance greatly enhanced at 1/2 filling factor

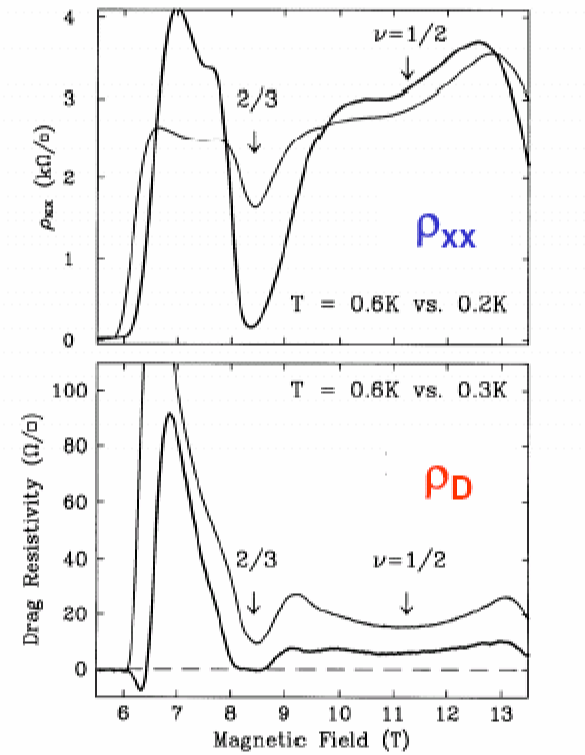

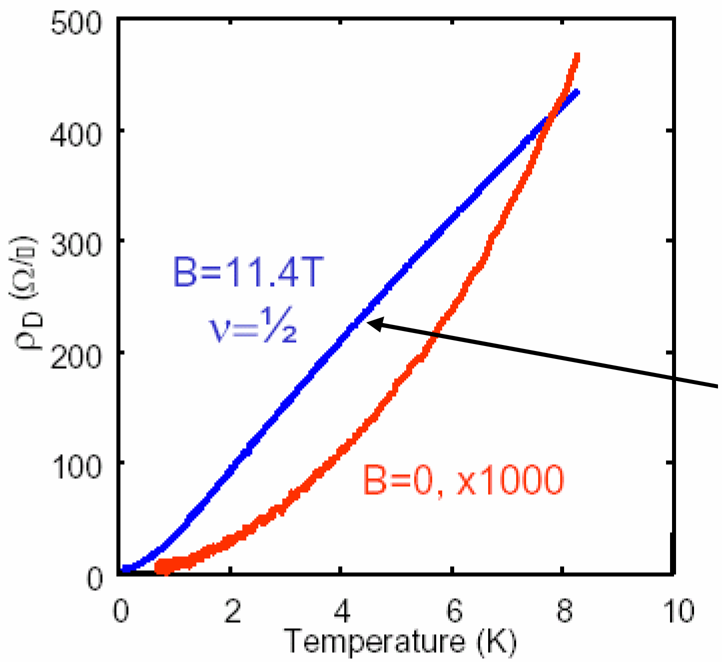

$R_D \sim$
Not T^2

Lilly, PRL '98

VI. Multicomponent systems: bilayers

Lilly, PRL '98

B. experiments: 1) drag and composite fermions

High B-field slow relaxation of charge density fluctuations

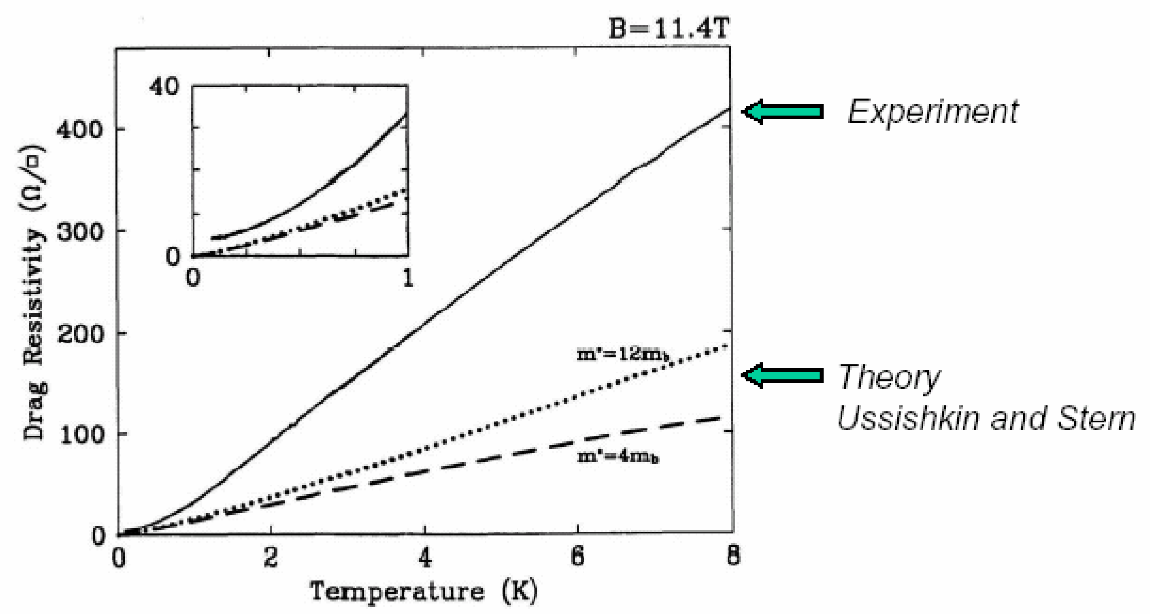

Kim and Millis
Sakhi
singular gauge field fluctuat...

Ussishkin and Stern — B = 0 theory + $\sigma_{xx}(q,\omega)$ at $\nu = 1/2$

B=0: $q_{max} \sim 1/d$

ν=1/2: $\sigma_{xx} \propto q$ → *Slow relaxation of charge fluctuations*

$q_{max} \sim T^{1/3}$

$$\rho_D \approx 0.8 \frac{h}{e^2}\left(\frac{T}{T_0}\right)^{4/3} \qquad T_0 \approx \pi e^2 N_s d / \varepsilon \approx 190\ K$$

$$\rho_D \approx 10\ \Omega/\square \quad @ \ T = 0.5K$$

Theory gets $T^{4/3}$, not overall magnitude.

Functional dependence due to composite particle conductivity wavevector dependence:

VI. Multicomponent systems: bilayers

B. experiments: 2) tunneling

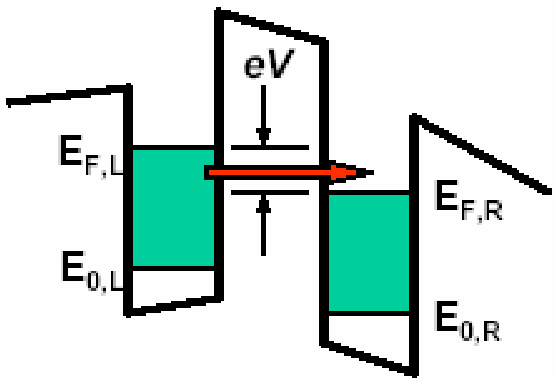

Murphy, PRB ‘95

Sharp resonance at B=0 due to momentum and energy conservation in 2D

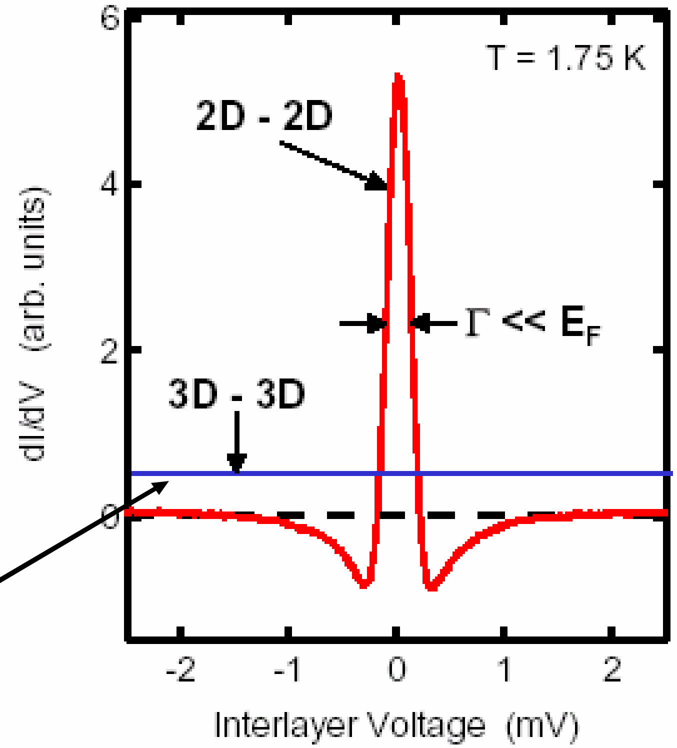

(Tunneling through oxide from and to normal metals)

VI. Multicomponent systems: bilayers

B. experiments: 2) tunneling

Tunneling in a Parallel Magnetic Field

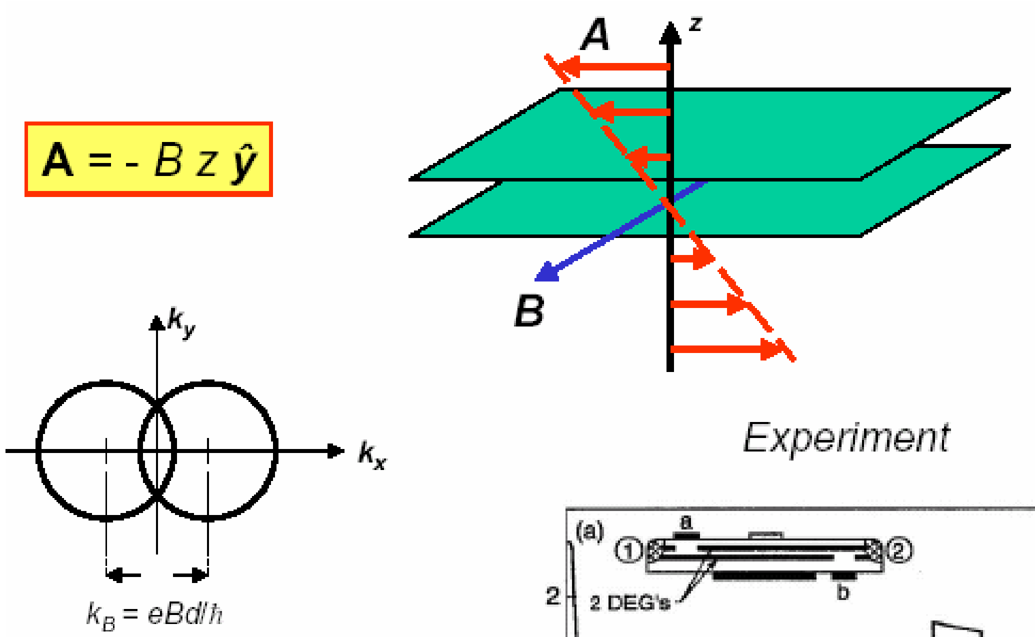

Experiment *Theory*

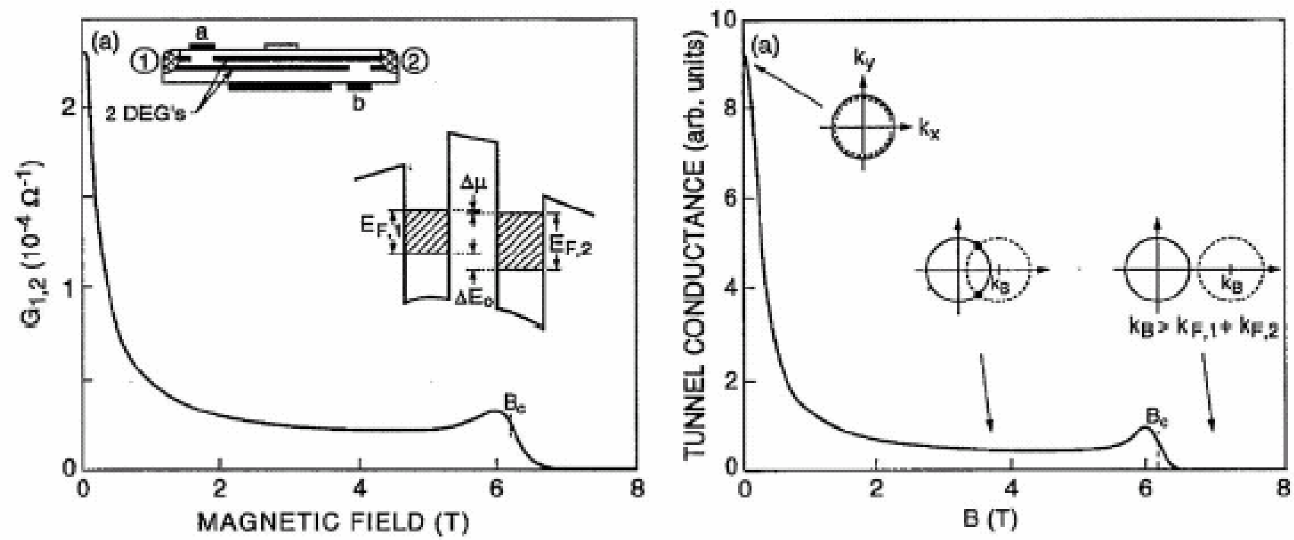

VI. Multicomponent systems: bilayers

B. experiments: 2) tunneling

Tunneling in a Parallel Magnetic Field

$\mathbf{A} = -B\,z\,\hat{\mathbf{y}}$

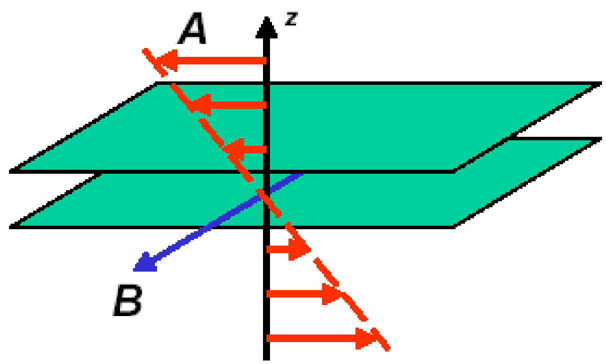

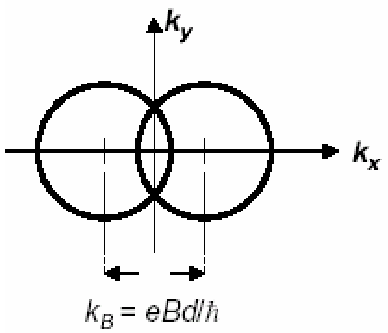

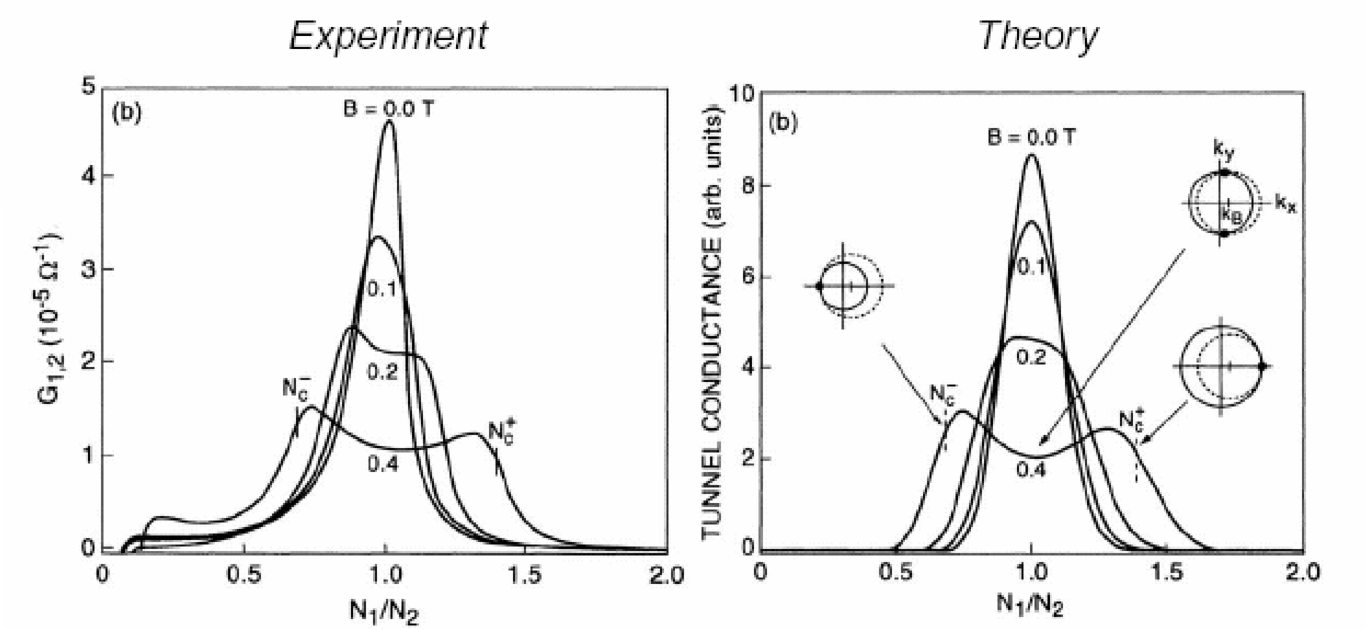

VI. Multicomponent systems: bilayers

B. experiments: 2) tunneling

Tunneling in a Large Perpendicular Magnetic Field

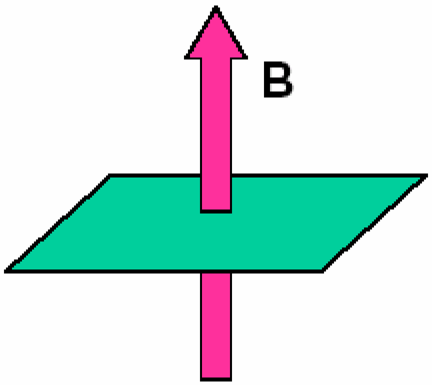

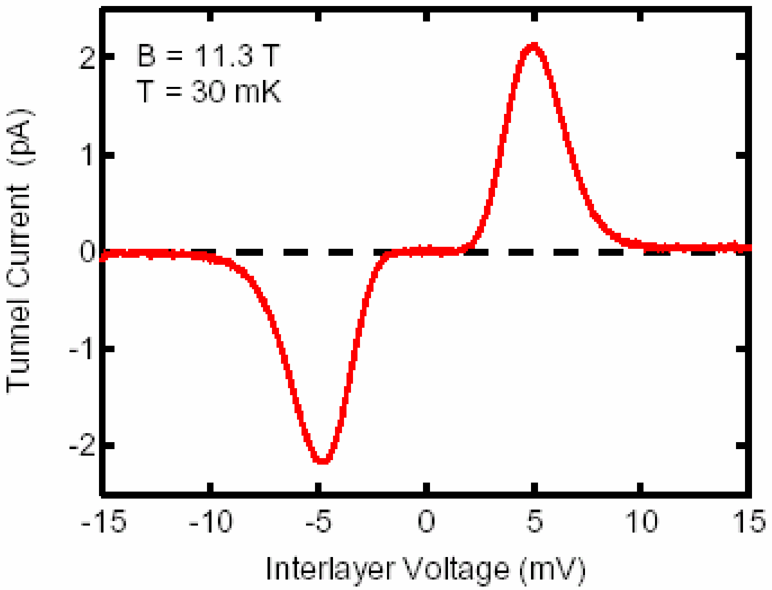

Zero bias suppression suggests Coulomb gap

VI. Multicomponent systems: bilayers

B. experiments: 2) tunneling

Tunneling in a Large Perpendicular Magnetic Field

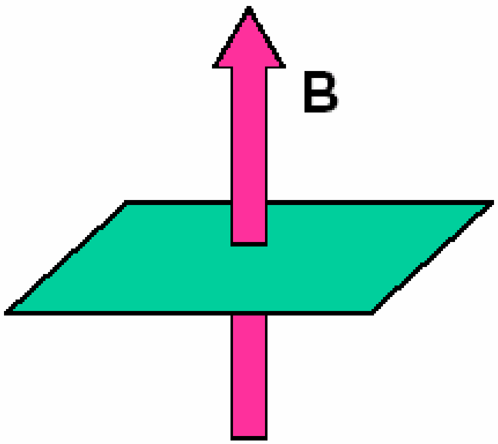

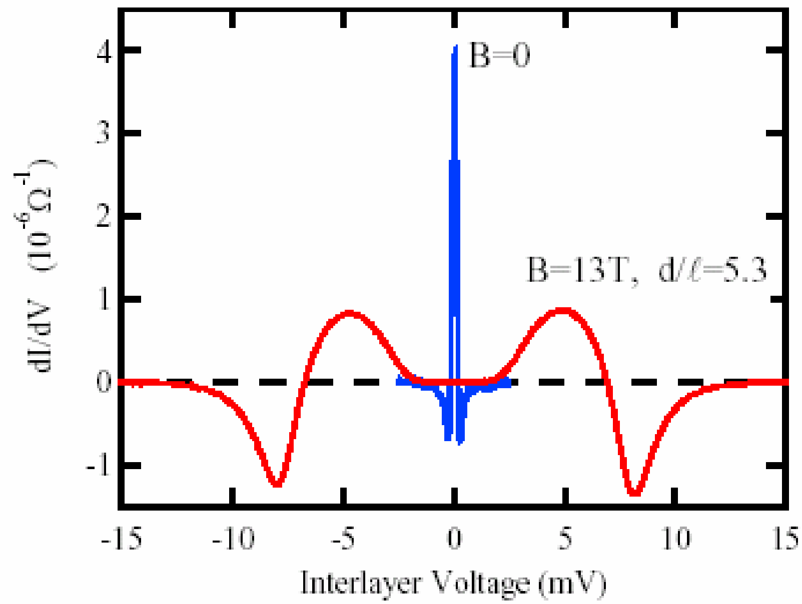

VI. Multicomponent systems: bilayers

B. experiments: 2) tunneling

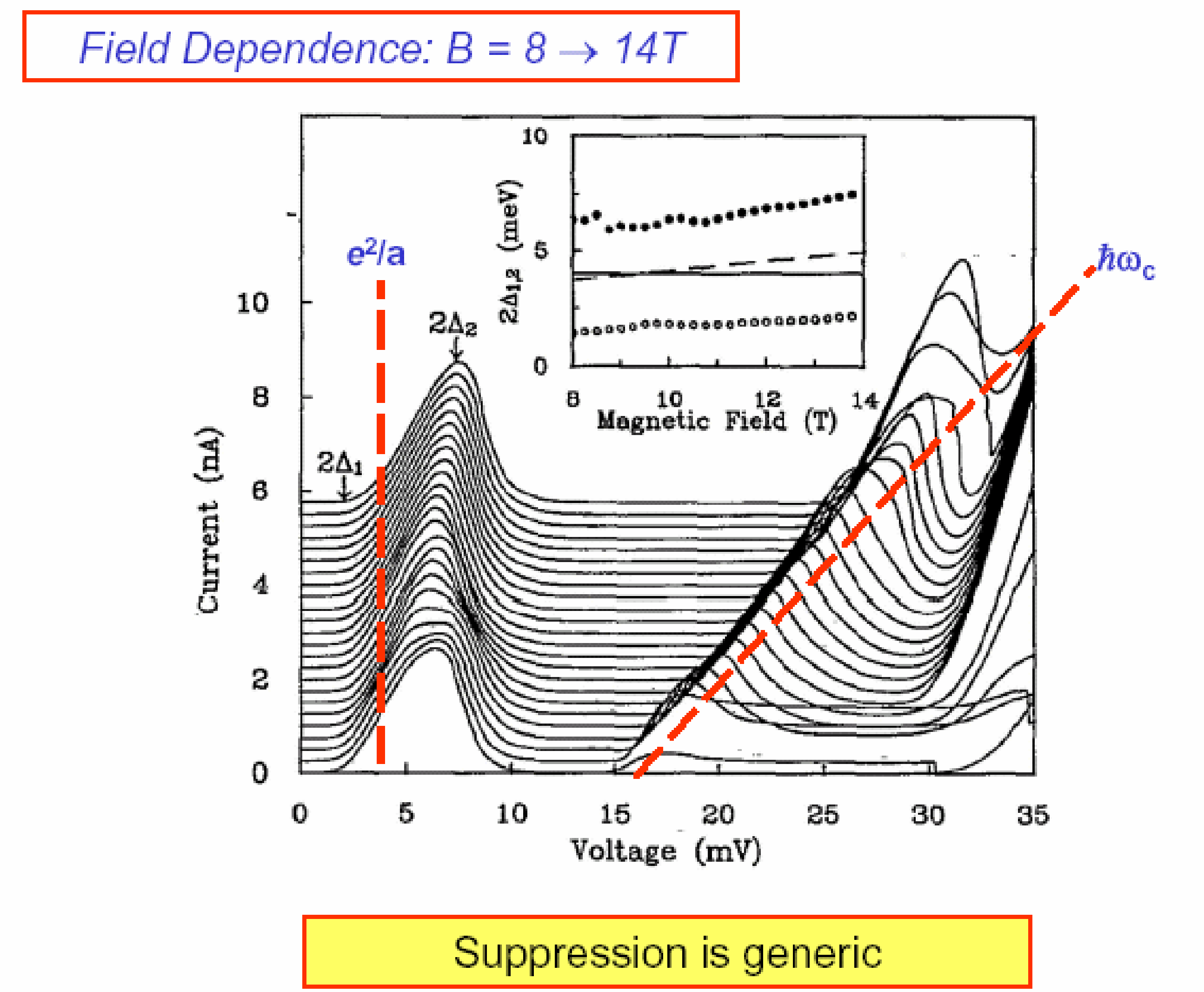

VI. Multicomponent systems: bilayers

B. experiments: 2) tunneling

Lowest Landau Level is a Strongly Correlated System

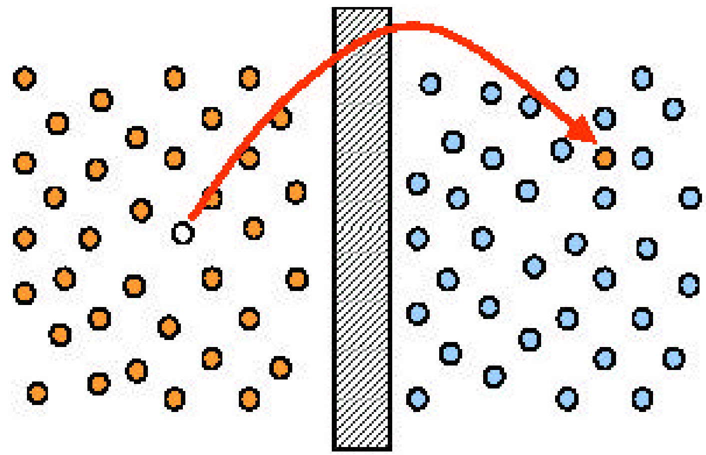

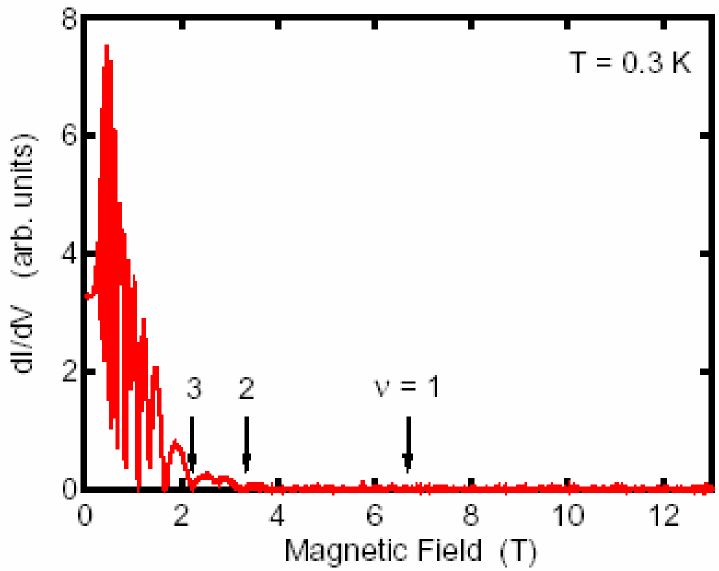

Tunneling is fast compared to relaxation time of charge defects.

Result: Tunneling is suppressed at voltages below mean Coulomb energy.

$$e\,\Delta V_{gap} \approx 0.3\frac{e^2}{\varepsilon\,\ell}$$

VI. Multicomponent systems: bilayers

B. experiments: 3) quantum Hall effect

Experiment = low temperature transport through bilayers with contacts to both layers (not independent)

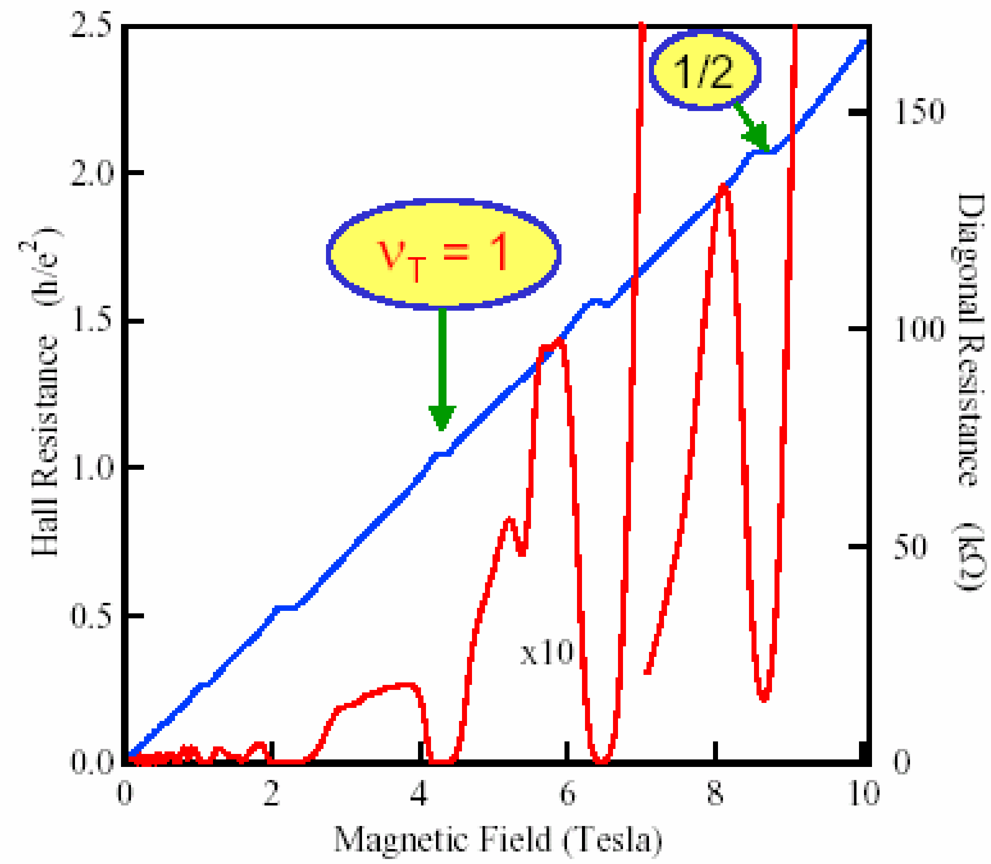

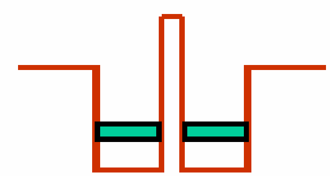

$\nu_T = 1 = ½ + ½$

$\nu_T = ½ = ¼ + ¼$

Quantum Hall effect observed at total filling factor 1 = ½ in each layer and at ¼ in each layer

VI. Multicomponent systems: bilayers

B. experiments: 3) quantum Hall effect

As d/l_o increases, the QHE is lost at total filling factor ½ , ¼ + ¼:

The interlayer Coulomb interactions are necessary for the QHE at these bilayer filling factors.

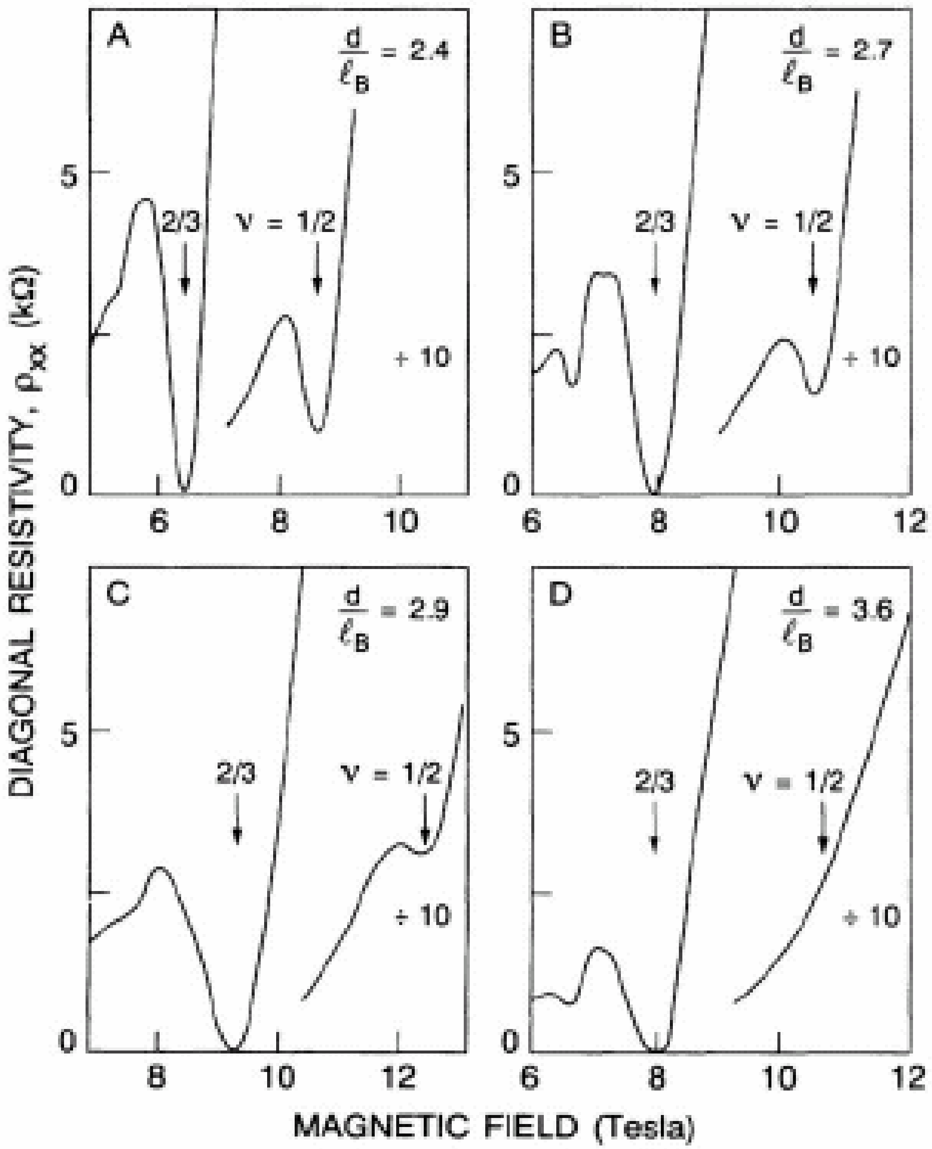

VI. Multicomponent systems: bilayers

B. experiments: 3) quantum Hall effect

Experiments show

1) Phase boundary
2) Phase boundary intercepts vertical axis at finite d/ l_o for ? = 1 state

31Å barrier

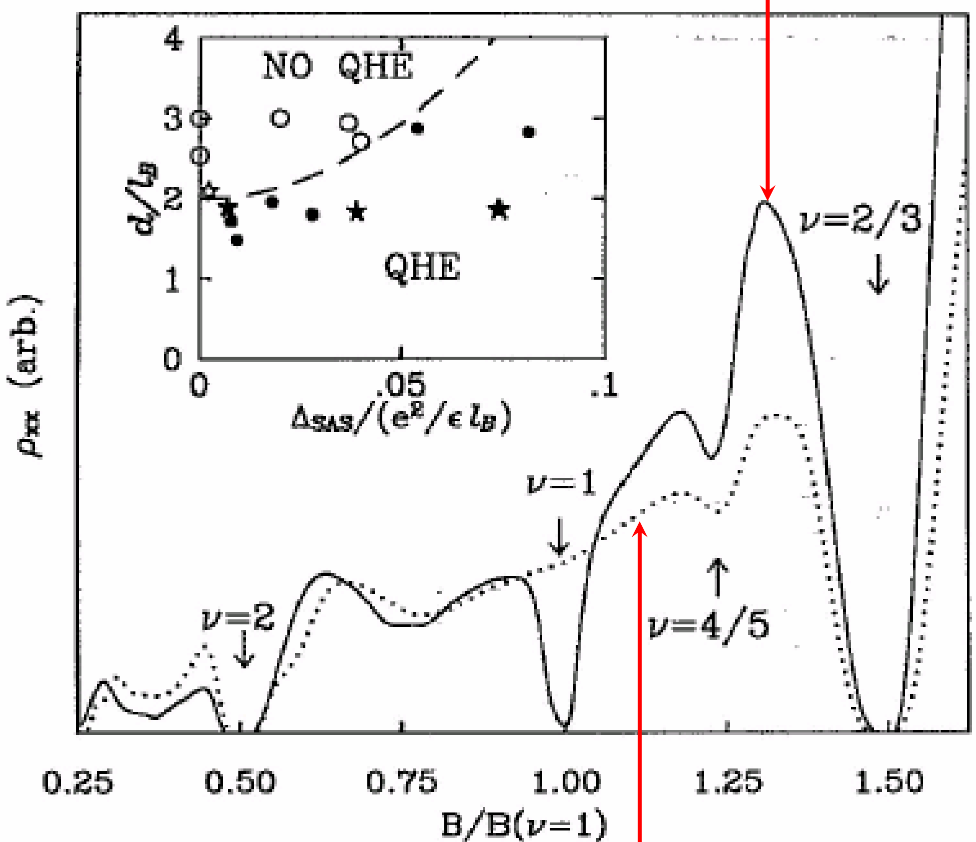

Murphy et al '90

40 Å barrier

VI. Multicomponent systems: bilayers

B. experiments: 3) quantum Hall effect

Halperin's Generalized Laughlin States

$$\Psi_{l\,m\,n}(z_1,\ldots;w_1,\ldots) \sim \prod_{i<j}(z_i - z_j)^l \prod_{i<j}(w_i - w_j)^m \prod_{i<j}(z_i - w_j)^n$$

At $\nu_T = 1/2$:

$$\boxed{\Psi_{331} \sim \prod_{i<j}(z_i - z_j)^3 \prod_{i<j}(w_i - w_j)^3 \prod_{i<j}(z_i - w_j)}$$

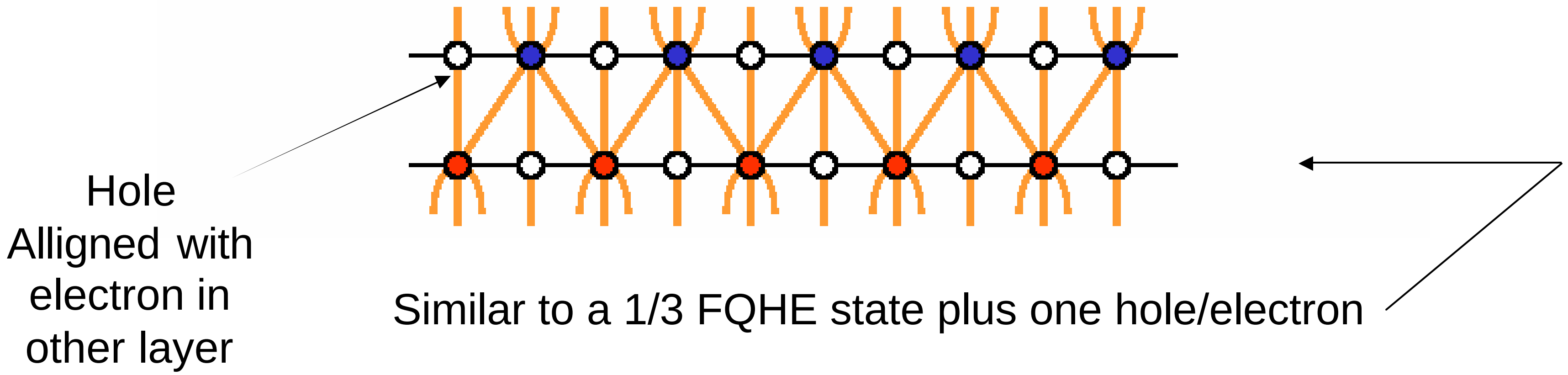

VI. Multicomponent systems: bilayers

B. experiments: 3) quantum Hall effect

At $\nu_T = 1/2$:
$$\Psi_{331} \sim \prod_{i<j}(z_i - z_j)^3 \prod_{i<j}(w_i - w_j)^3 \prod_{i<j}(z_i - w_j)$$

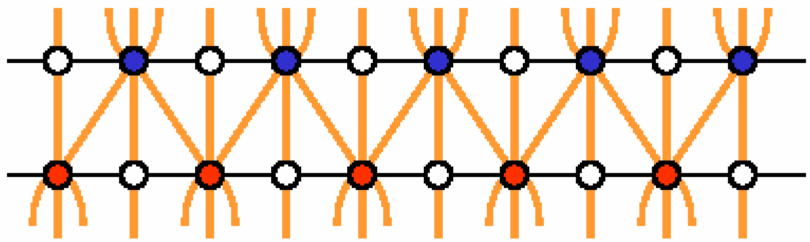

At $\nu_T = 1$
$$\Psi_{111} \sim \prod_{i<j}(z_i - z_j) \prod_{i<j}(w_i - w_j) \prod_{i<j}(z_i - w_j)$$

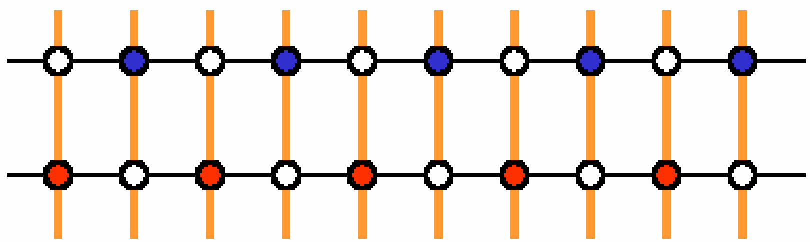

Bilayer QHE states related to Halperin generlized Laughlin states?

VI. Multicomponent systems: bilayers

B. experiments: 3) quantum Hall effect

?= 1 bilayer QHE has two possible origins:

Single particle
&
Many-body effect

1. Single Particle Tunneling

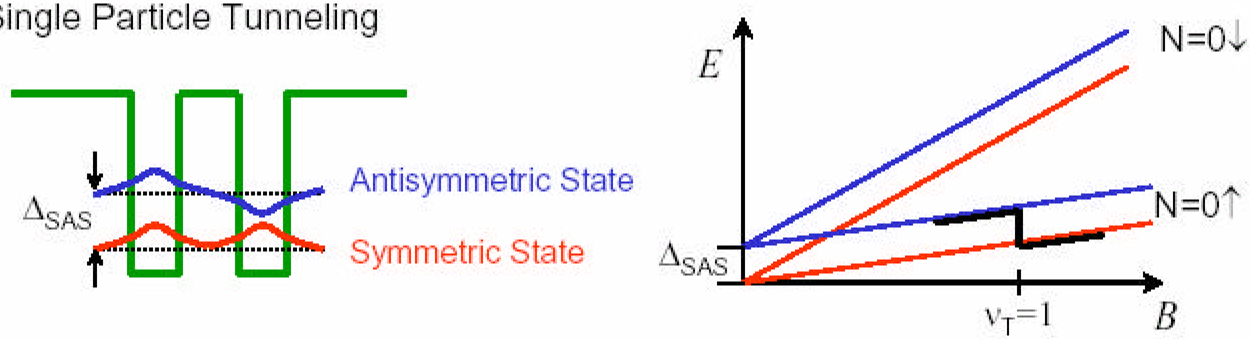

2. Pure Many-body Effect

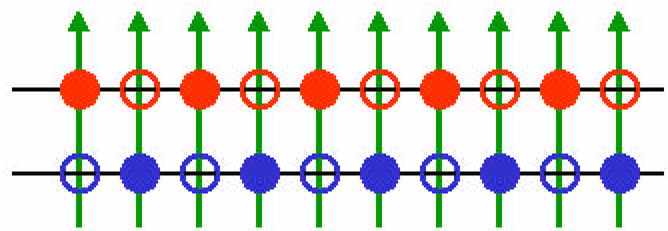

$$\Psi \sim \prod_{i,..,n} (z_i - z_j)\ (w_k - w_l)\ (z_m - w_n)$$

Reduce tunneling to get rid of the single particle origin

VI. Multicomponent systems: bilayers

C. Experiments – ?$_{\text{total}}$ = 1 excitonic Bose condensate

For low tunneling regime,
predicted that
the condensed state at
?$_{\text{total}}$ = 1 may be an
excitonic Bose
Condensate?

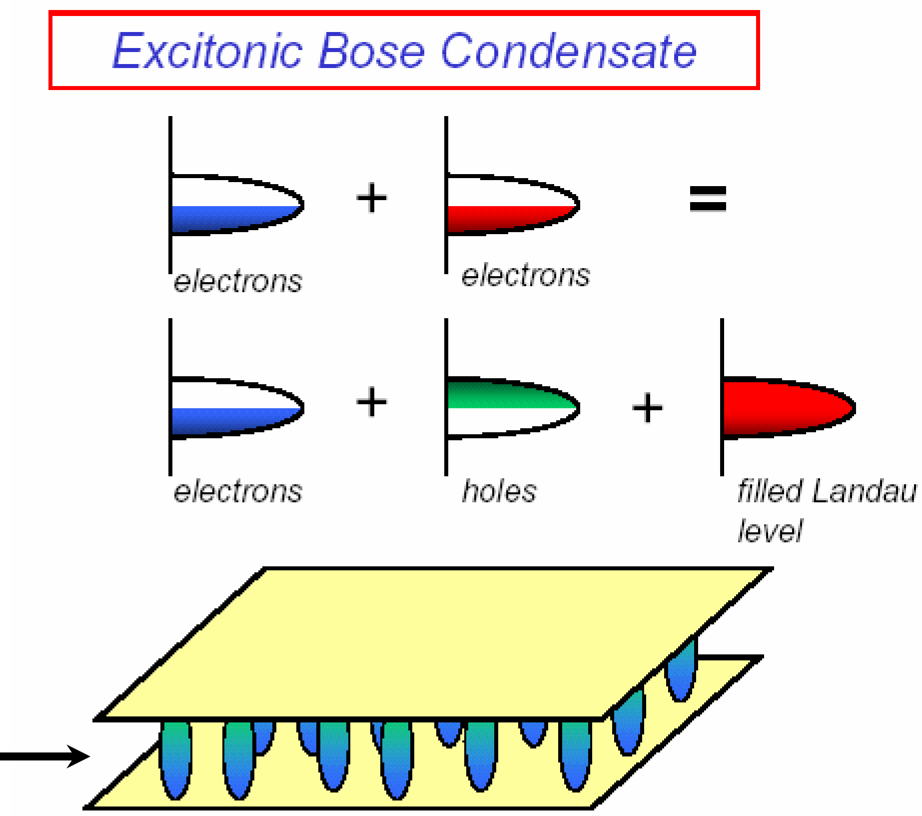

Charge neutral excitons

J.P. Eisenstein, ‘03

VI. Multicomponent systems: bilayers

C. Experiments – $?_{\text{total}}$ = 1 excitonic Bose condensate

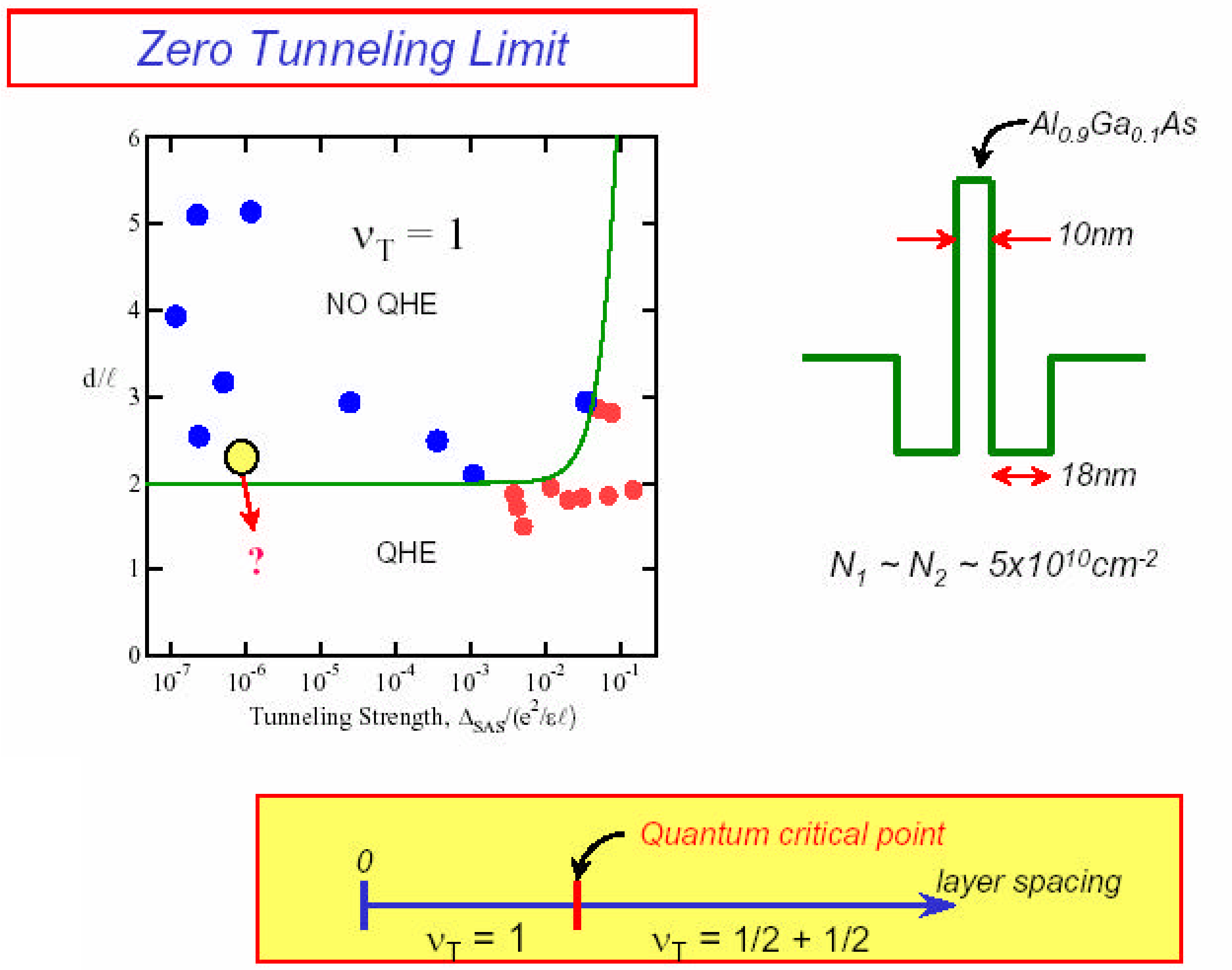

J.P.E. ‘04

VI. Multicomponent systems: bilayers

C. Experiments – ? $_{total}$ = 1 excitonic Bose condensate

? ?$_{total}$ = 1 QHE clearly not due to simple single particle spectrum

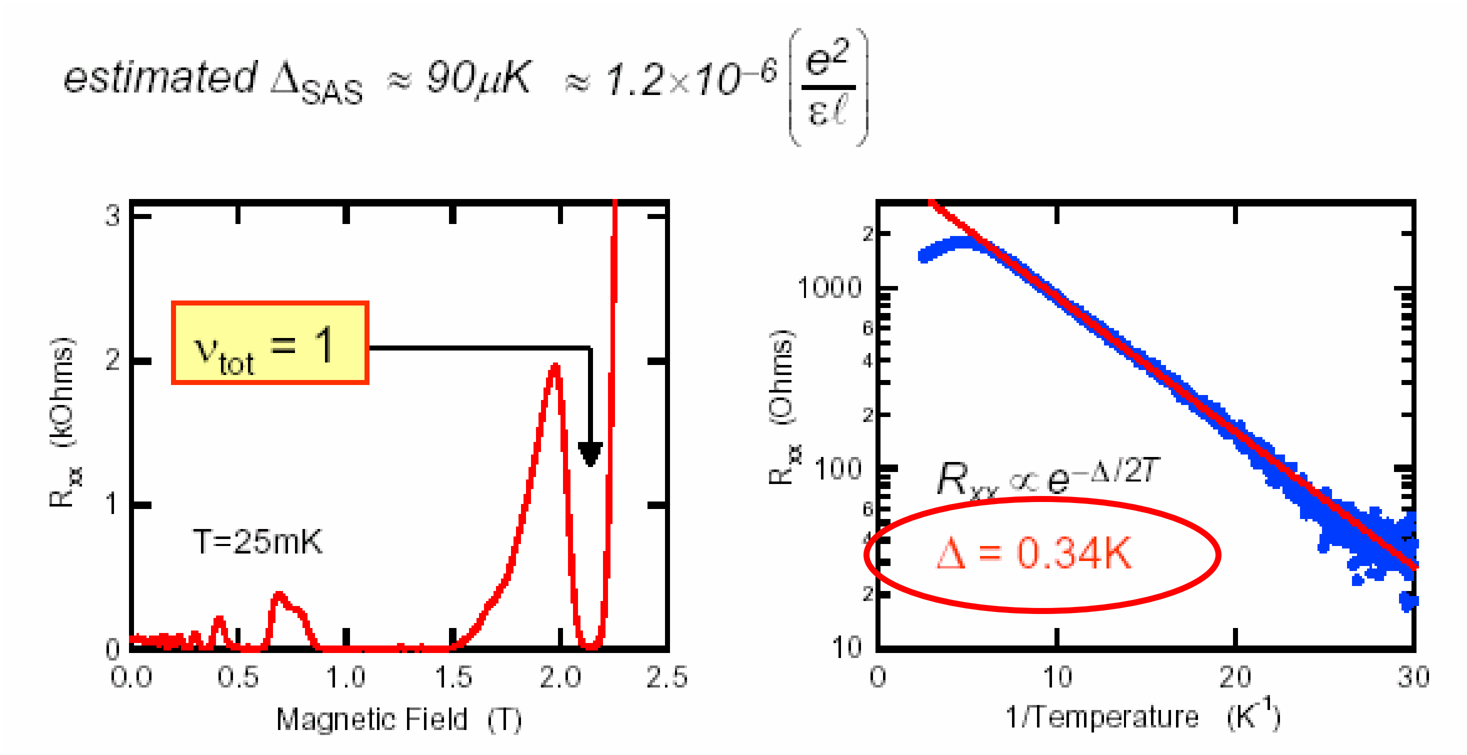

very low tunneling & large ? = 1 energy gap in these samples

VI. Multicomponent systems: bilayers

C. Experiments – ?$_{total}$ = 1 excitonic Bose condensate

Again, examine tunneling near the excitonic phase

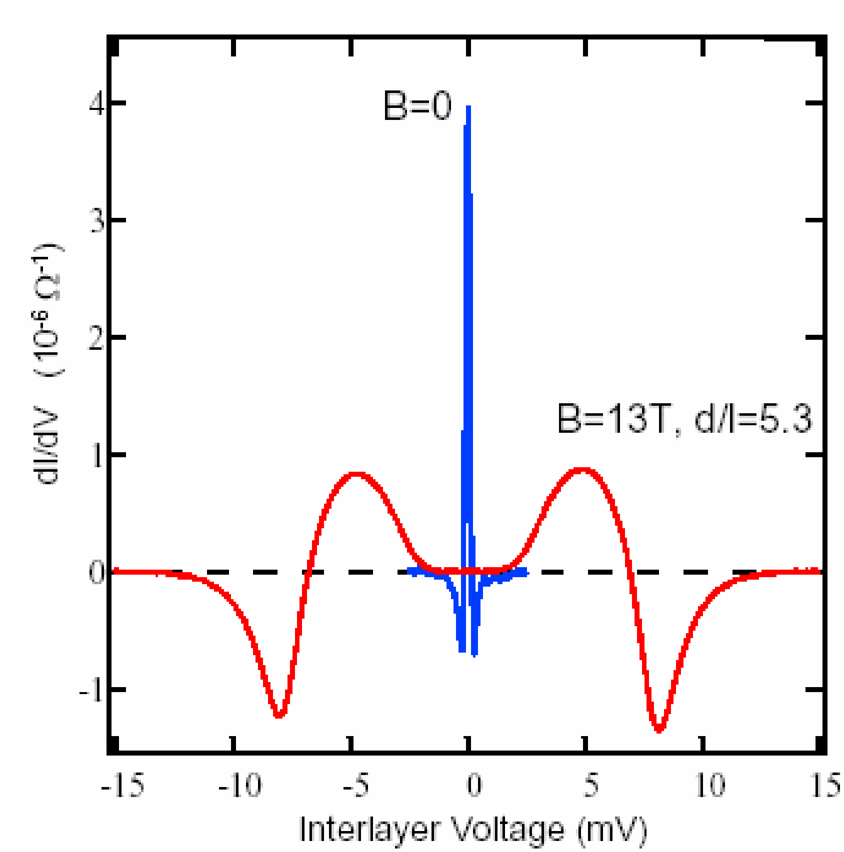

Remember:

B=0 Narrow resonance, created by momentum and energy conservation; a single particle effect. Γ~200μeV

B>>0 Strongly suppressed tunneling around zero bias, broad high energy response; a many-body-effect.

VI. Multicomponent systems: bilayers

C. Experiments – $?_{\text{total}} = 1$ excitonic Bose condensate

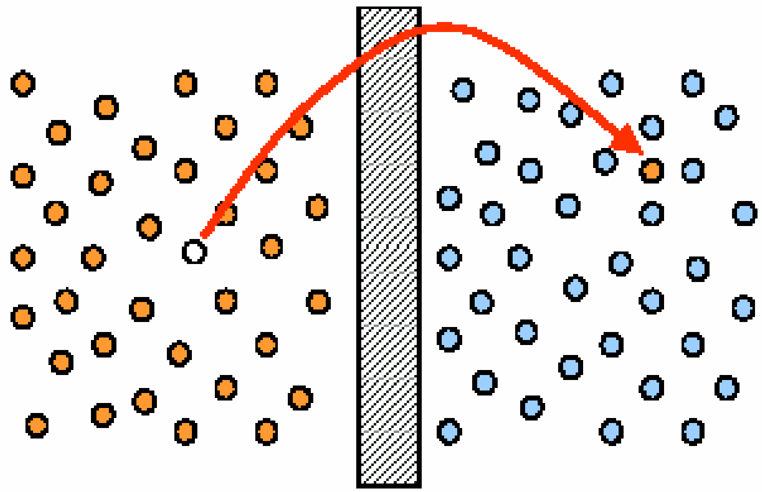

Vacancy + interstitial

However, near condensate……..

Tunneling is fast compared to relaxation time of charge defects.

Result: Tunneling is suppressed at voltages below mean Coulomb energy.

$$e\,\Delta V_{gap} \approx 0.3\,\frac{e^2}{\varepsilon \ell}$$

VI. Multicomponent systems: bilayers

C. Experiments – ? $_{total}$ = 1 excitonic Bose condensate

Crossing the ν_T =1 Phase Boundary

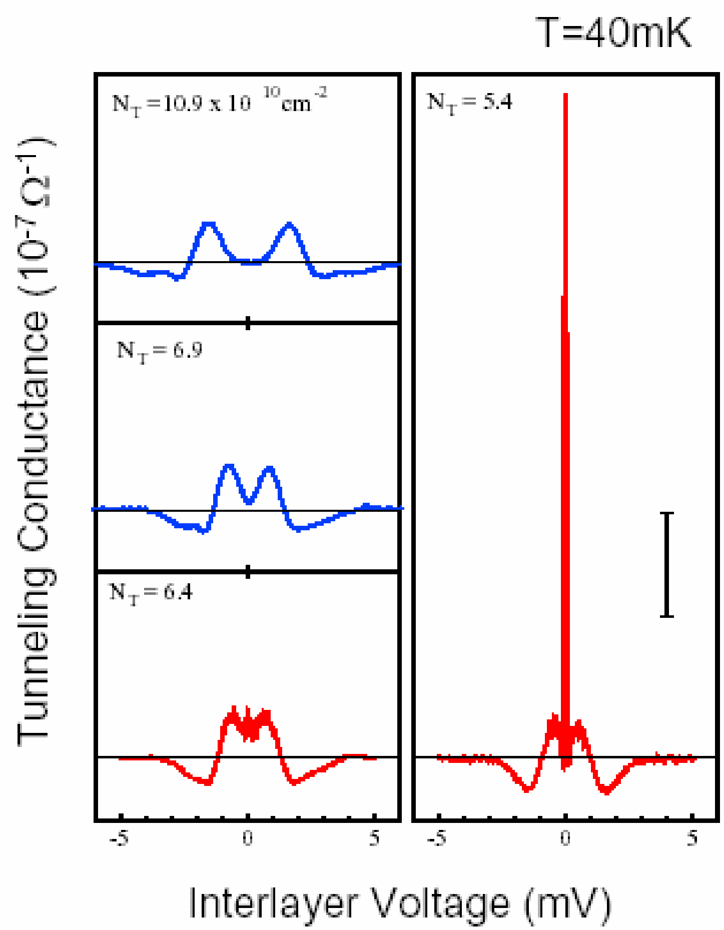

As phase boundary is crossed into the QHE range, tunneling peak occurs similar to B=0

VI. Multicomponent systems: bilayers

C. Experiments – ? $_{total}$ = 1 excitonic Bose condensate

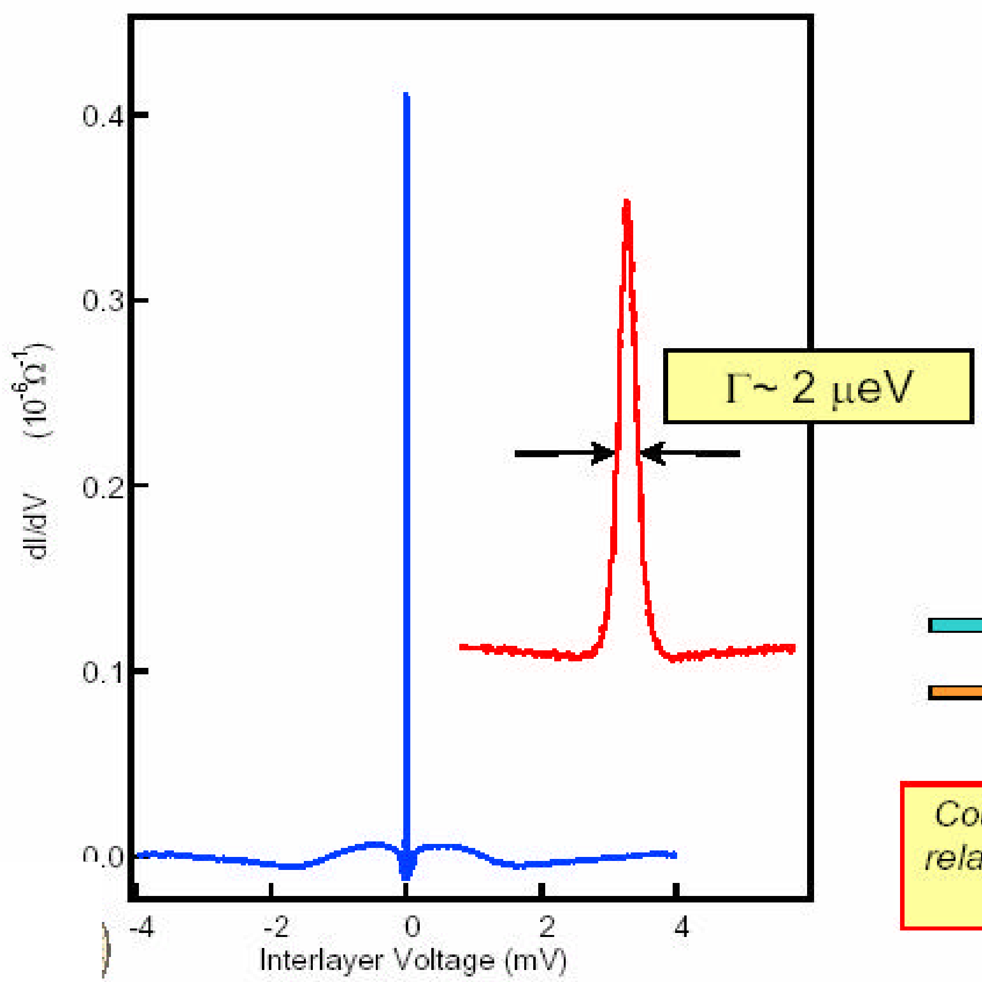

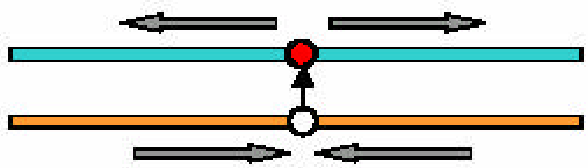

Counter-flow superfluidity rapidly relaxes charge defects created by tunneling.

VI. Multicomponent systems: bilayers

C. Experiments – ?$_{\text{total}}$ = 1 excitonic Bose condensate

What is expected in transport when the layers can be probed independently?

Counter-flow experiment

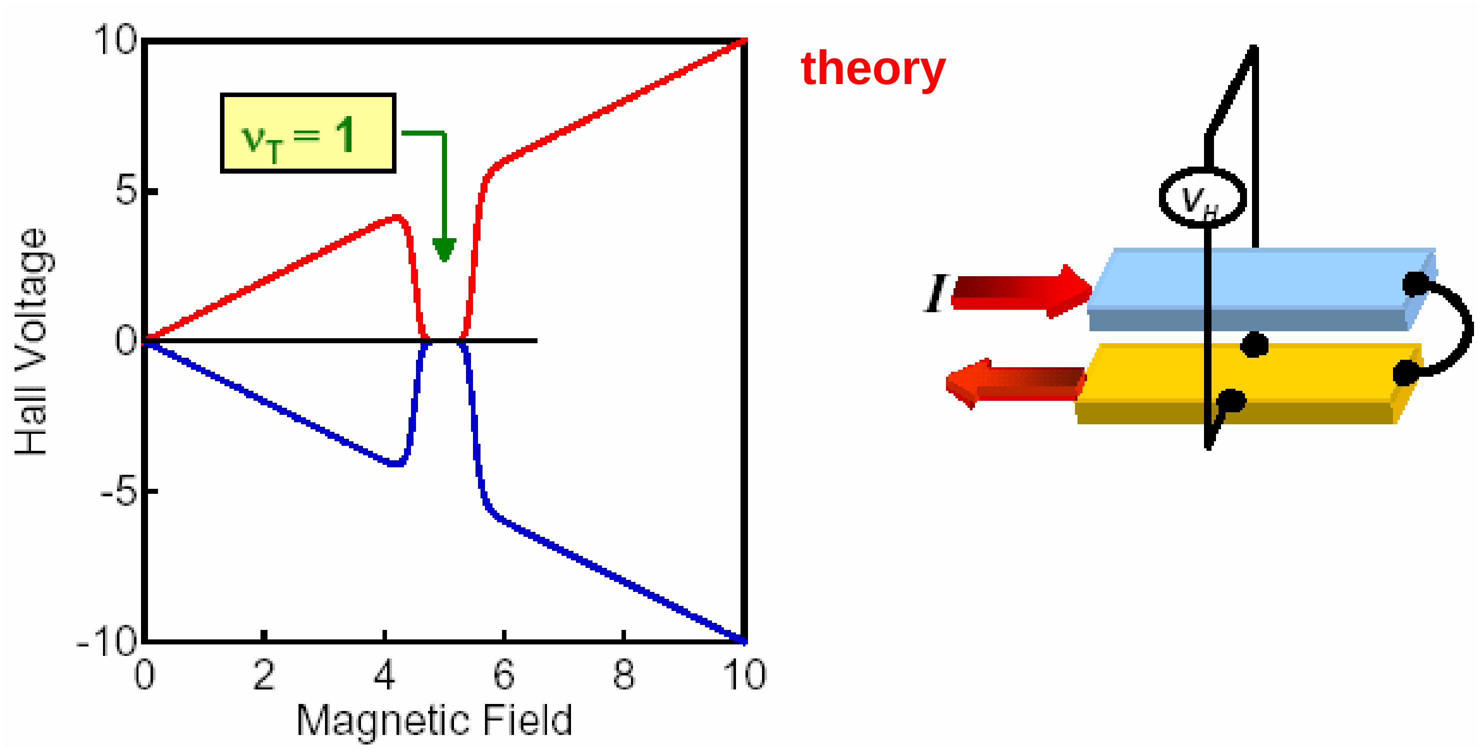

Charge neutral excitons should feel no Lorentz force!

VI. Multicomponent systems: bilayers

C. Experiments – ?$_{total}$ = 1 excitonic Bose condensate

What is expected in transport when the layers can be probed independently?
Counter-flow experiment – Hall resistance goes to zero

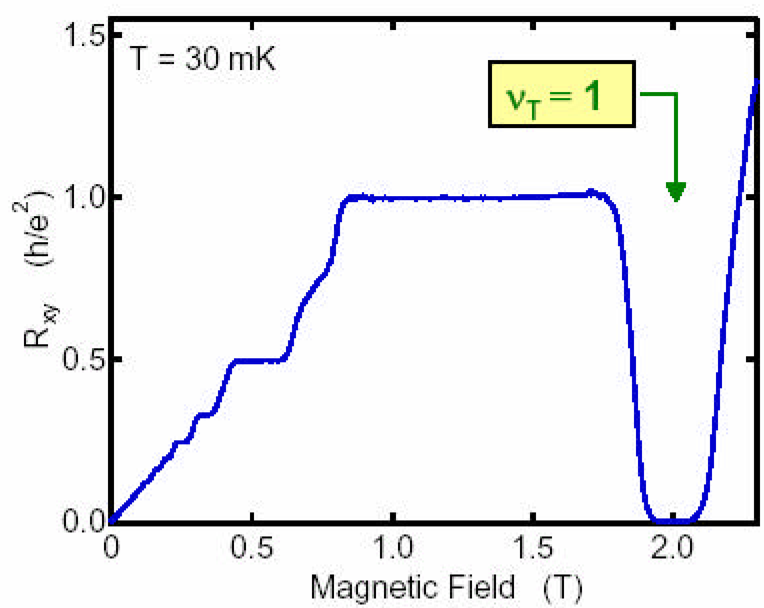

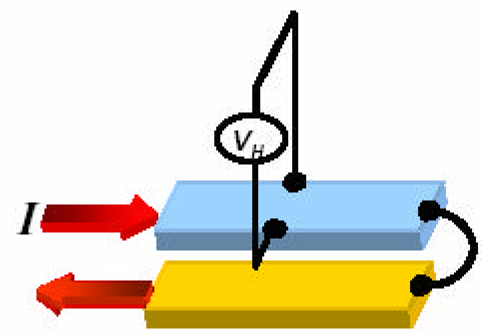

experiment

$At\ \nu_T = 1 \quad R_{xy}^{CF} \to 0\ \ as\ \ T \to 0$

exciton transport dominates counterflow

Kellogg, PRL ‘04

VI. Multicomponent systems: bilayers

C. Experiments – ? $_{total}$ = 1 excitonic Bose condensate

What is expected in transport when the layers can be probed independently?

Counter-flow experiment – longitudinal resistance goes to zero

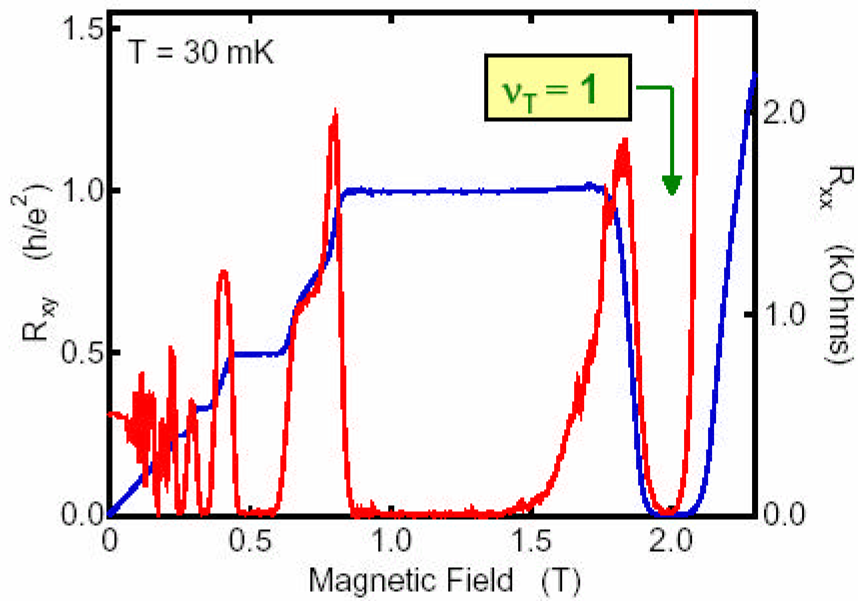

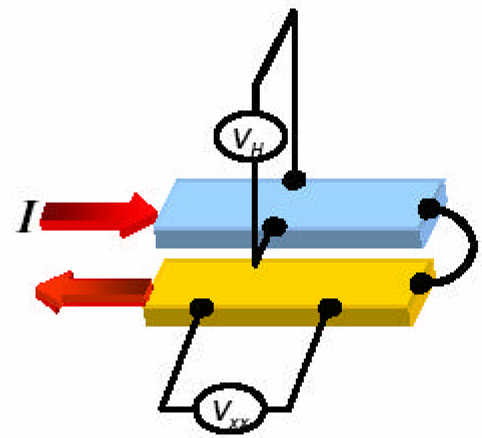

At $\nu_T = 1$: $R^{CF}_{xy} \to 0$ *and* $R^{CF}_{xx} \to 0$

Excitonic superfluidity?

See also results on drag at total filling factor 1

Kellogg, PRL '04

VI. Multicomponent systems: bilayers

C. Experiments – ? $_{total}$ = 1 excitonic Bose condensate

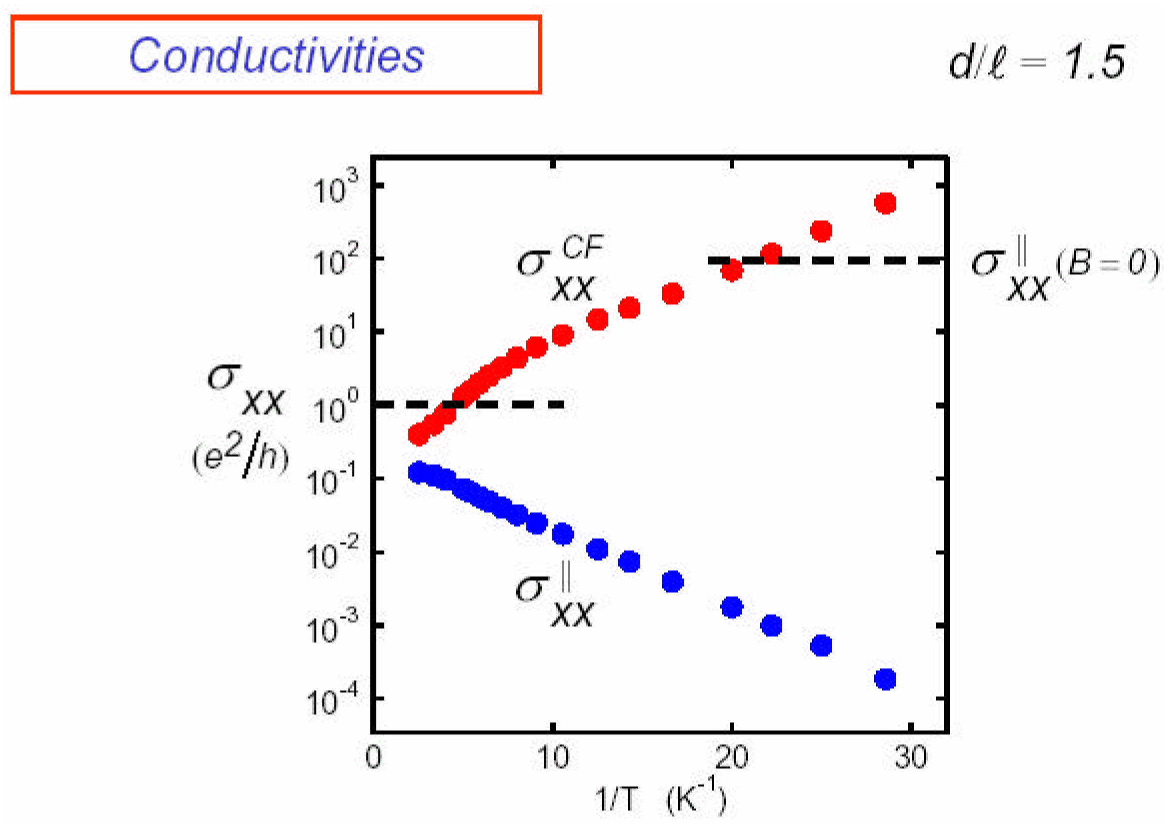

Counterflow dissipation small but non-zero at all finite T.

See also results on drag at total filling factor 1

VI. Multicomponent systems: bilayers

C. Experiments – ?$_{total}$ = 1 excitonic Bose condensate

J.P. Eisenstein ‘04

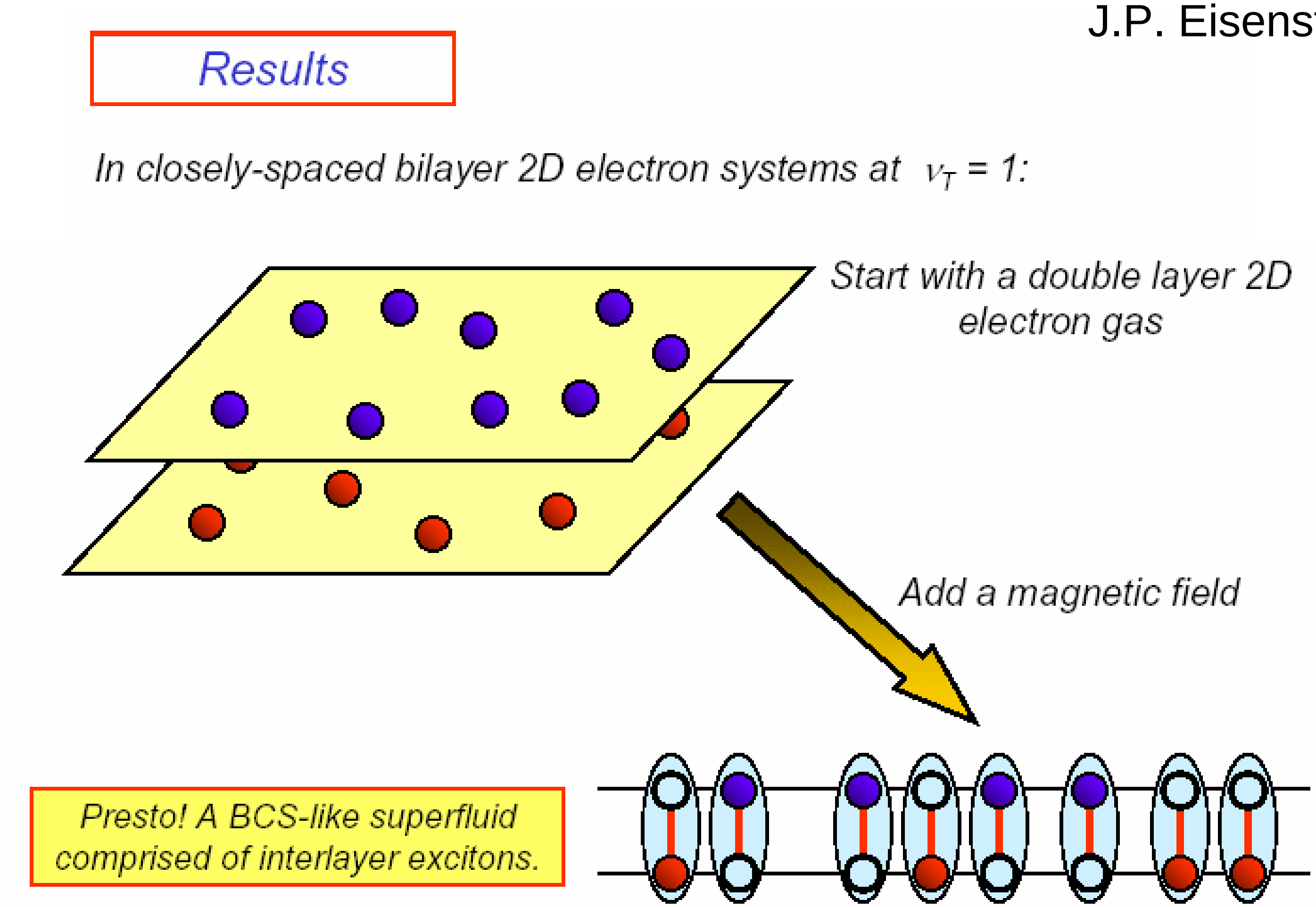

VI. Multicomponent systems: bilayers

Summary:

1) Multilayer systems of high mobility (correlations) possible
2) Drag experiments between layers expose Coulomb interaction properties
3) Tunneling measurements show the effects of correlations in the layers through their relaxation
4) Bilayer total filling factor 1 state shows ensemble of effects that are interpreted as a BEC of excitons

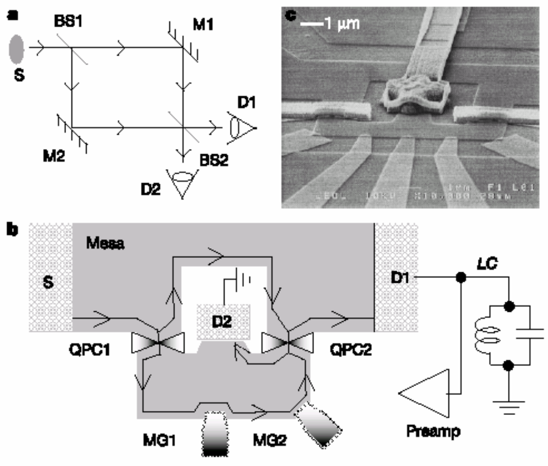

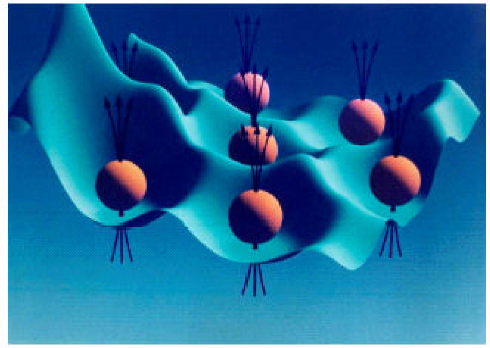

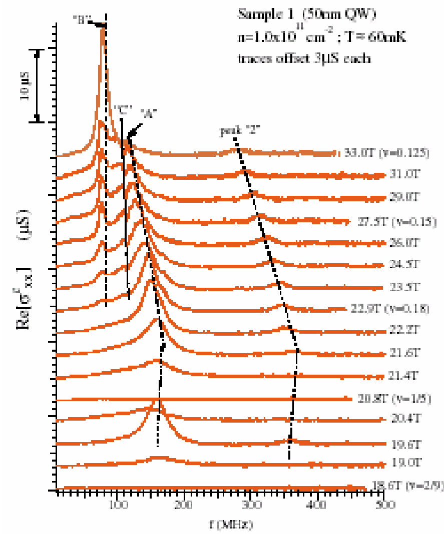

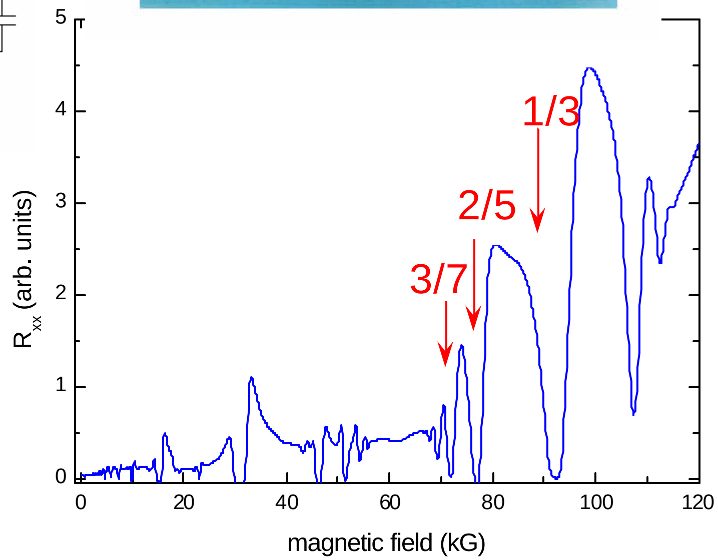

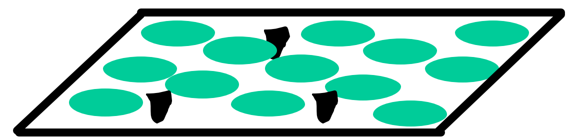

Pinned solid

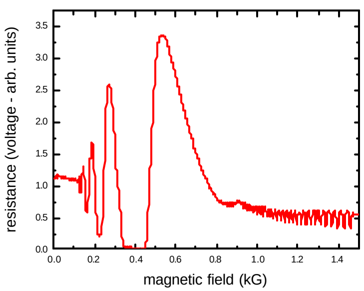

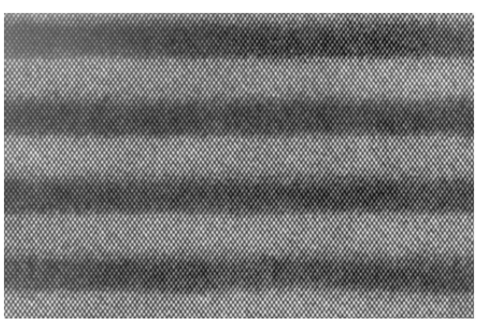

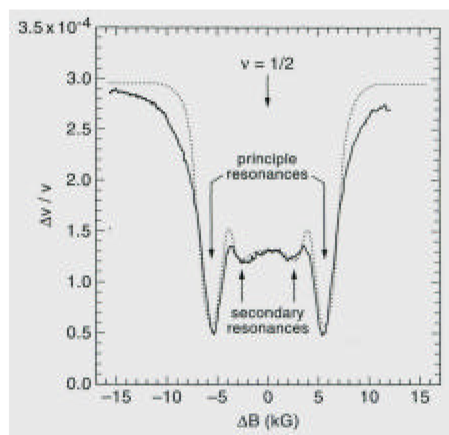

Excitonic Bose Condensate

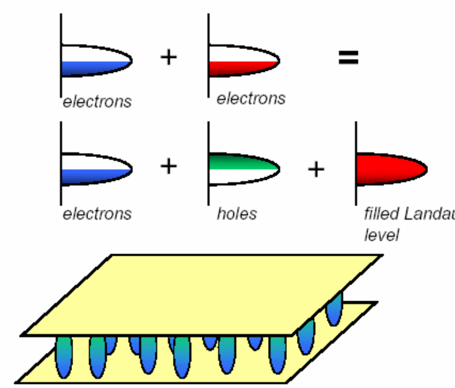

The end